Molecular and phenotypic studies of human antigen-specific effector- and memory B cells

D i s s e r t a t i o n

zur Erlangung des akademischen Grades

d o c t o r r e r u m n a t u r a l i u m

(Dr. rer. nat.)

im Fach Biologie

eingereicht an der Lebenswissenschaftlichen Fakultät
der Humboldt-Universität zu Berlin

von

Claudia Giesecke, M.Sc.

Präsident der Humboldt-Universität zu Berlin

Prof. Dr. Jan-Hendrik Olbertz

Dekan der Lebenswissenschaftlichen Fakultät

Prof. Dr. Richard Lucius

Gutachter/in: 1. Prof.Dr. Andreas Radbruch

2. Prof. Dr. Thomas Dörner

3. Prof. Dr. Kai Matuschewski

Tag der mündlichen Prüfung: 4. Dezember 2015

Table of contents

1. Abstract

Memory B cells and antibodies are major mediators of protective immune responses yet the mechanisms of their induction, maintenance and memory reactivation are poorly understood. Studies of secondary immunizations or recurrent infection courses, e.g. for tetanus and influenza, are abundantly available, while comparable detailed data with respect to primary immunizations in humans are so far lacking. Furthermore, as recall responses require memory B cell (mBC) maintenance, consequently, the question arises how and where this B cell memory is maintained.

To address this, in the first part of this study the characteristics of a human primary and secondary immune response to Keyhole Limpet Hemocyanin (KLH) was comprehensively examined, as an example for the principle plasma cell and mBC induction and reactivation of the latter. In the second part of this thesis mBC maintenance was investigated by a systematic analysis of mBC presence, frequency and phenotype within different lymphoid organs.

Primary parenteral KLH immunization resulted in a pronounced IgA response on both the serum and cellular level whereby discordances between both were detected, suggesting different restrictions for the humoral and B cellular layer. The unexpected simultaneous presence of low and highly mutated circulating KLH-specific (KLH^{spec}) plasmablasts (PB) 2-3 weeks after vaccination suggested not only the recruitment of naïve B cells but also of presumably cross-reactive mBC. Further detailed analysis of the clonal composition of blood KLH^{spec} primary PB, steady state mBC and PB 7 days upon secondary immunization revealed only little overlap of these three B cell repertoires suggesting that the respective progenitor cells underlay distinct recruitment and selection mechanisms.

With respect to the organ distribution of human mBC, the spleen was identified to harbor most mBC followed by tonsils, bone marrow (BM) and circulating mBC within the blood. All mBC pools exhibited a largely comparable phenotype. Yet interestingly, we found only tonsillar mBC to express CD69, while they rested in terms of proliferation comparably to mBC from the other tissues. This suggests that tonsillar mBC could constitute a tissue resident population. In line, tonsillectomy did not affect the circulating mBC pool.

The observations described allow insights into hitherto unknown potential mechanisms behind primary immune responses, i.e. prominent IgA induction by parenteral challenge and inclusion of cross-reactive mBC. The so far unclear regulatory players involved deserve future investigation as such knowledge may be crucial for therapeutic interventions in immune system disorders.

Furthermore, we found phenotypic similar mBC to distribute between lymphoid organs and to continuously recirculate in peripheral blood indicative of their potential permanent screening activities which differs strikingly to the resident plasma cells in the BM. Thus, the results suggest that quiescent human mBC do not require dedicated niches for their principle survival but rather represent a dynamic repertoire.

2. Zusammenfassung

Gedächtnis-B-Zellen und Plasmazellen sind essentielle Komponenten der protektiven Immunität. Die Mechanismen ihrer Induktion, ihres Überlebens und der Gedächtnis-B-Zellreaktivierung sind allerding bisher nur unvollständig verstanden. Detaillierte Untersuchungen zu sekundären Immunantworten oder Immunantworten zu wiederkehrenden Infektionen, wie zum Beispiel zu Tetanus oder Influenza Infektionen, gibt es viele im Menschen. Jedoch gibt es keine vergleichbar detaillierten Daten zu primären Immunantworten. Weiterhin setzen sekundäre B-Zellimmunantworten das Vorhandensein von Gedächtnis-B-Zellen voraus, woraus sich die logische Frage ergibt, wo und wie diese Zellen in der Zwischenzeit überleben.

Um unser Wissen diesbezüglich zu erweitern, wurden im ersten Teil der vorliegenden Arbeit Charakteristika von Primär- und Sekundärimmunantworten nach Immunisierung mit Keyhole Limpet Hemocyanin (KLH) untersucht. Im zweiten Teil dieser Arbeit wurden die Überlebensbedingungen der Gedächtnis-B-Zellen genauer untersucht. Dazu wurden in einem systematischen Ansatz die Frequenzen der Gedächtnis-B-Zellen sowie deren Phänotyp in verschiedenen lymphatischen Geweben erhoben.

Die primäre parenterale KLH Immunisierung führte zu einer deutlichen IgA Induktion auf serologischer und zellulärer Ebene. Beim Vergleich beider Kompartimente ergaben sich jedoch quantitative Unterschiede der IgG zu IgA Verhältnisse, was auf eine unterschiedliche Regulierung hinweist. Die unerwartete Präsenz von hochmutierten Plasmablasten parallel zu un- bis wenig mutierten Plasmablasten 2-3 Wochen nach der primären Immunisierung deutete darauf hin, dass in diese Immunantwort nicht nur naive B-Zellen rekrutiert wurden, sondern auch Gedächtnis-B-Zellen, die wahrscheinlich mit dem KLH kreuzreagierten. Weiterhin ergab die Analyse der klonalen Verwandtschaften von primären Plasmablasten, Gedächtnis-B-Zellen und den Plasmablasten induziert durch die Sekundärimmunisierung, dass es nur wenige Überschneidungen gab. Dies deutet darauf hin, dass die Zellen, bzw. deren Vorläufer bei Primär- und Sekundärimmunisierung individuellen Rekrutierungs- und Selektionsmechanismen ausgesetzt waren.

Die Untersuchungen der Gedächtnis-B-Zellverteilung in verschiedenen lymphatischen Geweben ergab, dass die meisten in der Milz, gefolgt von Tonsillen und Knochenmark zu finden waren und der zirkulierende Gedächtnis-B-Zellpool nur einen

kleinen Teil der Gesamtmenge ausmachte. Trotz des unterschiedlichen Vorkommens von Gedächtnis-B-Zellen fanden sich nur wenige phänotypische Unterschiede. Einer davon war die CD69 Expression auf tonsillären Gedächtnis-B-Zellen, die sich jedoch nicht teilten. Diese Kombination deutet darauf hin, dass tonsilläre Gedächtnis-B-Zellen tatsächlich sessil sein könnten und somit nicht am rezirkulierenden Gedächtnis-B-Zellpool teilhaben würden. Konsistent mit dieser Schlussfolgerung ist auch die Beobachtung, dass Tonsillektomien keinen quantitativen Einfluss auf den zirkulierenden Gedächtnis-B-Zellpool hatten.

Die in dieser Arbeit erhaltenen Ergebnisse bieten neue Erkenntnisse über bisher unbeschriebene Mechanismen von humanen primären Immunantworten. Zum einen wurde demonstriert, dass parenterale Impfungen IgA Antikörper induzieren können. Zum anderen scheinen an solchen primären Immunantworten kreuzreaktive Gedächtnis-B-Zellen teilzunehmen. Es bleibt zu klären, wie die Reaktivierung dieser Gedächtnis-B-Zellen reguliert ist. Dieses Wissen ist durchaus für die Therapie und das Verständnis von Erkrankungen des Immunsystems, wie z.B. von Autoimmunität, von Bedeutung.

Des Weiteren zeigen die Ergebnisse, dass sich phänotypisch weitgehend gleiche Gedächtnis-B-Zellen in unterschiedlicher Quantität in verschiedenen lymphatischen Geweben verteilen sowie auch kontinuierlich im Blut zirkulieren. Dieses patrouillierende Verhalten der Gedächtnis-B-Zellen ist ein deutlicher Unterschied zu den Nischen-abhängigen Plasmazellen. Die Ergebnisse deuten weitestgehend darauf hin, dass Gedächtnis-B-Zellen nicht auf derartige Nischen angewiesen sind und ein dynamisches Repertoire darstellen.

3. Introduction

The principle of immunity has already been described 430 BC by Thucydides. It arose from the original observation that when a person suffered from a disease once, such as the plaque for example, this person was in principle never attacked a second time or if, only suffered a mild course, even though that person still had contact to other infectious plaque patients (1). Thus, the person exhibited a certain non-susceptibility to the disease.

We now know that the key to this perceivable immunity is the primary infection itself and the survival of it, as our immune system fights off the pathogen and establishes an immunologic memory. We have even learned to use that principle in a controlled safe setting, i.e. vaccination. The vaccinee is usually inoculated with an attenuated pathogen or a detoxified or inactivated protein to which the immune system reacts, without the risk of permanent damages, and establishes immunological memory. This memory then protects the individual during future infections from the symptoms or a potentially fatal result. Vaccines led to the eradication of some widespread diseases, e.g. smallpox or tetanus, but the successful development of new vaccines proves difficult as often the induction of protective serum antibodies is inefficient. Examples of such cases are infectious diseases such as influenza or HIV or immune responses in immunocompromised individuals (2, 3). Although we have an overall idea of underlying mechanisms and processes of immune responses, many aspects of the induction, maintenance and reactivation of human immunological memory remain unclear. Yet such knowledge is of importance for the design of new vaccines and disease intervention strategies.

3.1 The vertebrate immune system

The immune system, consisting of organs, tissues, cellular and soluble components, is able to rapidly sense and respond to a vast array of invading pathogens and substances but can also eliminate own degenerated cells to maintain the bodies integrity. Thereby its arsenal contains on the one hand cells, e.g. dendritic cells (DC), macrophages, granulocytes and natural killer cells, and receptors (pattern recognition receptors (PRR)) that belong to the innate immune system, which recognize a de-

fined and restricted amount of pathogen patterns (pathogen-associated molecular patterns (PAMP)). This arm of the immune system triggers an immediate response to pathogens like bacteria, fungi, parasites and viruses. This response may already lead to elimination of the pathogen but moreover yields cytokine secretion and presentation of peptides from the pathogen's protein antigens in major histocompatibility complex (MHC) molecules by specialized phagocytes, collectively known as antigen-presenting cells, which include DC. This step marks the critical interface between the innate and the adaptive immune system, the latter which constitutes the other arm of the immune system.

The adaptive immune system consists of B- and T lymphocytes (B and T cells) carrying highly diverse specialized antigen recognition receptors on their cell surfaces. These receptors are capable of recognizing an almost unlimited variety of antigens, but in a specific fashion. Thereby, thymus-dependent cells (T cells) carry the T cell receptor (TCR) that recognizes the complex of a peptide:MHC molecule and confer classically either cellular immunity, i.e. they mount responses to intracellular pathogens or orchestrate a subsequent immune response.

The specialized antigen receptor of B cells (originally from Bursa fabricii (birds) derived cells) is the B cell receptor (BCR). It directly recognizes unprocessed extracellular epitopes that in concert with other signals activate the B cells. This response is referred to as humoral immunity. The B cells can either terminally differentiate into plasma cells (PC) which secrete the BCR in its soluble form, known as antibodies, or into memory B cells (mBC) or other effector B cells.

An important feature and hallmark of the adaptive immune system is its ability to adapt its measures of recognizing or responding towards a pathogen, e.g. the B and T cells can adjust cytokine secretion patterns, lower their activation thresholds or, exclusive to B cells, increase their antigen receptor affinity and alter its effector function. Finally, generation of immunological memory is also a distinctive feature of the adaptive immune system enabling a faster and stronger response upon pathogen re-encounter as well as establishment of protective antibody titers which potentially directly counteract the effective infection of the host at all.

These natural properties of the adaptive immune system are the underlying mechanisms to long-term protection, which is utilized by vaccination strategies. However, most successful vaccines have been found empirically with no or only little immunological insight and often confer protection by induction of humoral responses. Re-

flected in our current failure to develop new vaccines and treatments to immunodeficiencies and autoimmune diseases, gaining a deeper understanding of the formation and maintenance of immunological memory is clearly of importance.

3.2 B cells and the humoral immune response

3.2.1 The B cell receptor

Each B cell carries a unique membrane bound BCR that is in its secreted form referred to as antibody or often also simply as immunoglobulin (Ig). In humans, this Ig is a tetrameric molecule consisting of two identical Ig heavy chains (IgH) and two identical Ig light chains (IgL). Both, IgH and IgL, consist of several homologous domains of approximately 110 amino acids each. IgL consist of two, IgH of four to five of such globular Ig domains, depending on the isotype for the latter. The domains of the IgH and IgL chains are covalently linked by disulfide bonds which together with non-covalent interactions lead to the typical Y-shape three dimensional structure of an antibody (Figure 3-1). At the aminoterminal domain both chains possess a variable region and the adjacent part stretching towards the carboxyterminal end constitutes the constant region.

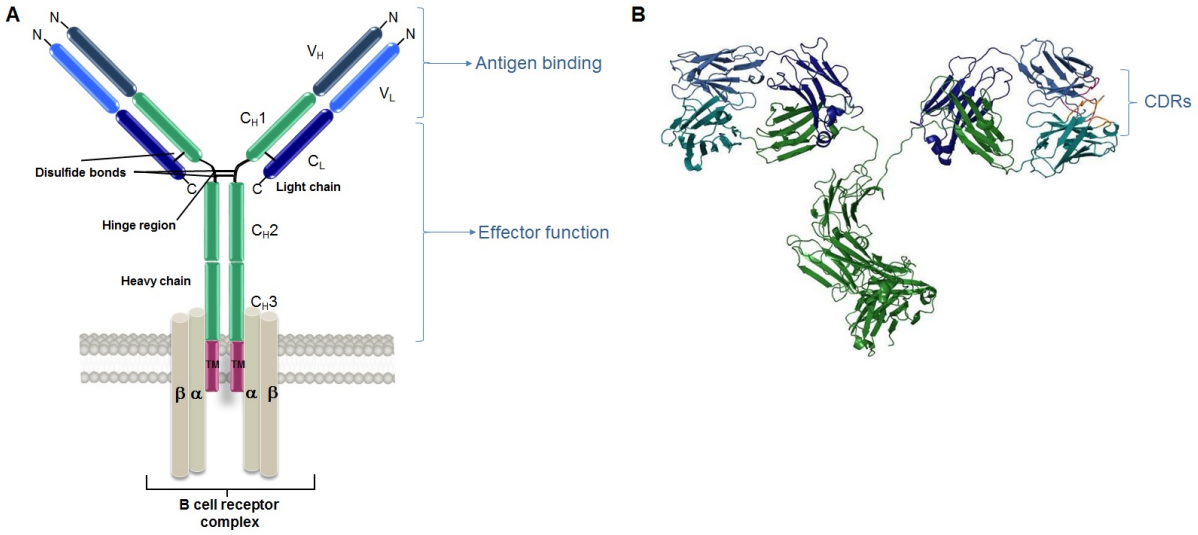

Figure 3-1 Schematic structure of a BCR molecule.
A BCR complex, i.e. membrane bound BCR with its accessory molecules Igα and Igβ. Indicated are the variable heavy (V_H) and variable light (V_L) regions as well as the constant light (C_L) and constant heavy (C_H) regions, for the latter subdivided in domains 1-3, as can be found e.g. in an IgG. TM: transmembrane domain. **B** Three dimensional structure of a secreted Ig. Indicated in orange, pink and purple are the loops comprising the complementary determining regions (CDR) on the right side. The 3D structure has been modified from the pdb file 1igt (www.pdb.org).

Functionally, the variable regions of the IgH and IgL contain the antigen binding region. Structurally, they consist of four framework regions (FWR1-4), which are β-folds providing the backbone and maintain the Ig's characteristic barrel like shape. These are intervened in a non-consecutive fashion by three complementary determining regions (CDR), termed CDR1, CDR2 and CDR3. In the tertiary structure, the CDR form loops that stick out of the barrel and constitute the antigen-binding site (Figure 3-1 B). Contact of the Ig to the antigen occurs through non-covalent interactions with complementary structures on the antigen, termed epitopes.

The constant regions, generally denoted by greek letters, of the IgL chains are termed κ and λ. A functional difference between them is currently not known. For the IgH chain, there are five different main constant region classes encoded by the μ, δ, γ, α and ε gene segments, resulting in IgM, IgD, IgG, IgA and IgE Ig isotypes, respectively (4). Further distinction of isotype subclasses exists for IgG, i.e. IgG1 to IgG4, and for IgA, namely IgA1 and IgA2. For the membrane bound form of the Ig, a transmembrane domain anchors the BCR into the cell membrane leaving a short cytoplasmic tail. For signal transmission, the accessory molecules Igα and Igβ are required which all together form the BCR complex.

This complex has two major functions. Firstly, signal transduction upon appropriate antigenic contact. This leads to different outcomes regarding the B cells' survival, proliferation and differentiation, depending on the subsequent signals and interactions with other cells. Secondly, antigen-BCR binding leads to internalization of the BCR-antigen-complex for subsequent antigen processing and presentation of peptides in MHC class II molecules. This is crucial for communication with other cells which potentially provide survival signals during immune responses.

In its soluble form, the differences of the IgH isotype classes with regard to their different composition, biological properties, location and their resulting mode of action, which is referred to as effector function, become of major functional importance. In short, antibodies can neutralize the pathogen, mark it for degradation by phagocytosis (opsonization) or complement, or activate other effector cells, inducing more or less inflammatory responses in consequence. While all isotypes can be found secreted as monomers, IgM and IgA can for pentamers and dimers, respectively.

3.2.2 Generation of the primary B cell repertoire diversity

The variable regions of the expressed BCR are not present as such in the germ line (5). Instead, the BCR is assembled during B cell development in a series from site-specific recombination events termed V(D)J recombination (illustrated in Figure 3-2), taking place in the bone marrow (BM) in human adults. This somatic rearrangement process is the central feature of the B (and T) cells' ability to generate a highly diverse set of antigen receptors.

The human IGH locus is located on chromosome 14 (14q32.33) and comprises multigene families of variable heavy (V_H), diversity (D) and joining heavy (J_H) segments (6, 7). The V_H gene cluster consists of 123 V_H segments of which 44 are classified as functional and can theoretically be expressed (8). These V_H segments were subdivided into seven distinct families based on their sequence homology. The J_H gene segment cluster contains six functional J_H segments (9) and the D gene segment cluster contains 27 functional segments (10). The IGH C_H locus comprises 11 genes of which two are pseudogenes (8). The human C_H genes for secretory Ig forms are composed of three (γ and α) or four (μ and ε) exons.

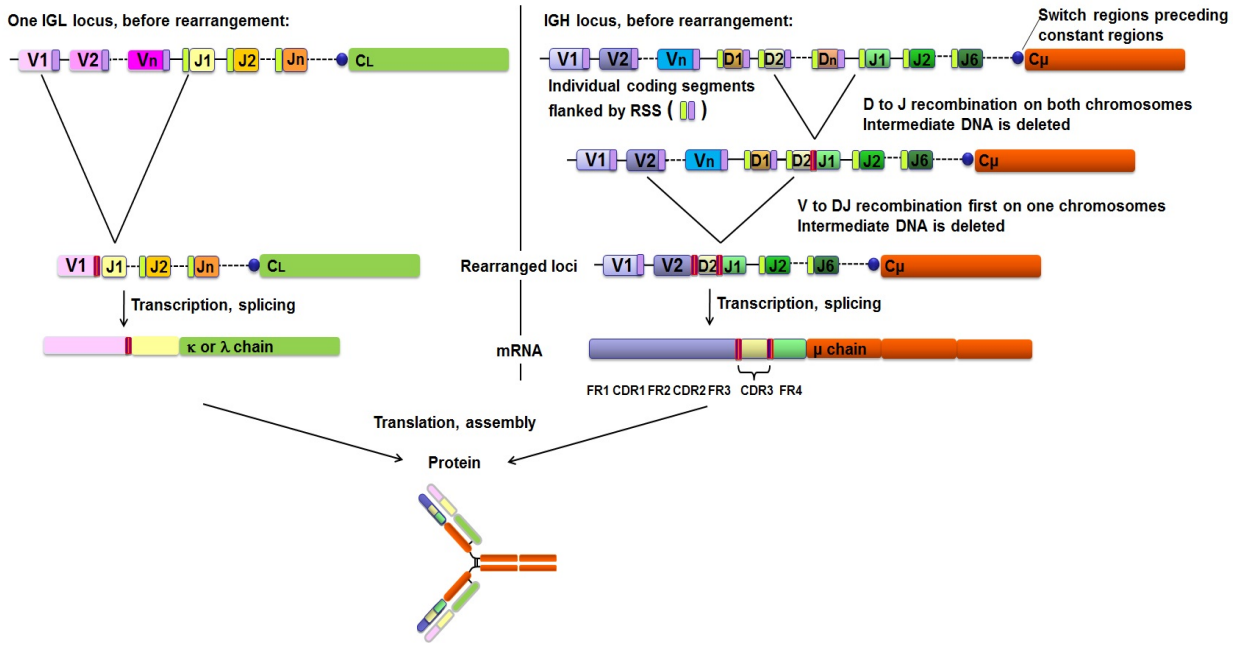

Figure 3-2 B cell Ig chain gene recombination and assembly.
Schematic illustration of the process of V(D)J recombination for IgL (left) and IgH (right) chain. Critical for the joining process during V(D)J recombination are the recombination signal sequences (RSS) which are directly adjacent to every segment's 3' and/or 5' coding region. RSS consist of a highly conserved heptamer (CACAGTG) and a less conserved nonamer (ACAAAAACC), interspersed with a non-conserved region known as the spacer, which is either 12 or 23 nucleotides long. During the recombination process, only gene segments flanked by an RSS with a 12-base pair spacer can be joined to one flanked by a 23 base pair spacer RSS, ensuring that V(D)J recombination is restricted to events that are biologically productive.

The hydrophobic transmembrane and short cytoplasmic segments for the BCR are encoded by one (α) or two (others) exons. Expression of either the secretory or membrane Ig form is controlled by alternative splicing. The V_H and C_H loci are physically linked on the chromosome in the order of 5'-V_H-D_H-J_H-C_H-3'.

Human κ and λ chain loci are located at 2p11.2 and 22q11.2, respectively, and comprise 40 and 30 Vκ and Vλ segments, respectively, and 5 Jκ and 4 Jλ, respectively and one C_L segment each (11, 12).

The underlying processes of V(D)J recombination and the factors involved have been extensively reviewed elsewhere (13-16). To shortly summarize, B cells develop from hematopoietic stem cells through well-defined stages. For the IgH and IgL chain together three major developmental stages were defined. In the first stage, lymphoid progenitor cells rearrange a D to a J_H segment, on both loci, to become a pro B cell followed by a second rearrangement joining an upstream V_H segment to the assembled D-J_H region, only on one locus first. If this is productive, then the second locus is not further rearranged. Otherwise, rearrangement on the other locus occurs which however silences the expression of the first locus. The principle that B cells express only one variable region combination is called allelic exclusion (17). The productive V_HDJ_H rearrangement is joined to a μ chain and expressed on the B cell precursor's surface as *pre*BCR. If this rearrangement is functional, the B cell precursor enters the next phase, i.e. pre-B cell stage, in which the cell divides a few times, exits the cell cycle and subsequently rearranges the IGL locus according to the same principles as for the IGH chain with the exception that no D segments exist (Figure 3-2). Thereby, the κ gene locus is rearranged up to several times first and if finally non-productive, the λ chain locus is rearranged leading eventually to expression of a functional BCR or otherwise to termination of the cell. Again, the B cell expresses only one type of IgL chain, termed isotype exclusion.

The pure combinatorial diversity from this process accounts theoretically for $2.3x10^6$ different BCR receptors. However, in addition to this diversity, during the V(D)J recombination itself the diversity is further increased by joining the gene segments imprecisely including addition of non-templated and palindromic nucleotides to the open DNA ends. Therefore, this junctional diversity is located and actually builds the so termed CDR3 regions which are the most variable of all CDR regions and are also considered as the major determinants of the specific interaction between BCR and

antigen. Furthermore, each single BCR or antibody can be uniquely identified by its CDR3 sequences, largely defining a B cell clone.

At the end of this developmental process stands an immature B cell. At this point, B cells with an auto-reactive BCR are largely negatively selected by either undergoing apoptosis (clonal deletion) (18), becoming unresponsive (anergic) (19) or re-entering into the rearrangement process (receptor editing) (20). B cells that pass this so termed central tolerance checkpoint, in mice approximately 10% of the generated clones (21), leave the BM and migrate to the spleen where they undergo further selection and maturation (22) into functional naïve B cells that subsequently recirculate and screen the periphery for pathogens/antigens.

3.2.3 Primary humoral response

A primary humoral immune response is mounted on the occasion the eliciting antigen is encountered for the first time (illustrated in Figure 3-3 B). B cell responses are classified as either T cell-dependent (TD) or T cell-independent (TI) largely determined by the nature of the antigen. TD response-eliciting antigens are usually proteins which engage the BCR in a highly specific fashion and which can be presented in MHC class II molecules. For initiation of division and differentiation of the specific B cells additional signals are required and these include the interaction of the specific B cells with T cells. TD responses generally result in generation of memory. Such responses and will be elaborated in this section.

Humoral responses to TI antigens, as intended by the name, do not require T cell help for their induction. Such antigens can be either of a mitogenic nature, e.g. CpG or lipopolysaccharide, which cause a polyclonal activation of B cells, i.e. independent of the BCR specificities. Or TI antigens can be large polymeric or aggregated proteins, or capsular polysaccharides that cross-link specific BCR and thus activate the B cells without requirement of additional signals. TI responses generally do not generate memory and are beyond the scope of this study.

At the beginning of an adaptive TD response stands the activation of the innate immune system. Most pathogens carry PAMP which can be bound by PRR on innate immune cells. Of importance for initiation of adaptive immune responses are the uptake and presentation of the pathogen by antigen-presenting cells, e.g. DC. Specifically DC carry a vast array of PRR enabling them to sense a wide range of

pathogens. In such a case, the activated DC take up the pathogen, process it and migrate to draining lymph nodes (LN) or spleen. Here they seek contact with T cells and present peptides of the pathogen via their MHC class II molecules (23). In primary cellular responses the process of antigen presentation is predominantly, if not exclusively, mediated through DC. Naïve $CD4^{pos}$ T cells with a specific TCR can recognize this peptide:MHC class II complex and become activated, proliferate and differentiate into $CD4^{pos}$ effector T cells. At the same time, recirculating naïve B cells screen the periphery, including secondary lymphoid organs, for matching antigens. Eventually they encounter also the pathogen or pathogen subunits. Binding of their specific BCR causes activation of the respective cells but also antigen uptake. The ingested antigen is then processed and presented as peptide:MHC class II complexes on their surface. Subsequent complete activation of these B cells does only occur if they encounter an activated cognate $CD4^{pos}$ effector T cell, usually happening at the T cell:B cell border in a secondary lymphoid organ (24, 25) to which the B cells and T cells locate in a chemokine-dependent manner (26). Most important interactions here include engagement of CD40 on B cells by CD40L, presented by the activated T cells, interaction of the B cells' peptide:MHC class II complex with the TCR and CD4, provision of CD80 and CD86 by the B cells to the T cells (27), inducible costimulator (ICOS)- inducible costimulator ligand (ICOSL) interaction and secretion of IL4 and IL21 by the T cells (28-32), collectively referred to as co-stimulatory signals. The completely activated B cells proliferate vigorously. They then either differentiate into extra-follicular PC, secreting unmutated and low affinity, mostly IgM, antibodies which can be detected in the serum (Figure 3-3 A and B). These PC are generated early during primary immune responses, i.e. after a couple of days (33), and are typically short-lived and of a non-migratory nature (34, 35).

Alternatively, the activated B cells migrate to a B cell follicle and become germinal centre (GC) founder B cells (33). These keep dividing subsequently generating a GC while they push the remaining non-dividing naïve B cells aside which then form the mantle zone. Plasmablasts (PB)/PC arising from the GC reaction are the source of the later detectable, higher affine class-switched antibodies.

Albeit B cells and T cells recognize quite distinct structures of the same molecule derived from a pathogen, the mechanism that only T and B cells with a specific receptor become activated and expanded is commonly referred to as clonal selection. Thus, from the existing receptor repertoires, which for human B cells could theoretically

comprise up to 10^{11} individual clones (36), only a small fraction of cells/receptors is engaged by any antigen. Studies from primary human responses are not available in this regard, but studies investigating secondary antigen-specific B cell repertoires, e.g. BCR specific to tetanus toxoid (TT), estimated these specific repertoires to range between 30- 200 clones (37-39).

3.2.4 The GC reaction – antigen-dependent B cell repertoire diversification

Antibodies produced initially in a systemic TD primary immune response are of low affinity and mostly of the IgM isotype, while antibodies produced later during that response are of higher affinity and comprise mainly switched isotypes, i.e. IgG antibodies (40) (Figure 3-3). The molecular analysis of IgL and IgH chains of B cells from mice undergoing TD immunization has further shown that in parallel somatic point mutations are introduced into the rearranged variable regions (41-47), responsible for the affinity increase. The underlying mechanism of these changes is the second major mechanism contributing to the B cell Ig repertoire's diversity, termed affinity maturation and occurs in a GC.

GC are compartmentalized into two zones: a dark zone (DZ) and a light zone (LZ) (48, 49) (illustrated in Figure 3-3 B). The dark zone consists almost exclusively of densely-packed proliferating B cells, named centroblasts (CB). Human CB diversify their Ig variable genes by somatic hypermutation (SHM), a process that modifies the Ig variable regions by introducing mostly single nucleotide exchanges but also small deletions and duplications (50, 51). The process of affinity maturation is catalyzed by the enzyme activation induced deaminase (AID) targeting the rearranged variable and constant Ig loci. This enzyme is critical to SHM but also to class switch recombination (CSR) (52).

Basically, the AID removes the amino group from a cytosine transforming it into a uracil, thereby creating a DNA mismatch. In the GC environment different complex (error prone) DNA repair mechanisms are then initiated leading either to a mutation or repair of the DNA lesion, which has been reviewed elsewhere (53-57).

As an indicator of T-B cell interactions, it has been shown that SHM are specifically targeted to mutation hotspots, e.g. the sequence motives RGYW/WRCY (R= purine, Y= pyrimidine and W= A/T) (53). Furthermore, SHM introduced during GC reactions seem to have a non-random pattern, with replacement (R) mutations found to be

overrepresented within the CDR and underrepresented within the FWR whereas the opposite is true for silent (S) mutations. This property has been assigned to the selection processes specifically occurring in the GC environment. Yet, the pure introduced SHM in the Ig variable regions only randomly change the affinity of the BCR and pattern of mutations.

An adjacent stringent selection process ensures that only those B cells expressing the highest affinity BCR survive. This occurs within the LZ to which CB migrate and give rise to smaller, non-dividing centrocytes (CC) which are then intermingled within a mesh of follicular DC (FDC), macrophages and few T follicular helper cells (TFH). Survival of CC is dependent on interaction with these cells (58). In short, FDC present antigen in the form of immune complexes on their surfaces (59). The CC re-expresses the diversified BCR and if the affinity of it is appropriate in a competitive fashion it gets access to the antigen, binds and internalizes it. The antigen is then again processed and presented in peptide:MHC class II complexes. The CC then competes for TFH survival signals. Current models suggest that the limited number of TFH in the GC creates a highly competitive environment with only the highest affinity B cells receiving sufficient T cell help (60). In consequence, the modified BCR can be positively selected for improved binding. CC producing an unfavorable BCR undergo apoptosis.

A further modification of the BCR within the LZ is the CSR by which B cells irreversibly switch their Ig isotype class expression, initially from IgM and IgD to other classes. This process depends on CD40-CD40L ligation as well as cytokines determining the resulting isotype (61).

Positively selected B cells either migrate back into the DZ to undergo further rounds of affinity maturation (26), leading to increasingly higher affinity BCR over time (43, 62). Or, B cells leave the GC. B cells emigrating from the GC reaction can either become mBC or PB and eventually PC. The mechanisms contributing to the B cell's fate decision and the time point of their fate determination are incompletely understood.

Yet, it is widely accepted that post-GC PB migrate via the blood to the BM. Antigen-specific primary PB were found to peak in blood not before day 10 upon primary immunization (63). In the BM, they presumably compete with resident long-lived PC for hypothetical survival niches, to become resident long-lived PC themselves. As long-lived PC they secrete protective antibodies over decades (64-68). In contrast, mBC

are functionally inactive, mostly quiescent, long-lived cells (69) that in part at least circulate through the blood and lymph (70).

After resolution of the response the immune system exhibits an altered state of its adaptive immune cells specific for the challenging antigen, known as memory. Thus, immunological memory is the persistence of resting memory T cell subsets, resting affinity maturated mBC and long-lived PC.

3.2.5 The secondary humoral response

B cell re-encounter with an anamnestic TD antigen triggers a secondary antibody response. Generally, in contrast to the primary response, secondary immune responses exhibit a faster onset, are of higher magnitude and more sophisticated regarding the array of effector functions (summary see Table 3-1 and Figure 3-3). This is a direct consequence of the generation of mBC and memory T cells during primary antigenic exposure. For B cells specifically, there are qualitative differences in the nature of the antibodies produced, for they are now predominantly of the IgG or IgA isotype class, depending on their site of induction, and of higher affinity than those detected during primary immunization. Moreover, during secondary responses, specific mBC are capable to present antigen peptides efficiently to T cells (71-73) inducing their activation whereas naïve B cells do not appear to possess that property.

Table 3-1 Features of primary and secondary humoral responses (adapted from Ademokun and Dunn Walters (74) and Janeway's immunobiology (75)).

Feature	Primary response	Secondary response
Antigen presentation	Mainly non-B cells, rather DC	mBC increasingly involved
Responding B cell	Naïve	Memory
Frequency of antigen-specific B cells	$1:10^4 – 1:10^5$	$1:10^2$-$1:10^3$
Inducing antigens	All antigens (TI and TD)	Protein antigens
Antigen dose required	Relatively high dose; optimally with adjuvant	Relatively low doses, works without adjuvant
Lag phase	4-7 days	2-5 days
SHM	None to low	High
Antibody isotype class	Predominantly IgM in the early response, later switched isotypes	Predominantly IgG or IgA (depending on site of induction)
Antibody affinity	Low	High

Consequently, mBC rapidly generate new antibody-secreting PB (38, 76), which peak in peripheral blood with a striking consistency independent of the eliciting antigen or pathogen between days 6-8 (77). These PB likely again migrate to the BM extruding some of the resident long-lived PC (78). Thus recall responses should lead to a continuous replenishment and improvement of the protective long-lived PC pool.

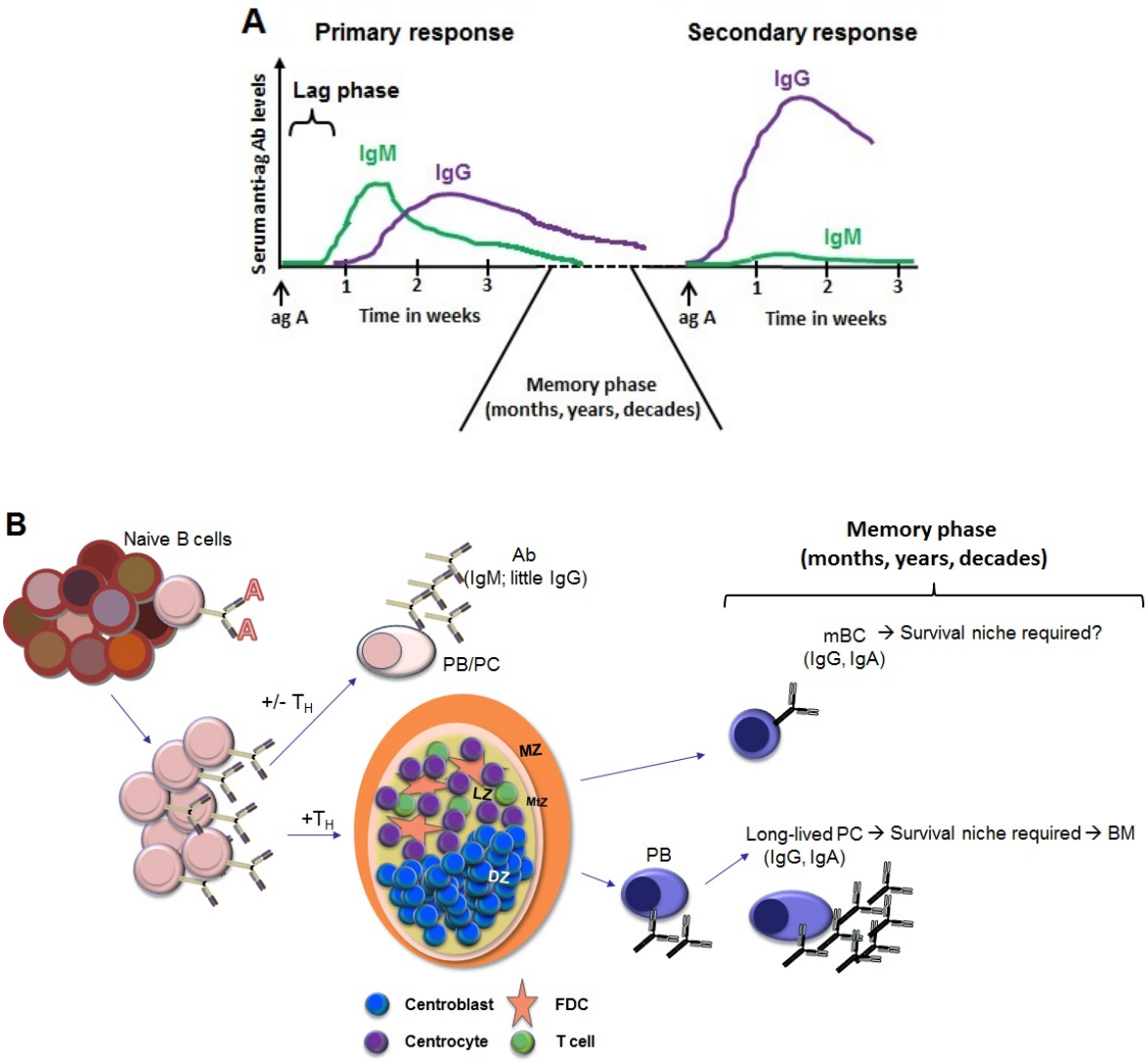

Figure 3-3 Schematic overview of a primary and secondary adaptive humoral response.
A Left: primary response. After an initial lag phase (time period between antigen (ag A) exposure and appearance of specific serum antibodies), specific serum antibodies (Ab) appear, which are predominantly of the IgM isotype. In the later phase of the primary response class-switched serum antibodies appear (mostly IgG in a systemic parenteral response). Right: secondary response. After a very short lag phase, a switched isotype dominated and heightened antibody serum response is measurable.
B Illustration of the serum antibody-underlying primary B cell response. To antigen A-specific naïve B cells become activated, proliferate and their descendants either generate antibody-secreting PB/PC which are the source of the early IgM serum antibodies. Alternatively, some B cells give rise to a GC reaction, which gives rise to affinity maturated and class-switched antibody secreting PB/PC and mBC. The PB presumably migrate to their protected niche (e.g. BM) to become long-lived PC. The life style and whereabouts of mBC during the memory phase remain unclear. Yet, upon secondary "ag A" contact, mBC mount a memory response which is the reason for the under **A** illustrated secondary response antibody kinetics. DZ: dark zone. LZ: light zone. MZ: Marginal zone. MtZ: mantle zone. FDC: follicular dendritic cell. T_H: T cell help.

The role of GC, whether they are re-initiated and the impact and requirement for T cell help in secondary responses is however unclear. With regard to the latter, mBC stimulated *in vitro* can generate PB independent of T cell help (79) whereas T cell help in fact suppresses the differentiation of mBC into PB in a CD40L dependent manner (80, 81), keeping them in a blastic state which potentially could make them prone to become GC founder cells again.

It remains currently unclear whether mBC or their descendants re-enter GC, however the antigen-specific mBC pool appears to repeatedly improve as determined by an increasing frequency of SHM from primary to secondary to tertiary responses (62, 82, 83). But this concept is not undisputed (84).

Especially for humans, these aspects remains unknown. Although B cell memory responses were intensively analyzed (38, 39, 77, 85), the identity and properties of the antigen-specific B cell repertoire before re-immunization has not been studied. The dimensions to which the effector B cell repertoire recalls sequences already employed during primary immunization and which fraction of the available specific repertoire is represented in peripheral blood at all is unknown. In line, it is not possible to draw conclusions on diversification and selection processes if only the memory response is analyzed. Therefore, detailed studies of primary together with secondary responses, focusing on antigen-specific B cells, would potentially deliver such insights but are lacking in humans so far.

3.2.6 Immunological B cell memory and its maintenance

Immunological memory is the feature of the adaptive immune system to respond more rapidly and effectively to already encountered pathogens. In essence immunological memory refers to the altered state of the immune system that as a net result provides improved passive and active immune protection.

With regard to the mediating lymphocyte subsets the altered state includes a) higher frequency of antigen-specific memory T and B cell subsets in contrast to low frequency of antigen-specific naïve cells, b) the memory cells are antigen-experienced and thus functionally superior compared to naïve cells, c) the memory cells exhibit extended life spans and d) they exhibit a lower activation threshold compared to the naïve lymphocytes.

Human B cell memory consist of two major components: reactive mBC and long-lived PC (Figure 3-3 B). Long-lived PC preferentially reside in niches in the BM (65) but were also identified in spleen (86) and tonsil (87) and appear to depend on survival signals delivered from stromal cells and eosinophils (88, 89). Outside of immunization or infection PB/PC are only rarely encountered in peripheral blood. In fact, long-lived PC are thought to be sentenced to death once they are extruded from their niche.

In contrast, potential survival niches for mBC and the role of certain organs and factors in mBC maintenance and functionality remain largely unknown. Yet, their lifestyle surely differs to that from long-lived PC which is already evident by the fact that their major effector function lies in their reactivation and that they can be found circulating in blood without immunization. Specifically, in humans mBC constitute up to 40% of peripheral blood total B cells (90, 91). With regard to their tissue localization, based on certain observations, eligible candidate lymphoid tissues, that may provide niche conditions and soluble survival factors for mBC, are the BM, mucosal tissues, tonsil and the spleen.

The BM already provides a unique survival niche for long-lived PC but also for reactive memory T cells (92-94) and thus it is only logic to assume that it also may provide a niche to mBC. However, data on mBC in the BM are scarce. Solely, the presence of mature IgM^{pos} B cells with mutated BCR gene rearrangements has been described (95, 96) but more detailed data on their proportion and characteristics are unavailable.

In gut-associated lymphatic tissues (GALT) $CD27^{pos}$ B cells were found under the dome epithelium of Peyer's patches (97) and in the inner wall of the subcapsular sinus of mesenteric lymph nodes (98). On B cells, moderate CD27 expression (i.e. $CD27^{pos}$) has been proven useful to identify quiescent B cells that carry somatically mutated Ig gene rearrangements (91, 99), which is a hallmark of antigen-experienced B cells as well as $CD27^{pos}$ B cells resemble mBC in functional terms (reviewed in (100)). However, further studies of the $CD27^{pos}$ GALT B cells are also not available.

With regard to the tonsil, the presence and functionality of reactive mBC have been described (71, 80, 101-103). Further their location has been determined to be mainly the mucosal crypt epithelium. But again, more detailed studies of the tonsillar mBC pool are lacking.

Finally, the spleen has been considered as a major reservoir for mBC and thus may also provide a niche to them as supported by the following observations. Firstly,

$CD27^{pos}$ mBC are present in the spleen (99), usually organized around B cell follicles (104-107). Secondly, splenectomy greatly diminishes peripheral mBC numbers of both pre-switch mBC and post-switch mBC (108-110). Moreover, mBC generated during TD responses (vaccinia virus) were shown to persist in the spleen even 30 years after the last antigen exposure (70). Interestingly, that study also identified vaccinia virus-specific mBC circulating in peripheral blood, albeit at smaller numbers.

The fact that mBC can be found in peripheral blood at the same time as they are spread out in different lymphoid tissues and organs suggests their recirculation. Yet, it remains to be determined, whether a certain proportion of them is sessile once they have reached their favored location or niche, waiting to become reactivated, as would be suggested by experiments conducted by Gowans and Uhr (111).
To gain insight into these aspects, a comprehensive mapping, including enumeration and phenotyping of mBC within different lymphoid organs would be a starting point and has so far not been performed, neither in mice nor in humans. Yet, gaining more knowledge about mBC lifestyle is of obvious interest not only for enhancing our understanding of immune memory but therapeutically more important also for autoimmune conditions and other long lasting immunological disorders, as when autoantigen-specific or allergen-specific B cells establish a mBC pool their long-term survival and reactivation characteristics can become of dramatic pathogenic importance.

3.3 Aims and objectives

B cell memory is an essential component of immunologic memory. A thorough understanding of it will assist the development of new vaccination strategies but also to improve current therapeutic strategies of immunological disorders. The medical need became apparent by our recent limitations to provide efficient vaccinations to current pandemics (Ebola, HIV), due to failure of induction of protective antibody titers, or inducing remission of autoimmune diseases as the long-term efficacy of current therapies is impeded by pathogenic immune memory maintenance and reactivation. Thus, we lack knowledge of the molecular and cellular mechanisms underlying primary B cell responses in humans during which memory is established. Furthermore, the life style and maintenance of human B cell memory remains also largely unknown.

Therefore, the current thesis investigated the initial induction of human antigen-specific plasma- and memory B cells and also reactivation of the latter. The main aim was to enhance our understanding of the induction of antigen-specific Ig and principles of B cell selection and recruitment into the B cell memory pool. Further, memory B cells were enumerated and characterized in tissues likely providing a protected environment. Peripheral blood memory B cells were monitored during absence of the one or other organ in humans to better identify the role of potential survival organs or niches.

Therefore, firstly, primary and secondary KLH immunization was employed and the induced KLH-specific serum antibody levels as well as plasma- and memory B cells quantified. The results should provide first insights into the serologic and B cellular response kinetics and characteristics permitting conclusions on the principles of these responses.

Secondly, the quality of the resulting B cell responses were studied by molecular analyses of Ig heavy chain gene rearrangements of circulating KLH-specific B cell subsets. In order to do so, KLH-specific sequences were analyzed for their Ig gene family usage, repertoire composition, frequency of somatic mutations and clonal ex-

pansion. The results should permit insights into repertoire recruitment characteristics and the process of affinity maturation during primary and secondary immunization as well as they should allow conclusions on the B cells' origin.

Thirdly, antigen-specific Ig repertoire comparisons between the primary and secondary response as well as the steady state KLH-specific memory B cell repertoire were performed. The results should reveal relationships between the KLH^{spec} B cell pools and thus allow conclusions on memory formation, characteristics of reactivation and Ig diversification.

Fourthly, the distribution and organ-specific phenotype of the overall human memory B cells and antigen-specific memory B cells in spleen, tonsil and bone marrow compared to peripheral blood were studied. Finally, the impact of the absence of spleen or tonsil on memory B cell maintenance was investigated. The results should grant insight into compartmentalization of reactive B cell memory and its organization.

The overall aim of the study was to gain deeper insights into the principles of memory induction, maintenance and reactivation by using a defined vaccination model in humans. The thesis studies led to innovative insights that allow to roll out new concepts of memory B cells and will fertilize vaccination and immunotherapeutic approaches.

4. Materials and Methods

4.1 Materials

Table 4-1: Universal materials

Reagent / Material	Manufacturer
Microcentrifugation / Safe-Lock Tubes 1,5 mL / 2,0 mL	Eppendorf AG, Hamburg, Germany
Serological Pipettes (10 mL, 25 mL, 50 mL)	Becton Dickinson (BD) Falcon, Heidelberg, Germany
EDTA Vacutainer and serum Vacutainer tubes	BD Biosciences, San Jose, CA, USA
50 mL Conical Centrifuge Tube	Corning Incorporated | Life Sciences, Acton, MA, USA
15 mL Conical Centrifuge Tube	Corning Incorporated | Life Sciences
Phosphate buffered saline (PBS) w/o Ca^{2+} w/o Mg^{2+} low endotoxin	Biochrom AG, Berlin, Germany
Albumin, Bovine Fraction V (BSA)	Sigma-Aldrich Chemie GmbH, Steinheim, Germany
Ultra Pure Water (H_2O)	Biochrom AG
DAPI (4,6 diamidino-2-phenylindole; 220 nM)	Molecular Probes, Eugene, OR, USA

Table 4-2: Isolation of mononuclear cells from blood and tissue

Reagent	Manufacturer
Ficoll–Paque Plus	GE Healthcare Bio-science AB, Uppsala, Sweden
70 µm cell strainer	BD Biosciences, San Jose
Quiagen Buffer EL	Quiagen GmbH, Hilden, Germany
Ultra Pure™ 0.5 M EDTA (Ethylenediaminetetraacetic acid), pH 8.0	Life Technologies, Carlsbad, CA, USA

Table 4-3: Staining materials for flow cytometry and FACS

Reagent	Manufacturer
BD Cytofix Fixation Buffer	BD Biosciences, San Jose
BD Phosflow Perm Buffer III	BD Biosciences, San Jose
5 mL Polystyrene Round Bottom Tube	Falcon, Corning Incorporated, NY, USA
BD Trucount™ tubes	BD Biosciences, San Jose

Table 4-4: Antigens

Reagent	Manufacturer
Tetanus toxoid (TT) Lot 317470	Novartis Deutschland GmbH, Nürnberg, Germany
Keyhole Limpet Hemocyanin (KLH)	Biosyn, Fellbach, Germany

Table 4-5: Conjugated antigens for flow cytometry and FACS

Antigen	Fluorochromelabel/ conjugated to	Conjugated at
TT	Digoxigenin (Dig)	DRFZ, Berlin, Germany
TT	Cy5	DRFZ, Berlin
KLH	Dig	DRFZ, Berlin
KLH	Cy5	DRFZ, Berlin

Table 4-6: Antibodies for flow cytometry and FACS

Specificity of antibody	Clone	Fluorochromelabel/ conjugated to	Manufacturer
CD3	SK7	Allophycocyanin-H7 (APC-H7)	BD Biosciences, San Jose
CD3	UCHT1	Pacific Blue (PacB)	BD Biosciences, San Jose
CD14	MOP9	APC-H7	BD Biosciences, San Jose
CD14	M5E2	PacB	BD Biosciences, San Jose
CD19	SJ25C1	Phycoerythrin-Cyanine7 (PE-Cy7)	BD Biosciences, San Jose
CD19	SJ25C1	APC-H7	BD Biosciences, San Jose
CD20	L27	Peridinin-chlorophyll-protein complex (PerCp)	BD Pharmingen™, Heidelberg, Germany
CD20	HI47	Pacific Orange (PacO)	Invitrogen Corporation, Frederick, MD, USA
CD27	2E4	Cyanine5 (Cy5)	Kind gift from René van Lier, Academic Medical Centre, University of Amsterdam, The Netherlands
IgA	M24A	Fluorescein isothiocyanate (FITC)	Chemicon, Temecula, CA, USA
IgD	IA6-2	PE	BD Biosciences, San Jose
IgM	G20-127	PerCpCy5.5	BD Biosciences, San Jose
IgG	G18-145	PE-Cy7	BD Biosciences, San Jose
CD24	ML5	FITC	BD Biosciences, San Jose
CD21	B-Ly4	PE-Cy7	BD Biosciences, San Jose
CD31	WM59	PE	BD Biosciences, San Jose
CD38	HIT-2	PerCpCy5.5	BD Biosciences, San Jose

Specificity of antibody	Clone	Fluorochromelabel/ conjugated to	Manufacturer
CD45	2D1	PerCp	BD Biosciences, San Jose
CD54	HA58	PE	Biolegend, San Diego, CA, USA
CD62L	Dreg-56	PE-Cy7	ebioscience, San Diego, CA, USA
CD69	FN50	APC	Miltenyi Biotec GmbH, Bergisch Gladbach, Germany
CD95	DX2	PerCpCy5.5	BD Biosciences, San Jose
β7 integrin	FIB504	PE	BD Biosciences, San Jose
CXCR5	RF8B2	Alexa488	BD Biosciences, San Jose
CXCR4	12G5	PE	BD Biosciences, San Jose
ICOSL	HIL131	PE	kind gift from Andreas Hutloff
HLADR	L243	FITC	Kind gift from DRFZ
Ki67	MIB-1	FITC	Dako Denmark A/S, Glostrup, Denmark
Dig, Fab fragments	polyclonal	FITC	Roche Diagnostics GmbH, Mann-heim, Germany

Table 4-7: ELISpot

Reagent	Manufacturer
MultiScreen flat-bottom 96-well plate (MSIPN4450)	Merck Millipore, Ireland
Ethanol 70%	Carl Roth GmbH & Co. KG, Karlsruhe, Germany
1640 RPMI medium	Gibco, NY, USA
Fetal calf serum (FCS)	Gibco, NY, USA
Penicillin-Streptomycin	Gibco, NY, USA
Tween-20	Sigma-Aldrich, St. Louis
Biotinylated anti-IgA antibody (mix of anti-IgA1 and anti-IgA2, clone G20-359)	BD Biosciences, San Jose
Biotinylated anti-IgM antibody (polyclonal)	Sigma-Aldrich, St. Louis
Biotinylated anti-IgG antibody (polyclonal)	Sigma-Aldrich, St. Louis
ExtrAvidin-Peroxidase	Sigma-Aldrich, St. Louis
3-amino-9-ethylcarbazole	Sigma-Aldrich, St. Louis
N,N-dimethylformamide	Sigma-Aldrich, St. Louis
Sodium actetate	Sigma-Aldrich, St. Louis
Acetic acid buffer	Sigma-Aldrich, St. Louis
H_2O_2	Sigma-Aldrich, St. Louis

Table 4-8: RT-PCR and cDNA synthesis

Reagent	Manufacturer
Titan One Tube RT-PCR System - 5x R- PCR-Buffer - Enzyme mix (reverse transcriptase, AMV) - DTT (100 mM)	Roche Diagnostics GmbH
Deoxynucleotide (dNTP) Mix (each 10 mM)	Sigma-Aldrich Chemie GmbH, Steinheim
Primer $p(dT)_{15}$ (800 ng/mL)	Roche Diagnostics GmbH
RNasin Plus Rnase inhibitor® (40 U/µL)	Promega,Madison, WI, USA
Spermidin (50 nM)	Sarka Ruzickova, Prague,Czech Republic
Triton-X-100	Sigma-Aldrich Chemie GmbH, Steinheim

Table 4-9: Nested PCR

Reagent		Manufacturer
AmpliTaq DNA Polymerase kit (N808-0153) - AmpliTaq® DNA Polymerase - GeneAmp® 10x PCR Buffer II - GeneAmp® $MgCl_2$-Solution (25 mM)		Applied Biosystems, Foster City, CA, USA
Primer for external PCR (100 pmol/µL)		Metabion, Martinsried, Germany
VH1 LC	5' CC ATG GAC TGG ACC TGG A 3'	(112)
VH2 LC	5' ATG GAC ACA CTT TGC T(AC)C AC 3'	
VH3 LC	5' CC ATG GAG TTT GGG CTG AGC 3'	
VH4 LC	5' ATG AAA CAC CTG TGG TTC TT 3'	
VH5 LC	5' ATG GGG TCA ACC GCC ATC CT 3'	
VH6 LC	5' ATG TCT GTC TCC TTC CTC AT 3'	
IgA : IgVH-cα	5' GGA AGA AGC CCT GGA CCA GGC 3'	(113)
IgG: Ecγ*	5' AC GCC GCT GGT CAG GGC GC 3'	
IgM: Ecµ	5' TCA GGA CTG ATG GGA AGC CC 3'	
Primer for internal PCR (100 pmol/µL)		Metabion, Martinsried
VH1 FM	5' CAG GTG CAG CTG GTG CAG TCT GG 3'	(114)
VH2 FM	5' CAG GTC ACC TTG AAG GAG TCT GG 3'	
VH3 FM	5' GAG GTG CAG CTG GTG GAG TCT GG3'	
VH4 FM	5' CAG GTG CAG CTG CAG GAG TCG GG3'	
VH5 FM	5' GAG GTG CAG CTG GTG CAG TCT GG3'	
VH6 FM	5' CAG GTA CAG CTG CAG CAG TCA GG3'	
IgA: IgAex2	5' ACC AGG CAG GCG ATG ACC AC 3'	
IgG: IgGex*	5' AAG TAG TCC TTG ACC AGG CAG C3'	(115), modified
IgM: IgMin,neu	5' AGG AGA CGA GGG GGA AAA GGG TTG 3'	(115), modified

Table 4-10: PCR product purification

Reagent	Manufacturer
10x Tris-borate-EDTA (TBE)	Carl Roth GmbH & Co
Biozym LE Agarose	Biozym Scientific GmbH, Oldendorf, Germany
mi-100bp+ DNA Marker (0.1 µg/µL)	Metabion, Martinsried
GelRed™ Nucleic Acid Gel Stain	Biotium, Inc., Hayward, CA, USA
tRoti®-Load-DNA short-run (supplemented with 1 mL glycerol, 8 mL H_2O and 1:5000 GelRed™)	Carl Roth GmbH & Co
QIAquick®Gel Extraction Kit (250) - QG Buffer - PE Buffer - EB Buffer - QIAquick spin column	Qiagen, Hilden, Germany
Isopropanol	Carl Roth GmbH & Co
Ethanol 96%	Carl Roth GmbH & Co

Table 4-11: Other reagents and materials

Reagent/ Material	Manufacturer
Abgene®PCR Plates Thermo-Fast®96, Low Profile	Thermo Fisher Scientific, Bonn, Germany
PCR-adhesive foil	VWR International GmbH, Dresden, Germany
Domed cap strips	Thermo Fisher Scientific
Glycerol	Merck, Darmstadt, Germany
96 well microtiterplates, V-form	VWR International GmbH

Table 4-12: Devices

Device	Manufacturer
BD FACSAria flow cytometer special order system	BD, Heidelberg, Germany
BD FACSCanto II flow cytometer	BD, Heidelberg
Centrifuge 5415C / 5415D	Eppendorf AG
DS34 Direct Screen Instant Camera with GH26 Electrophoresis Hood	Polaroid, Dreieich-Sprendlingen, Germany
Electrophoresis chamber	C.B.S. Scientific Co, Del Mar, CA, USA
Labofuge 400e	Heraeus Instruments, Hanau, Germany
MaxiCycler PTC-100	Biozym Diagnostic GmbH
MultiCycler PTC-200	Biozym Diagnostic GmbH
Transilluminator 312nm	Herolab GmbH, Wiesloch, Germany
ELISpot Reader and Immunospot Software	CTL, Aalen, Deutschland

4.2 Methods

4.2.1 KLH immunization and study participants

Five healthy volunteers (HD; 1 male, 4 female, age range 27 to 54 years) were enrolled in the KLH immunization study. Donors received a parenteral immunization of either 0.6 mg KLH subcutaneously (s.c.; HD1) or 0.1 mg KLH s.c. (HD2 and HD3) or 0.5 mg KLH s.c. and 0.5 mg KLH intradermally (i.d.; HD4 and HD5) in the deltoid region. A booster dosis was injected 7 (HD4 and HD5) or 10 days (HD1-HD3) afterwards with 1 mg s.c. or 0.1 mg s.c., respectively. Donors HD1, HD2 and HD3 received a secondary immunization 18 months (HD1; 0.1 mg s.c.) or 6 months (HD2 and HD3; 0.01 mg s.c.) after the primary immunization cycle. 10 mL serum and 10-20 mL EDTA venous blood (BD Vacutainer) was obtained before and at several time points after immunization as depicted in the figures (see section 5.1). The study was approved by the local ethics committee and informed consent was obtained by the individuals participating in this study.

4.2.2 Tissue distribution of B cells and mBC study participants

For the comparative analysis of mBC between blood and lymphoid organs, 10-50 mL venous peripheral blood (EDTA, BD Vacutainer) from 40 HD (23 female, 17 male, age range 23-63 years), from 10 tonsillectomized HD (TX, 3 female, 7 male, 26-65 years) and 6 splenectomized donors (S1-S6, 4 female, 2 male, 36-73 years) was collected. S1, S2, S4 and S5 were splenectomized because of immune thrombocytopenia (ITP) and S3 and S6 because of non-immunological diseases. To confirm the absence of splenic function, blood smears were examined for Howell-Jolly-bodies (116).

Altogether 23 tonsils were obtained from patients (12 female, 3 male, 8 unknown, 11-51 years) undergoing tonsillectomy due to tonsillitis. A total of 10 spleen samples were obtained from patients (6 female, 4 male, 16-79 years) of that four underwent splenectomy because of ITP and the other six for non-immunological reasons. Thirty-four BM samples were obtained from patients (23 female, 10 male, 1 unknown, 35-82 years) undergoing hip joint replacement surgery. Written informed consent was obtained in all cases in accordance with the local ethics' committee of the Charité Universitätsmedizin Berlin.

4.2.3 Mononuclear cell- and serum isolation

Peripheral blood mononuclear cells (PBMC) were isolated from fresh EDTA blood by density gradient centrifugation using Ficoll-Paque Plus (according to the principle described by Bøyum (117)). Therefore, blood was 1:1 (V/V) mixed with PBS and 30 mL of this mixture layered on to 15 mL Ficoll-Paque Plus solution in a 50 mL conical centrifugation tube and centrifuged for 20 min at $400_x g$ (brakes off, all at RT). Due to different cell densities and with respect to the properties of the Ficoll-Paque Plus solution, differential migration during centrifugation resulted in the formation of layers containing the different cell types. In short, erythrocytes and granulocytes form a layer at the bottom of the tube, followed by a layer of Ficoll-Paque Plus solution on which a ring like interface contains the lymphocytes, monocytes and platelets, followed by the top layer, i.e. the plasma. The lymphocyte-containing ring was recovered from the interface and transferred into a new 50 mL conical centrifugation tube and washed twice with 4 °C cold PBS/0.2% BSA at $200_x g$ at 4 °C for 10 min. The obtained PBMC were then filtered through a 70 µm cell strainer.

Spleen and tonsil specimens were minced, respectively, and vortexed in PBS/BSA. The resulting cell suspensions were filtered (70 µm cell strainer) and mononuclear cells (MNC) isolated as performed for PBMC. BM samples were either treated as described for spleen and tonsil specimens but using PBS/BSA/5mM EDTA or after filtration residual erythrocytes were lysed using Quiagen Buffer EL. Therefore, the filtered BM cell suspension was mixed 1:4 (V:V) with the Quiagen Buffer EL in a 50 mL conical centrifugation tube and incubated for 15 min on ice. This suspension was centrifuged afterwards at $180_x g$ at 4 °C for 10 min, and washed twice with cold PBS/BSA/EDTA and finally filtered (70 µm cell strainer).

For serum collection, serum blood was centrifuged at $1500_x g$ for 10 min at RT. Serum was stored at -21 °C until use.

4.2.4 Flow cytometric analysis

Flow cytometry is a laser-based widely used biophysical technique for the rapid analysis of multiple characteristics of single cells. In short, cells from a suspension are hydrodynamically focussed in a stream of fluid and passed by several laser beams

and an electronic detection apparatus recording how the cell or particles scatter incident laser light and emit fluorescence. Hence, it measures optical and fluorescence characteristics of these single cells based on their physical properties (e.g. size, granularity) and cellular components or reaction products labeled with fluorescent dyes, either directly (e.g. DNA or RNA intercalating reagents) or indirectly by fluorochrome-labeled antigens or antibodies targeting specific proteins. The underlying principles and applications of flow cytometry and also of fluorescence activated cell sorting (FACS), which provides a method for isolating individual cells from the heterogeneous cell suspension, has been expertly summarized in detail elsewhere (118).

4.2.4.1 Surface staining procedures

To characterize and isolate KLH-specific (KLH^{spec}) B cells, PBMC were stained with a basic mix of antibodies against CD3, CD14, CD19, CD20, CD27 (Table 4-6) and KLH which was either labeled to Cy5 or to Dig. For the latter combination a second staining step after washing with anti–Dig-FITC was required. KLH^{spec} B cells were identified by their binding to the labeled KLH. The specificity of the antigen staining was confirmed each time by blocking with unconjugated KLH (50x-200x excess) which was added 5 min prior to the regular staining. TT^{spec} B cells were identified by their binding to Cy5-labeled TT (TT-Cy5) and the specificity of this staining was also confirmed each time by blocking using unconjugated TT, as described for KLH.

For the stainings designed to characterize lymphoid organ and blood B cells and mBC, a basic staining mix containing CD3, CD14, CD19, CD20 and CD27 was used in different combinations of antibodies (Table 4-6) were added. Additionally, for each of the antibodies, the respective isotype control was stained in a fluorescence minus one control manner.

For the principle cell surface staining procedure, a volume of 50 µL containing ~$1x10^6$ PBMC/MNC in PBS/BSA was used. To this, the respective antibodies or antigens were added. Stainings were performed in the dark at 4°C for 15 min, followed by washing in 2 mL PBS/BSA at $200_x g$ for 5 min. DAPI was added immediately before flow cytometric analysis. PBMC/MNC were analyzed using a BD FACSCanto II flow cytometer.

4.2.4.2 Intracelluar staining for Ki67

Intracellular Ki-67 staining was performed upon surface staining with the basic B cell staining mix, as described above, only that 100 µL containing ~2x10^6 PBMC/MNC were used. PBMC/MNC were then washed three times with 3 mL PBS followed by their thorough resuspension in the reflux after discarding the supernatant. For fixation, 250 µL BD Cytofix Fixation buffer was added while vortexing and the cells incubated for 10 min at 37 °C followed by washing with 2 mL PBS at 400x*g* for 5 min. Resuspended cells were again washed (400x*g* for 5 min) with 2 mL PBS/1% BSA followed by their thorough resuspension in the reflux after discarding the supernatant. For permeabilization, 500 µL BD Phosflow Perm Buffer III was added slowly while gently vortexing and cells were incubated for 30 min on ice in the dark. Permeabilized cells were washed twice with 3 mL PBS/BSA at 400x*g* for 5 min. Resuspended cells were stained with the Ki-67-FITC antibody at RT for 30 min in the dark and washed afterwards in PBS/BSA.

4.2.5 Enzyme-linked immunospot assay (ELISpot) for detection of individual PB secreting KLH-specific antibodies

ELISpot is a method which enables the monitoring of individual cells within a cell population or generally PBMC by detection of their secreted products, as a modification of a traditional sandwich ELISA immunoassay. In brief, a suspension of cells is seeded ideally in an adequate dilution to form a monolayer on a polyvinylidene fluoride-membrane microtiter plate which has been coated either with e.g. an antigen or a capture antibody followed by incubation and subsequent detection steps. Each spot that develops represents a single cell and thus provides qualitative and quantitative information. In this study it is used to detect antigen-specific antibody secreting cells from peripheral blood, i.e. PB, from KLH immunized donors. The technique's principle is expertly explained in the original work by Czerkinsky et al. (119).

To test for the KLH stainings' general effectiveness to extract KLH^{spec} B cells, KLH-binding versus non-binding antibody-secreting cells, i.e. PB, gates as $CD3^{neg}CD14^{neg}CD19^{pos}CD20^{low/neg}CD27^{high}KLH^{pos}$ and KLH^{neg} cells, respectively, as well as bulk $CD3^{neg}CD14^{neg}CD19^{pos}CD20^{low/neg}CD27^{high}$ cells were isolated by FACS and subsequently seeded on a KLH-specific ELISpot. Therefore, prior to cell seeding a MultiScreen flat-bottom 96-well plate was prepared by pre-wetting with 35% ethanol for 1 min, followed by washing with PBS and incubation with 50 µL of 0.04 mg/mL

KLH at 37 °C for 1 hour. As controls, wells were incubated with undiluted human serum and as well as with PBS/3% BSA. Afterwards, the plate was washed with PBS and the membrane blocked with PBS/3% BSA at 37 °C for 1 hour followed by washing with PBS/BSA. The by FACS isolated PB populations were seeded onto that plate and incubated overnight in 1640 RPMI medium, supplemented with 10% FCS and 1% penicillin/streptomycin in a humid atmosphere (plate covered) at 37 °C/5% CO_2. On the following morning the cells were removed by thorough washing six times with PBS/1%BSA/0.05% Tween-20. For detection of secreted KLH-specific antibodies, a mix of biotinylated anti-IgA, anti-IgM and anti-IgG was added in a 1:200 PBS dilution. The plate was then again incubated at RT for 1 hour followed by vigorous washing six times with PBS. For detection of the biotinylated antibodies, the plate was incubated at RT for 30 min with ExtrAvidin-Peroxidase diluted 1:3000 in PBS. Afterwards the plate was again washed with PBS. Subsequently, 5 min incubation with 3-amino-9-ethylcarbazole dissolved in N,N-dimethylformamide, diluted in a 0.2 M sodium actetate/0.2 M acetic acid buffer supplemented with H_2O_2, was used to develop bound antibody and was followed by thorough washing under the tap (deionized water). The plate was analyzed by an ELISpot reader after drying overnight.

4.2.6 ELISA for detection of anti-KLH serum antibodies

ELISA for quantification of serum anti-KLH IgM, IgA and IgG antibodies, respectively, were performed by the laboratory of Dr. J.F.M. Jacobs (Radboud University Medical Centre, Nijmegen, The Netherlands) according to their published protocol by Aarntzen et al. (120). In short, KLH antibodies were purified from each serum sample by washing the serum over a KLH-coated column (Alpha Diagnostics International, San Antonio, Texas, USA) followed by washing and elution of the antibodies. Different concentrations of each respective eluate were added on 96-well plates coated with 5 µg/mL KLH (Biosyn) at RT for 1 hour. After washing, specific antibodies against human IgM, IgG and IgA, respectively, labeled with horseradish peroxidase (all Invitrogen, San Diego, CA, USA) were added and incubated at RT for 1 hour. Upon subsequent washing, peroxidase activity was revealed using 3,3′,5,5′-Tetramethylbenzidine (Sigma-Aldrich) as substrate. The reaction was stopped with sulphuric acid and absorbance was determined at 450 nm. A detection limit of the anti-KLH ELISA was determined by the laboratory as described (120).

4.2.7 Single-cell PCR for IgH sequence analysis

Single-cell analyses generally provide powerful tools to gather information not only on an entire cell population but on a cell individual level, which yet can be expanded to a population level again, depending on the quantity of analyzed events, as can be very easily comprehended from FACS analyses.

Single-cell DNA or RNA analysis is an informative tool in the analysis of genetic material providing information on e.g. cell clonality, detection of genetic disorders from embryos, analysis of transgenic animals and/or the absolute abundance of e.g. mRNAs or microRNAs and their up- or downregulation in a single cell compared to neighboring cells. In this regard and with respect to the current study, polymerase chain reaction (PCR) is a particularly useful tool when the amount of genetic material is very limited because single copies of (expressed) genes can be detected. PCR relies on a principle where a DNA polymerase synthesizes a new strand of DNA complementary to the offered template strand during cycles of repeated heating and cooling required for the different PCR steps, i.e. DNA denaturation, primer annealing and template elongation. At the end, the specific target sequence will be accumulated in millions of copies, so termed amplicons, which can be made visible on e.g. an agarose gel.

In the here conducted study, expressed IgH genes were reverse transcribed by reverse transcription- (RT-) PCR and the target sequences subsequently amplified by a nested PCR protocol, i.e. a two-step amplification PCR. The first PCR step is called external PCR with a set of external primers of which the product is used as template for the second PCR step termed internal PCR using internal primers, which are indented in the product from the external PCR. The correct PCR product (according to size) is isolated from an agarose gel and sequenced. The process is illustrated in Figure 4-1.

Therefore, PBMC were stained as described under section 4.2.4.1 and individual KLH^{spec} PB or mBC sorted into a 96-well plate, using a BD FACSAria flow cytometer. DAPI was added immediately before cell sorting to exclude dead cells. Each well already contained 30 µL of a mix for cell lysis and RNA stabilization, consisting of 8.3 mM DTT, 0.5 µg BSA, 1.7% TritonX-100, 0.8 nM Spermidin, 0.4 ng $p(dT)_{15}$ Primer and 20 U RNasin Plus RNase inhibitor.

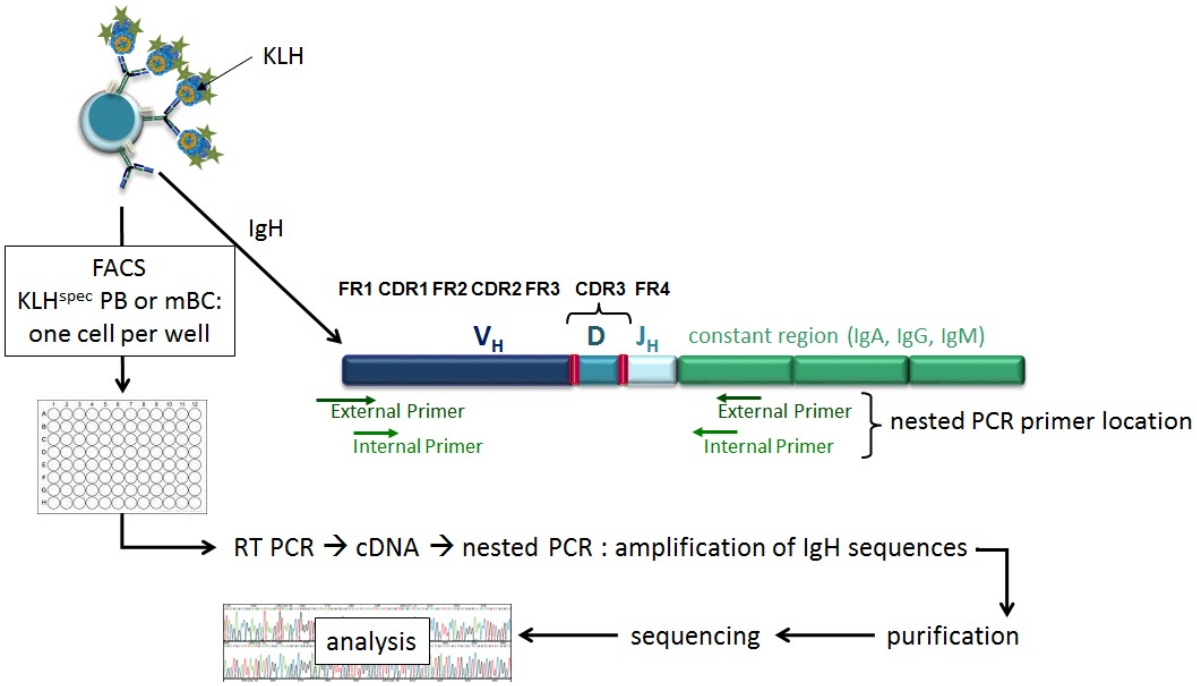

Figure 4-1 Schematic overview of KLH^{spec} B cell isolation by FACS and the single-cell PCR approach for amplification of the KLH^{spec} IgH chain.
The amplification of IgH sequences from KLH^{spec} PB and mBC, respectively, was achieved by RT PCR from mRNA of single isolated cells, followed by a multiplex nested PCR. The external forward primers were located in the leader sequence of the mRNA. Six V_H family specific forward primers were used in the external and internal PCR, respectively, amplifying segments from all V_H families, including V_H7. For the constant region (reverse primers), for each major isotype (IgA, IgG or IgM) an individual primer was used.

Afterwards, 20 µL of a second mix was added containing the Titan One Tube kit's RT-PCR buffer (10 µL) and 1 µL AMV reverse transcriptase supplemented with 0.5 mM dNTPs. Exemplarily for one well, individual component volumes for mix 1 and mix 2 are shown in Table 4-13. Complementary DNA (cDNA) was generated at 50 °C for 60 min.

Table 4-13 Example mix RT PCR

Mix 1	Volume per well	Mix 2	Volume per well
H_2O	20.95 µL	H_2O	8 µL
0.1 M DTT	2.5 µL	5x RT-PCR-Buffer	10 µL
40 U/µL RNasin	0.5 µL	dNTP Mix (10 mM ea)	1 µL
50 nM Spermidin	0.5 µL	Enzyme mix (AMV)	1 µL
10 µg/mL BSA	0.05 µL		
800 ng/mL $p(dT)_{15}$ Primer	0.5 µL		
10 % Triton-X-100	5 µL		

Amplification of rearranged $V_HDJ_HC\gamma/\alpha/\mu$ sequences from the bulk of generated cDNA was facilitated by nested PCR using 5 µL of the cDNA, followed by product

purification and sequencing. For both, the external and internal PCR, the reaction mix consisted of the AmpliTaq DNA Polymerase kit components prepared according to the manufacturer's instruction, supplemented with 0.2 mM dNTP and 0.07 µM of each of the external and internal primers (Table 4-9), respectively. 5 µL of the external PCR products were used as template for the internal PCR. Table 4-14 shows an example mix for external and internal PCR, containing all V_H forward primers for full repertoire analysis and reverse primers for IgM, IgA and IgG transcript amplification. The external PCR cycle program consisted of 7 min at 95 °C, 1 min at 50 °C, 90 sec at 72 °C, followed by 50 cycles of 1 min at 94 °C, 30 sec at 50 °C, 90 sec at 72 °C and to finish 1 min at 94 °C, 30 sec at 50 °C, 10 min 72 °C. For the internal PCR, the same cycle program was used with the exception of the primer annealing temperature which was 58 °C.

Table 4-14 External and internal PCR reaction mix example with all forward and reverse primers

External PCR mix	Volume per well	Internal PCR mix	Volume per well
H_2O	56.4 µL	H_2O	56.4 µL
10x PCR Buffer II	8 µL	10x PCR Buffer II	8 µL
$MgCl_2$ Solution	8 µL	$MgCl_2$ Solution	8 µL
dNTP Mix (10 mM ea)	1.6 µL	dNTP Mix (10 mM ea)	1.6 µL
Amplitag DNA Polymerase	0.5 µL	Amplitag DNA Polymerase	0.5 µL
VH1 LC	0.056 µL	VH1 FM	0.056 µL
VH2 LC	0.056 µL	VH2 FM	0.056 µL
VH3 LC	0.056 µL	VH3 FM	0.056 µL
VH4 LC	0.056 µL	VH4 FM	0.056 µL
VH5 LC	0.056 µL	VH5 FM	0.056 µL
VH6 LC	0.056 µL	VH6 FM	0.056 µL
IgA : IgVH-cα	0.056 µL	IgA: IgAex2	0.056 µL
IgG: Ecγ*	0.056 µL	IgG: IgGex*	0.056 µL
IgM: Ecµ	0.056 µL	IgM: IgMin,neu	0.056 µL

25 µL to 50 µL of PCR products were mixed with 20 µL tRoti-Load loading buffer and were separated by agarose gel electrophoresis, on a 1.8% agarose gel dissolved in a 0.5% TBE buffer. DNA fragments were visualized with GelRed by exposition to UV light, cut out and purified using QIAquick Gel Extraction kit according to the manufacturer's instructions. In short, each gel slice (equalling a volume of ~200 µL) was incubated with 600 µL QG buffer for 10 min at 50 °C until the gel slice dissolved

completely. Then, 200 µL isopropanol were added and the mix vortexed and placed on to a QIAquick spin column and centrifuged for 1 min at $10000_x g$. The flow-through was discarded and 500 µL QG buffer added, the tube centrifuged again and the flow-through discarded. To wash, 750 µL PE buffer (supplemented with 96% ethanol) were added, let stand for 5 min and the column centrifuged again. The flow-through was discarded and the residual PE buffer-ethanol mix removed by another centrifugation step. The QIAquick column was then placed into a new 1.5 mL microcentrifugation tube and let stand open for 10 min so the residual ethanol could volatilize. To elute the DNA, 30 µL of EB buffer was added and the column centrifuged again at $10000_x g$ for 1 min. Products were sequenced at Eurofins MWG Operon (Martinsried, Germany).

4.2.8 Data analysis

4.2.8.1 Flow cytometry data

Flow cytometry data were analyzed using FlowJo software 7.6.5 (TreeStar, Ashland, OR, USA) or BD FACSDiva 6.1.3. software. Absolute numbers of B cells, mBC or TT^{spec} mBC were approximated by multiplying the described tissue-specific lymphocyte number (121), with the ratio of gated B cells, mBC or TT^{spec} mBC, respectively, to gated total lymphocytes.

4.2.8.2 IgH sequence analysis

IgH sequences were analyzed using the Chromas 2.33 sequence viewer (Chromas Technelysim, Helensvale, Australia) and the joinsolver software (accessed between May 2012 and June 2014) using the Kabat database (122). Thereby, the joinsolver algorithm assigned V_HDJ_H germline genes based on the highest homology. SHM were counted within V_H genes from FWR1 to FWR3, which includes IgH chain CDR1 (CDRH1) and CDRH2 and excludes the CDRH3 region. Isotype subclasses were determined by sequence comparison to the genomic sequence references from the ensemble human genome browser data base.

Genomatix (123) was used for alignments and homology analyses of the sequences. As basis for construction of genealogic trees, firstly phylograms were created using phylogeny.fr (124). A search for common sequence motifs within CDRH3 regions was conducted using the MEME suite, ClustalW and Weblogo (125-128).

Mutation rates of primary KLH^{spec} PB sequences were calculated with the formula

Equation 1 Mutation rate.

$$\frac{\#\ \text{mutations}}{V_H\ \text{length (bp)}} * \frac{1}{\#\ \text{of generations}} = \text{mutation rate } (bp^{-1} * \text{division}^{-1})$$

with the V_H length given in base pairs (bp) of the respective corresponding V_H region length and an assumed generation time of 8 hours, according to the estimated division time of GC CB (129). Of note, this hypothetical natural mutation rate calculation was taken to its extremes by assuming that the division was maintained over the entire course of the 14-18 days from time point zero, i.e. injection of the KLH.

Since the number of isolated sequences was larger than the number of unique rearrangements (Figure 5-17) a statistical prediction of actual repertoire sizes could be made using an approach described by Behlke et al. (130). Accordingly, the probability of observing exactly *d* distinct gene rearrangements among a total number of *r* examined sequences for a fixed number *n* of distinct gene rearrangements can be described as the likelihood (repertoire size) estimates with the equation

Equation 2 Repertoire size.

$$P(d) = S(r,d) * \binom{n}{d} * d! * n^{-r}$$

whereby S(r,d) are the Stirling's numbers of the second kind and with the assumption that no significant skewing of the data set by nonrandom gene segment usage occurred. For each day and donor, a maximum likelihood estimate (*n* for $P(d)_{max}$) of the the clonal repertoire and a 95% one-sided confidence limit (*n* for $P(d)_{<0.05}$) of the maximum likelihood estimates was calculated.

4.2.8.3 Statistical analysis

GraphPad Prism Version 5 for Windows (GraphPad Software, San Diego California, USA), Microsoft Excel 2010 (Santa Rosa, CA, USA) and R (131) were used for statistical analyses. To determine significant differences between B cell populations regarding distributions of V_H and J_H gene usage, respectively, the χ^2- goodness-of-fit statistic was calculated. Where appropriate to compare the distributions of two groups, the Mann-Whitney test was used. To compare paired values the Wilcoxon matched pairs test and paired t-test was performed, respectively. Which test was used for the respective data set is specified in the figure legends.

To calculate for statistical dependence between two variables the Spearman's rank correlation coefficient was calculated.

Generally, an alpha of 0.05 or 0.01 was chosen as cutoff for statistical significance.

5. Results

Immunological memory mediates our long-term protection from ubiquitous or recurring pathogens. Yet its induction and maintenance are so far incompletely understood, especially in humans. To address these aspects, this study investigated the induction, maintenance and reactivation of human antigen-specific B cell memory. Therefore, a comprehensive characterization of human primary- and secondary immune responses was conducted. Secondly, a so far unique systemic quantification and characterization of mBC within different human lymphoid organs compared to those detectable in peripheral blood was performed.

5.1 Direct comparison of a human KLH^{spec} B cell response induced by primary versus secondary immunization

To gain insights in to the underlying processes of PB and mBC generation as well as of reactivation of the latter we firstly utilized parenteral immunization with Keyhole Limpet Hemocyanin (KLH) in 5 naïve donors. KLH is a naturally occurring respiratory protein of the giant keyhole limpet *Megathura crenulata* living in shallow coastal waters in the sea (132, 133) and is usually not encountered by humans wherefore prior exposure or sensitizations of the immune system is unlikely. In the past, it has been utilized in studies addressing the phenomenon known as oral tolerance which resulted in useful insights how parenteral immune responses can or even cannot be manipulated by oral antigen feeding (134-136). Albeit soluble proteins are supposed to be poorly immunogenic when injected without adjuvants, KLH is immunogenic after all and elicits robust B- and T cell responses. Therefore, most recently it is used as a protein carrier to numerous poorly immunogenic cancer antigens, e.g. in melanoma (137), non-Hodgkin lymphoma (138) and follicular lymphoma (139). Hence, these applications underpin its functionality and principle safety for human studies.

To determine antibody and B cell kinetics and examine the employed specific BCR repertoire in response to KLH administration the present study used direct staining of PBMC with fluorochrome-labeled KLH and FACS-isolated KLH-specific (KLH^{spec}) B cells for molecular analyses.

5.1.1 Establishing a KLH-specific B cell staining

Popular methods to determine the frequency of antigen-specific B cells include B cell ELISpot (140) and limiting dilution assay (141), which however both preclude a further downstream isolation and characterization of the specific cells. To overcome this limitation, I established the direct staining of human KLH^{spec} B cells using KLH coupled to a fluorochrome or hapten, i.e. Cy5 or Dig, and flow cytometry allowing enumeration, further characterization and isolation of the specific cells. Figure 5-1 illustrates the staining's principle.

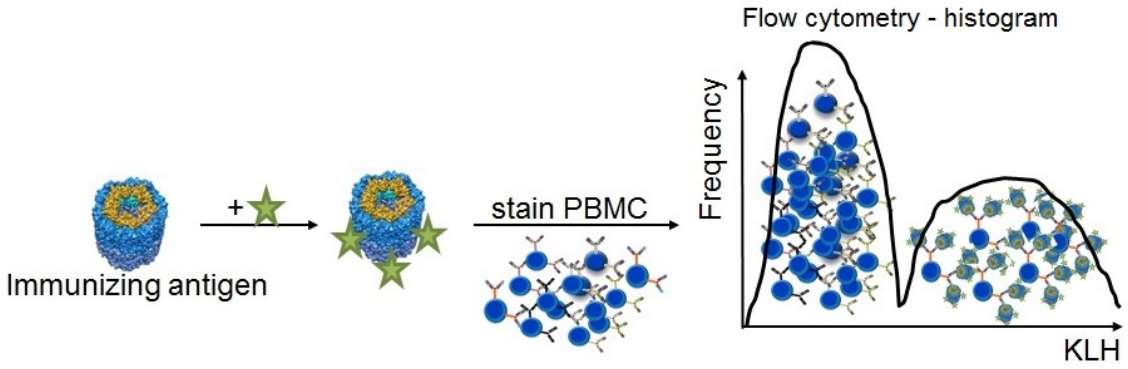

Figure 5-1 Staining principle of antigen-specific B cells and flow cytometry.
The green star indicates the fluorochrome or hapten that is covalently coupled to the immunizing antigen, here KLH, followed by the product's usage to stain PBMC. Stained PBMC are then analyzed on a flow cytometer. Only B cells (shown as blue cells) with an antigen-specific BCR should recognize the antigen and stain as positive cells while the rest should be unstained and therefore only exhibit a fluorescence intensity equivalent to their autofluorescence and potential background, i.e. are detected as antigen-negative cells.

To test for the staining's specificity, three approaches were used. Firstly, competitive blocking controls with unlabeled antigen were performed. Secondly co-stainings with an irrelevant antigen, i.e. here tetanus toxoid (TT), were used to determine unspecific binding. An example of a KLH^{spec} B cell staining, where KLH was stained in two channels simultaneously and the corresponding block, is shown in Figure 5-2 A. In Figure 5-2 B co-staining with the irrelevant antigen and its corresponding block is shown. The TT blocking control did not influence the binding of KLH^{spec} mBC to KLH while the KLH blocking control did, as would be expected for specific B cells.
As a result, in all following KLH experiments competitive blocking controls of the KLH staining were performed each time.

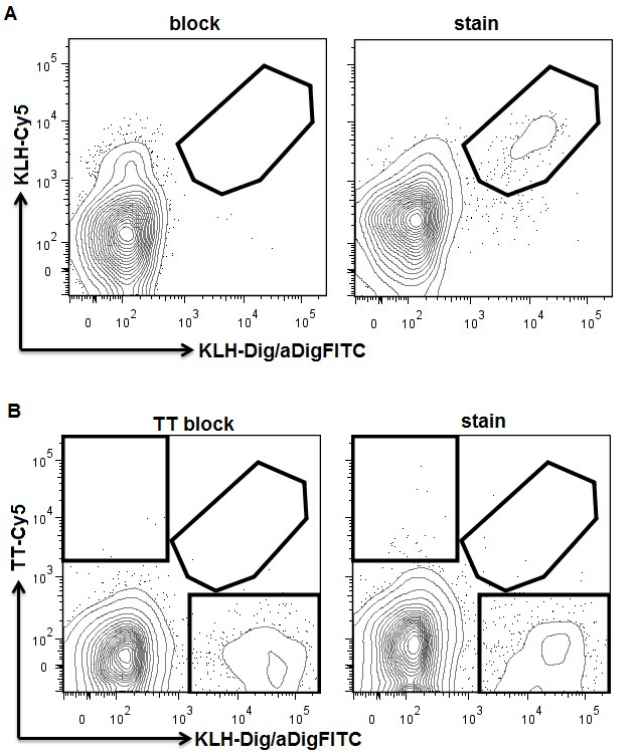

Figure 5-2 Specificity controls of the KLH^{spec} B cell staining.
A Shown are exemplarily mBC, gated as CD3^{neg}CD14^{neg}CD19^{pos}CD20^{pos}CD27^{pos} cells, from HD1 7 days upon secondary KLH immunization, which were stained with both simultaneously, KLH labeled to Cy5 and KLH labeled to Dig for the latter with secondary detection using a digoxigenin-specific FITC-labeled F(ab)$_2$ (aDigFITC). Left: unlabeled KLH (block) was added to the staining prior to adding the labeled KLH. Right: KLH staining without block. The gate marks the KLH-positively stained mBC, i.e. mBC carrying a KLH-specific BCR. **B** MBC were stained for KLH and tetanus toxoid (TT) simultaneously. Left: TT blocking control equivalently done as described under **A** for KLH. The gates show the areas where the specific B cells would be expected. Clockwise, starting from the top: TT^{spec} mBC; double TT^{spec} and KLH^{spec} mBC, which would be considered as unspecific fluorescent labeling unless they would share a common epitope, and the right-corner rectangle gate marks the KLH^{spec} mBC.

Thirdly, to further also test for the staining's efficacy to separate specific from non-specific B cells, from blood obtained at day 16 after primary immunization for donors HD2 and HD3, KLH-binding PB (KLH^{pos}) versus KLH-nonbinding PB (KLH^{neg}) were isolated by FACS and seeded on an ELISpot plate specific for KLH (Figure 5-3, one representative example of two is shown).

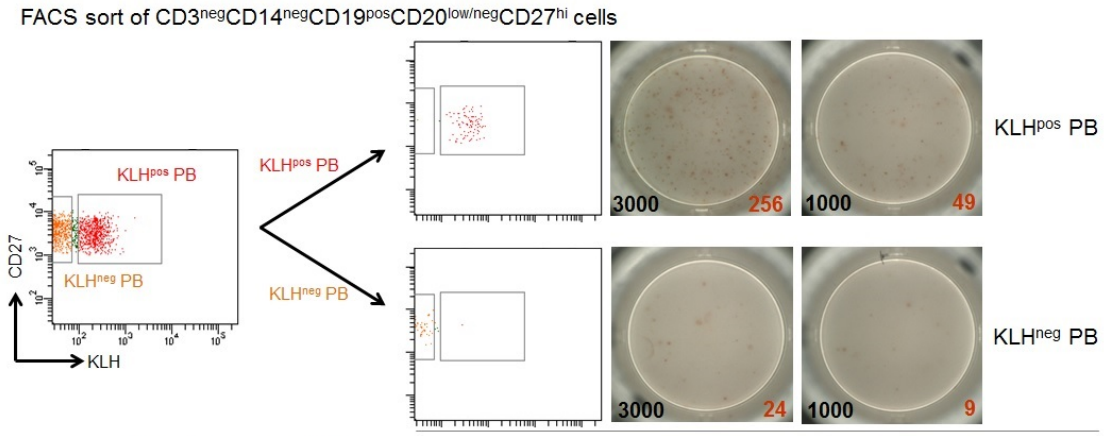

	Number of spots in sorted fraction			
Seeded PB	KLH^{pos} PB	KLH^{neg} PB	bulk PB	Frequency of spots from seeded PB
3000	256			8.53
1000	49			4.90
3000		24		0.80
1000		9		0.90
2000			47	2.35
5000			129	2.58

Figure 5-3 Control of the KLH^{spec} B cell staining's efficacy to isolate specific cells.
Sixteen days upon primary KLH immunization, KLH-binding (here: KLH^{pos}) and KLH-non-binding (here: KLH^{neg}) as well as a bulk PB population, respectively, were isolated from PBMC from HD2 by FACS and subsequently seeded overnight on a KLH-coated ELISpot plate (coated with 40 µg/mL KLH). Detection of secreted anti-KLH antibodies was carried out using a mix of anti-human IgM, IgG, and IgA-biotinylated antibodies, followed by secondary incubation with avidin-peroxidase and its substrate 3-amino-9-ethylcarbazole. Black numbers in ELISpot-well-image indicate number of seeded PB. Orange numbers in ELISpot-well-image indicate number of spots.

For both donors, we detected an enrichment of anti-KLH Ig secreting PB in the KLH^{pos} fraction. In contrast, the PB bulk population contained very few anti-KLH Ig secreting PB and thus anti-KLH Ig producing PB were clearly de-enriched after sorting in the KLH^{neg} PB. This approves the staining efficacy and identification approach employed to extract KLH^{spec} B cells from the bulk B cell population.

5.1.2 Primary parenteral KLH immunization induced simultaneous increase of anti-KLH IgM, IgG and IgA antibodies

Initially, the pre-immunization status of the 5 volunteers hitherto unexposed to KLH was analyzed by testing for specific serum antibodies. Here, we found that pre-immunization anti-KLH IgM, IgA and IgG antibody levels were either below or just above the lower limit of the assay's detection level. In detail, where possible to determine, specific titer levels ranged between 4.9 mg/L - 26 mg/L for IgG levels and 1 mg/L - 13 mg/L for IgA. Subsequent parenteral immunization with soluble KLH did not cause a change of anti-KLH antibody levels until day 14. Interestingly, at this time point anti-KLH antibodies of all three major isotypes showed a rather simultaneous

increase, i.e. the appearance of IgM antibodies did not precede that of IgA or IgG antibodies. Further, anti-KLH IgA antibodies showed a similar increase as IgG antibodies, i.e. 2- to 32- and 2- to 12-fold, respectively, yet specific IgA antibody levels remained below that of IgG antibodies at all times. Nevertheless, this clearly demonstrates that IgA antibodies can be induced by a parenteral immunization.

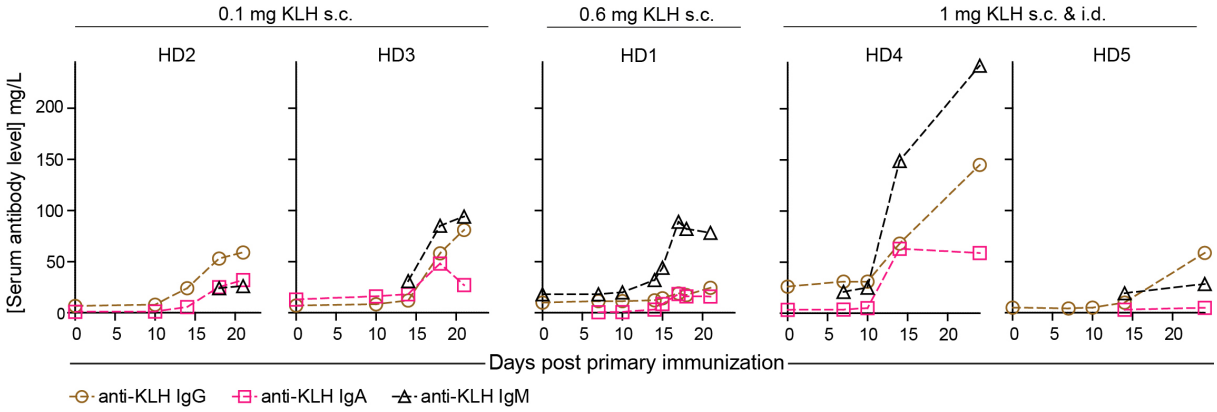

Figure 5-4 Kinetics of anti-KLH serum antibodies after primary parenteral KLH immunization. Donor HD1 received 0.6 mg KLH s.c., HD2 and HD3 received 0.1 mg KLH s.c., and HD4 and HD5 received 1 mg KLH split into 0.5 mg s.c. and 0.5 mg i.d. in the upper arm. The KLH used for immunization was in a soluble form without any adjuvant added. No value plotted means value was below detection limit.

5.1.3 The majority of induced KLH^{spec} B cells belonged to the CD27^{pos} and CD27^{high} B cell populations

Next, upon primary KLH immunization it was determined in which CD19^{pos} B cell subpopulations KLH^{spec} B cells appeared, as shown in Figure 5-5. As a result, KLH^{spec} B cells were found within the CD27^{high} B cell compartment, equaling the circulating antibody-secreting PB/PC population (see Figure 5-3 and (142)), and the CD27^{pos} B cell compartment, constituting the circulating mBC compartment in their majority (143, 144). Only in donor HD3, we found similar frequencies of KLH^{spec} B cells in CD27^{pos} and CD27^{neg} B cell compartments, the latter comprising mainly naïve B cells, but also few mBC and transitional B cells.

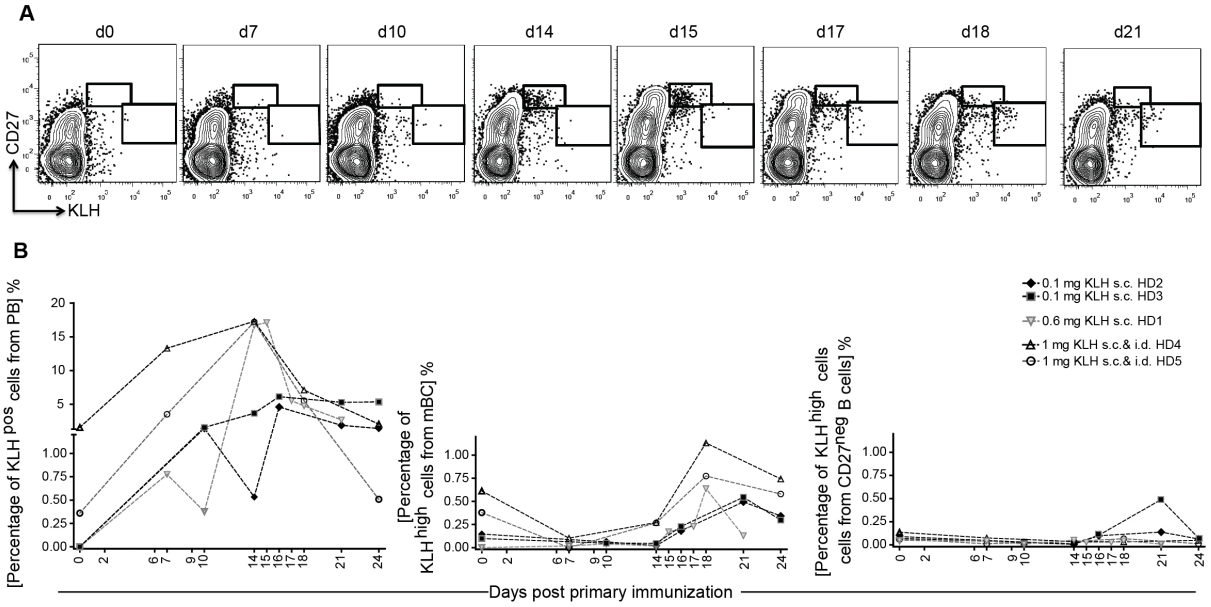

Figure 5-5 Circulating KLH^{spec} B cells are found in the CD27^{high} and CD27^{pos} B cell compartments.
A Dot plots of the appearance of KLH^{spec} human CD3^{neg}CD14^{neg}CD19^{pos} B cells exemplarily shown from donor HD1 on indicated days (d) after primary KLH immunization. For orientation, gates refer to KLH^{spec}CD27^{high} (upper gate) and KLH^{spec}CD27^{pos} (lower gate) cells, respectively. **B** Kinetics of the frequency of peripheral blood KLH^{spec} PB detected by flow cytometry (left, gated as CD3^{neg}CD14^{neg}CD19^{pos}CD20$^{neg/low}$CD27^{high}KLH^{pos} cells), KLH^{spec} mBC (middle, gated as CD3^{neg}CD14^{neg}CD19^{pos}CD20^{pos}CD27^{pos}KLH^{high} cells) and KLH^{spec} CD27^{neg} B cells (right, gated as CD3^{neg}CD14^{neg}CD19^{pos}CD20^{pos}CD27^{neg}KLH^{high}) on indicated time points after primary immunization expressed as percentages of the parent gate, respectively.

5.1.4 Peripheral blood appearance of primary KLH^{spec} PB preceded that of KLH^{spec} mBC

Next, the kinetics of increase of blood KLH^{spec} PB and mBC was determined. Generally, an increase of KLH^{spec} PB was detectable in peripheral blood between days 7-24 after primary immunization whereby variations between the individual donors were identified (Figure 5-5 B). Specifically, in HD1 KLH^{spec} PB were detectable between days 7-21, but did not show an increase from day 7 (0.8%) to day 10 (0.4%). From day 10 to day 14, where also the peak increase was found (17.7%), KLH^{spec} PB exhibited a 44-fold increase. In HD2 and HD3, KLH^{spec} PB were observed in peripheral blood on day 10 and thereafter until the last sampling time point, i.e. day 24. The peak response for both donors was detected on day 16 (4.6 % (HD2) and 6.1% (HD3)). In HD4 and HD5, few KLH^{spec} PB were detectable on day 0 which however were not blockable. From day 7 to day 14 KLH^{spec} PB were found 1.3- to 5-fold increased to 17.3% (HD4) and 17.2% (HD5), respectively. These cells decreased thereafter but still were detectable until the end of the sampling period in a comparable manner as found in the other donors.

In contrast to the appearance of primary KLH^{spec} PB, KLH^{spec} mBC exhibited slightly delayed and principle different kinetics of appearance. Firstly, KLH-binding mBC were detectable before immunization in 4 out of 5 donors, however, this KLH binding could be blocked poorly to 0% - 64% by pre-incubation with unlabeled KLH whereas at later time points, when KLH^{spec} mBC re-appeared in blood (see below), the block was more efficient, i.e. a significant reduction of positively stained mBC of 57-100% was achieved (days 21/24; Figure 5-6).

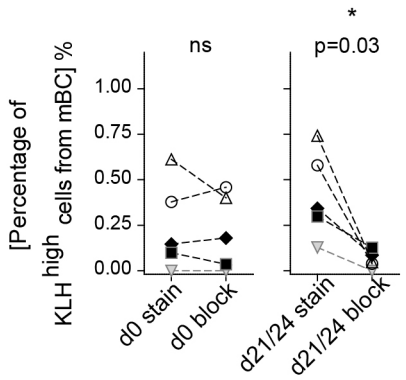

Figure 5-6 KLH-binding pre-primary immunization mBC were poorly blockable in contrast to post-immunization mBC.
Frequency of KLH^{pos} mBC with and without block before primary immunization (left) and 21 or 24 days after primary immunization (right). Paired t-tests were performed, with p≤0.05 considered to represent a significant change.

Secondly, compared to day 0, KLH^{spec} mBC were reduced or absent at day 7 and/or 10 (HD2-HD5), i.e. the next time points measured, but found to be increased at day 14 (HD4 and HD5) or a later time point (HD1-HD3; Figure 5-5 B middle graph). Thereby, KLH^{spec} mBC showed their maximum increase between day 18 (HD1, HD4 and HD5) and day 21 (HD2 and HD3), which was consistently later than the corresponding KLH^{spec} PB.

5.1.5 Circulating KLH^{spec} mBC and long-term anti-KLH serum antibodies were detectable after primary immunization

Donors HD1-HD3 were re-analyzed 18 months (HD1) or 6 months (HD2 and HD3) after the primary, prior to secondary KLH immunization. Here, circulating KLH^{spec} PB were absent in contrast to KLH^{spec} mBC, which were readily detectable, ranging from 0.084% to 1.76% from their parent-gated mBC population (Figure 5-7 A and B). Anti-KLH IgG antibodies were reduced compared to the last sampling time point after primary immunization but still detectable at 20 mg/L - 40 mg/L corresponding to a 2.0-

to 6.0-fold increase to the pre-primary immunization levels (Figure 5-7 C). Anti-KLH IgA was also still detectable at levels 1.2- to 12-fold above the baseline levels before primary immunization.

5.1.6 The secondary KLH serum response was dominated by IgG and exhibited an earlier onset compared to the primary one

To determine whether the primary KLH immunization led to establishment of a functional reactive memory, we next we examined the KLH^{spec} B cell response to KLH booster immunization. Compared to primary immunization, secondary KLH immunization induced different kinetics of appearance of peripheral blood KLH^{spec} PB and mBC as well as a faster and heightened IgG dominated humoral response (Figure 5-7).

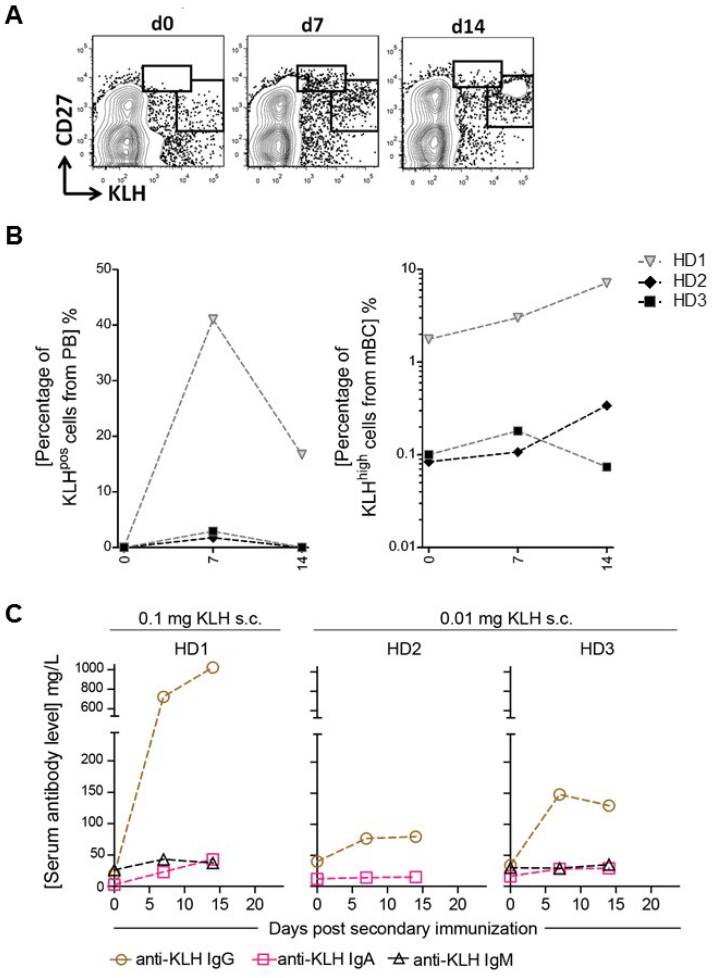

Figure 5-7 KLH^{spec} PB, mBC and anti-KLH serum antibodies showed faster increase upon secondary immunization.
A Dot plots of the appearance of KLH^{spec} human CD3^{neg}CD14^{neg}CD19^{pos} B cells exemplarily shown from donor HD1 on indicated days (d) after secondary KLH immunization. For orientation, gates refer to KLH^{spec}CD27^{high} (PB, upper gate) and KLH^{spec}CD27^{pos} (mBC, lower gate), respectively. **B** Appear-

ance of KLH^{spec} PB (left) and mBC (right) after secondary KLH immunization in peripheral blood. For secondary immunization which was performed 6 months (HD2 and HD3) or 18 months (HD1) after primary immunization, HD1 received 0.1 mg KLH s.c., and HD2 and HD3 both received 0.01 mg KLH s.c. each. **B** Serum titers of anti-KLH IgA, IgM and IgG antibodies after secondary immunization. No value plotted means value was below detection limit.

In detail, circulating KLH^{spec} PB and mBC were increased on day 7 in all three donors with subsequent contraction of KLH^{spec} PB frequencies by day 14 (Figure 5-7 A and B). A further 2.4- to 3.2- fold increase of KLH^{spec} mBC was detected in donors HD1 and HD2, respectively. Anti-KLH IgG antibodies showed a strong 2.0- to 36-fold increase, whereas IgA antibodies showed only a minor increment of 1.2- to 8-fold and IgM antibodies remained largely unchanged (Figure 5-7 C).

These data suggest that primary KLH immunizations induced a reactive immunological memory, i.e. a faster onset and higher magnitude response even to lower dosages. The frequency increment levels of circulating KLH^{spec} primary and secondary PB and mBC further revealed a slight but definite dose-dependence while this was not consistently observed on the serologic level.

5.1.7 Parenterally-induced circulating KLH^{spec} PB exhibited a high incidence of IgA1 isotype usage in their IgH sequences

Next, the composition of the by KLH engaged circulating KLH^{spec} PB and mBC BCR repertoires was analyzed. This analysis was conducted to unravel IgH characteristics related to the underlying diversification and selection processes. Therefore, individual KLH^{spec} PB and mBC were isolated at different time points by single-cell FACS followed by RT-PCR and amplification of IgH variable and constant chain gene rearrangements.

After primary immunization between days 14-18, a total of 207 functional IgH sequences from circulating primary KLH^{spec} PB could be obtained. In these KLH^{spec} PB a predominance of the Ig alpha-1 constant heavy chain region (Cα1) usage was detectable during all days, i.e. 42% - 90% of the sequences used the Cα1, apart from HD2 on day 14 (Figure 5-8 A). Only in 3 of the 5 donors we found KLH^{spec} PB using the Cμ (26 from 207 sequences). IgG subclass usage varied within and between donors with yet frequent emergence of sequences using Cγ1 and Cγ2. Although we frequently detected Cγ sequences, the relative molecular isotype distribution of the circulating KLH^{spec} PB did not correspond well with the relative IgG to IgA isotype ratio of the serologic data (Figure 5-8 B). Nevertheless the somewhat surprising but

consistent appearance of IgA on the serologic and molecular level provides a very interesting finding for this systemic response, without intended or identifiable mucosal contribution (see section 5.1.8). The underlying mechanisms and nature of the Cα class-switch remain to be delineated (145-147).

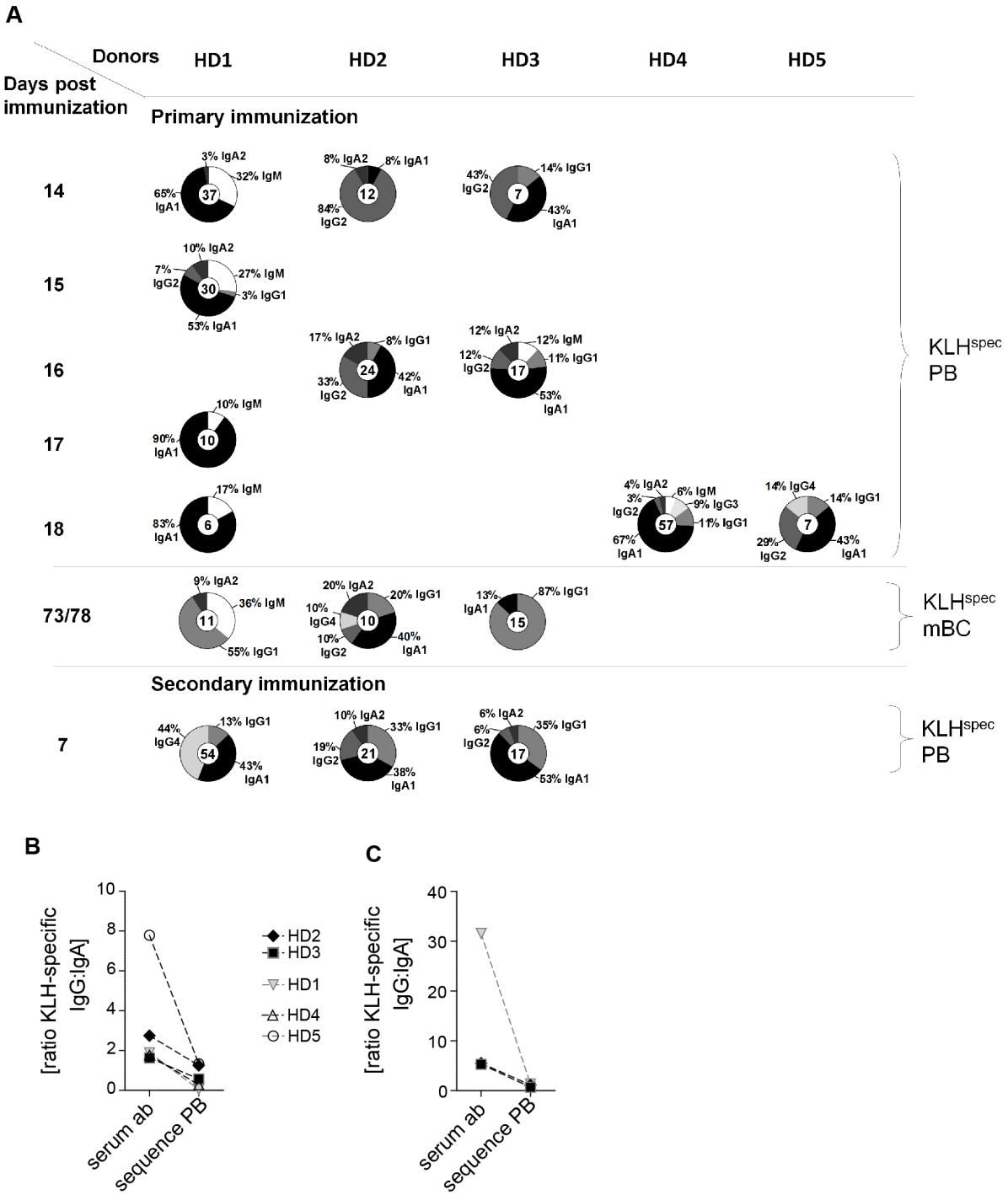

Figure 5-8 IgH sequence isotype usage of KLH^{spec} PB and mBC.
A Pie charts of the heavy constant chain isotype distribution of KLH^{spec} PB and mBC on indicated days after primary (HD1-HD5) and secondary immunization (HD1-HD3). Numbers in circles denote the number of productive sequences included. **B** Ratio of anti-KLH IgG to IgA levels from mean serum

antibody (ab) titers (from days 14-24 after primary immunization) and KLH^{spec} PB IgH sequences (mean of each isotype from primary PB). **C** Ratio of anti-KLH IgG to IgA levels from serum antibodies and KLH^{spec} PB IgH sequences, 7 days after secondary immunization.

Seven days upon secondary immunization, individual circulating KLH^{spec} PB were again isolated using single-cell FACS for sequence analysis. Here, from the three donors, in total 92 sequences could be recovered. Again the Cα1 was employed by a large proportion of these PB (38%-53%), however, we detected a more frequent usage of IgG isotype subclasses (41%-57%) including an increased Cγ1 usage. Yet, the ratio of the IgG to IgA isotype usage again did not correspond with the relative serum levels of anti-KLH IgG to IgA antibodies (Figure 5-8 B).

5.1.8 Adhesion receptor profile of the circulating KLH^{spec} PB

To gain cues on the circulating KLH^{spec} PBs' origin, which expressed IgA1 to a large proportion, the PB were analyzed for their $\alpha4\beta7$ integrin and CD62L homing and adhesion receptor profile (Figure 5-9). The homing receptor $\alpha4\beta7$ integrin is typically expressed on cells activated in the intestinal mucosa, which is associated with IgA expression on B cells. Thereby the $\alpha4\beta7$ integrin homing receptor supposedly guides circulating cells back into mucosal tissues (148). CD62L (L-selectin) is expressed on cells activated or generated in the non-mucosal periphery (i.e. parenteral) and guides the cells to peripheral lymph nodes (149-151). In humans, it has been shown that mucosally activated circulating PB expressed $\alpha4\beta7$ integrin to 99% with only a minor fraction co-expressing CD62L. In contrast, parenterally induced circulating PB literally all expressed CD62L and up to 50% of these co-expressed also $\alpha4\beta7$ integrin (152, 153). Here, the phenotypic analysis of the circulating PB revealed that the majority of the primary KLH^{spec} PB carried a systemic adhesion receptor profile, i.e. 65-97% of day 14-24 KLH^{spec} PB expressed CD62L and 0-47% of these co-expressed $\alpha4\beta7$ integrin while only a minor fraction expressed $\alpha4\beta7$ integrin without CD62L co-expression. The proportion of the latter fraction does not correspond to the frequencies of Cα1 expressing PB. Thus, the circulating KLH^{spec} IgA^{pos} PB were most likely not of mucosal origin.

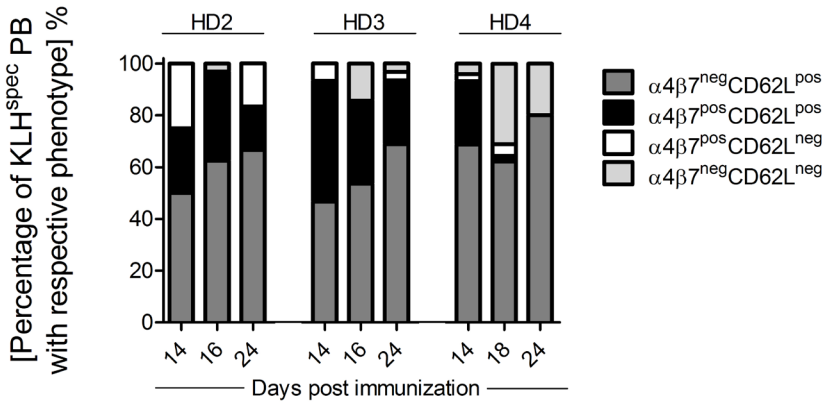

Figure 5-9 Homing receptor expression of circulating KLH^{spec} PB after primary immunization. Phenotypic analysis of $\alpha4\beta7$ integrin and CD62L expression of circulating primary KLH^{spec} PB on indicated days after primary parenteral KLH immunization in donors HD2, HD3 and HD4.

5.1.9 Isotype usage of circulating KLH^{spec} mBC showed only little overlap to primary and secondary KLH^{spec} PB

2.5 months after primary immunization KLH^{spec} mBC were isolated by single-cell FACS from donors HD1-HD3 and their IgH sequence characteristics analyzed. Here, from the 3 donors in total 36 single-cell sorted KLH^{spec} mBC IgH sequences were recovered (Figure 5-8 A). For HD1 and HD3 we found that the IgH isotype usage differed to that observed for KLH^{spec} primary and secondary PB, i.e. more pronounced Cγ1 chain and reduced Cα1 usage. Notably, in HD1 we found KLH^{spec} mBC using Cμ. Although this is so far only an isolated finding, the principle presence of IgM mBC in parallel to switched mBC both specific to the same TD antigen could be a hint that in humans a similar labour division of mBC subsets exists as has been discussed for the murine mBC compartment (154, 155). Thereby IgM mBC are thought to play a role in maintaining the mutational flexibility of the memory repertoire by being poised to re-enter into the GC response upon re-challenge, contrasting the behaviour of switched mBC which were shown to generate PB more vigorously upon re-exposure (155).

5.1.10 V_H and J_H segment repertoire usage

A major structural restriction in the reactivity of an antibody towards an antigen lies in the employed variable region gene segments, wherefore the KLH^{spec} IgH variable region gene repertoire was investigated in more detail. This analysis comprised the description of V_H- and J_H segment and family usage and pairings for each donor, cell

type and day post vaccination. The V_H and J_H usage was further compared with the V_H and J_H repertoire of peripheral blood naïve B cells described by Wu et al. (156). As a result, we found that in all donors and KLH^{spec} PB and mBC, respectively, segments of either the V_H3 or V_H4 families were used most frequently, i.e. by more than 66% of all rearrangements (Figure 5-10).

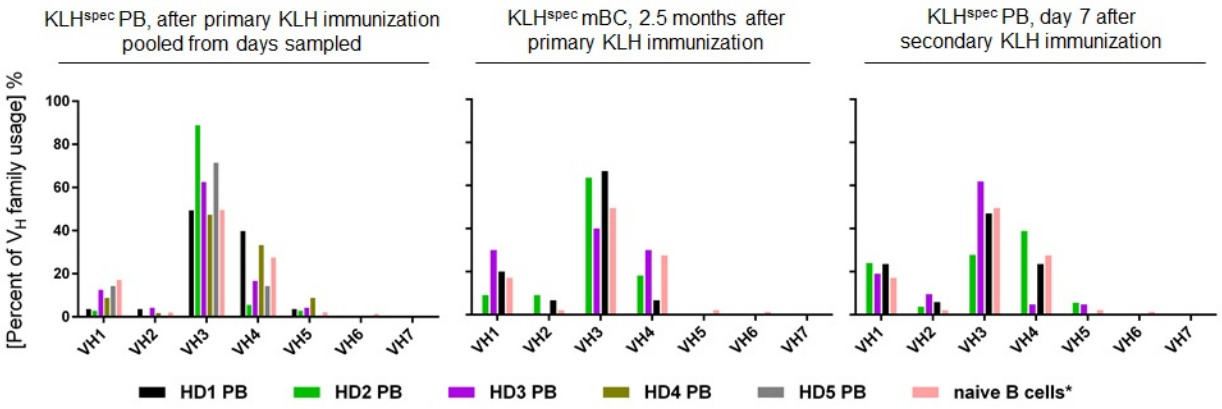

Figure 5-10 V_H family usage within the expressed variable heavy chain regions from KLH^{spec} B cell subsets.
Distribution of V_H family segment usage for KLH^{spec} PB pooled for each donor from all respective sampled days after primary immunization (left), from KLH^{spec} mBC isolated 2.5 months post primary immunization (middle) and from day 7 KLH^{spec} PB after secondary immunization (right). For orientation frequencies of V_H usage from naïve B cells* are additionally shown, from Wu et al. 2010 (156).

In relative terms, for V_H1, V_H3 and V_H4 usage differences to the naïve B cell repertoire appear only of minor nature. Yet, employing a χ^2 goodness-of-fit-statistical test to compare the individual used V_H distributions (absolute numbers) with the V_H segment usage distribution of naïve B cells (156) revealed that KLH^{spec} B cells differed significantly from the naïve B cell repertoire in this aspect ($p<0.001$ in all cases) especially in conjunction with the fact that V_H6 and V_H7 family segments were not used in any of the KLH^{spec} IgH variable regions in contrast to naïve B cells. Hence this analysis indicated general selection of the KLH^{spec} B cell repertoires.
In HD1 and HD2, significant variations between the different KLH^{spec} B cell pools were observed, i.e. in HD1, secondary PB exhibited a significant different V_H distribution compared to primary PB ($p\chi^2<0.001$) while mBC did not. In HD2, both mBC and secondary PB differed in their V_H family usage distribution from the primary KLH^{spec} PB (both $p\chi^2<0.001$) suggesting ongoing selection processes during the responses.
A more detailed analysis of the individual V_H segments employed in the KLH^{spec} PB and mBC sequences revealed that the KLH^{spec} B cell clones were not randomly selected from across the entire gene locus repertoire but appeared to distribute in a

biased fashion, i.e. some segments were overrepresented while others were not used at all (Figure 5-11).

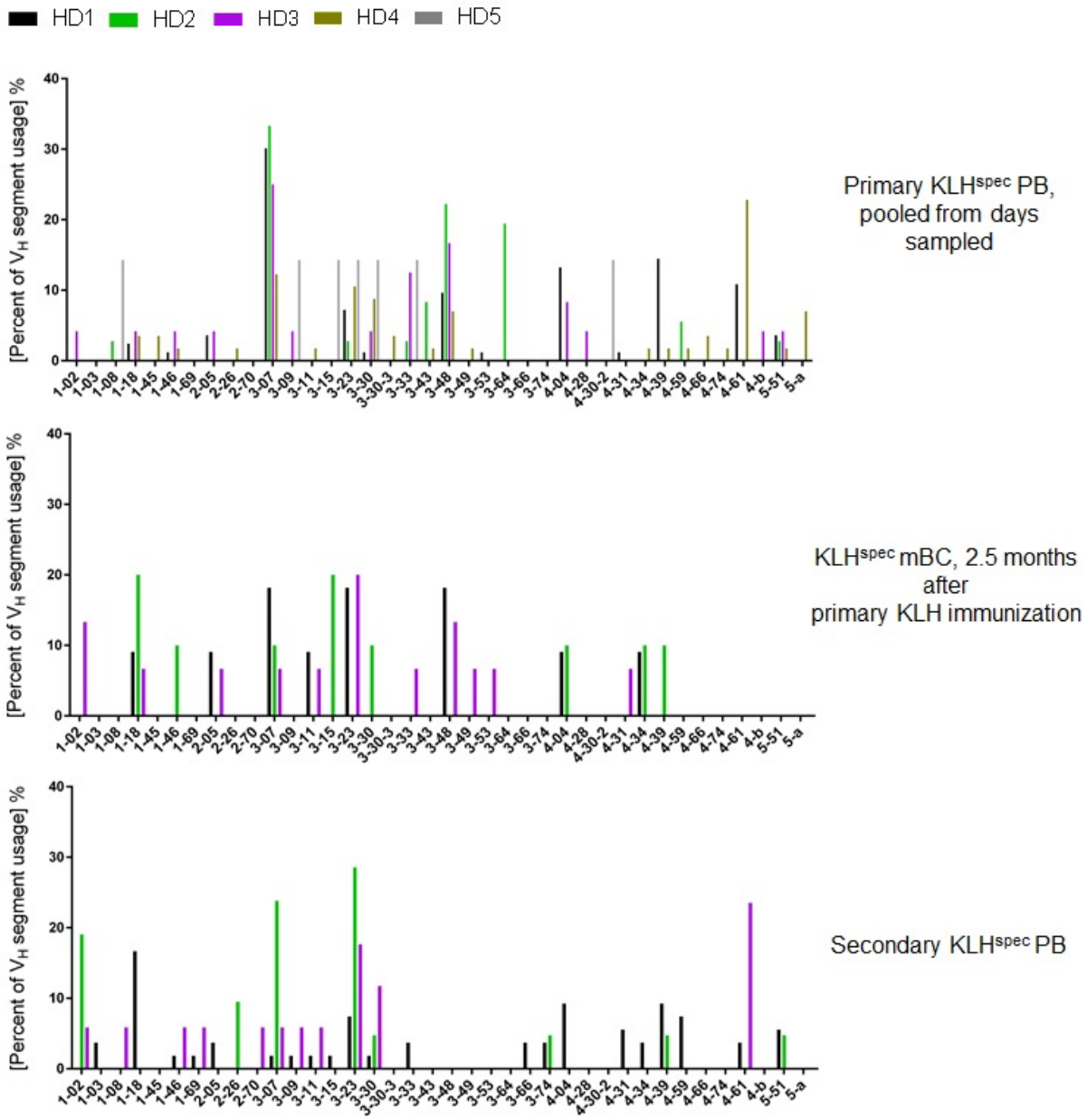

Figure 5-11 V_H segment usage within the expressed variable heavy chain region genes from KLH^{spec} B cell subsets.
Distribution of V_H segment usage from KLH^{spec} donor-individual pooled primary PB, mBC and secondary PB, respectively.

Due to the partial presence of only one sequence employing the one or other segment further statistical calculations were not carried out at this point. Noteworthy though is the repeated presence of V_H3-07 and V_H3-48 segments in primary KLH^{spec} PB consistent in all donors, while secondary KLH^{spec} PB still employed V_H3-07 but no V_H3-48 segments in their sequences, i.e. V_H3-48 segments apparently underwent negative selection in the course of the KLH (re-challenge) response.

Analysis of the J_H family usage revealed that all of the known functional J_H family genes were employed in the KLH^{spec} B cell repertoire (Figure 5-12). The relative overall J_H gene segment usage followed the general distribution of the relative segment family usage of a naïve B cell repertoire, i.e. J_H4 segments (J_H4) were the most frequently used J_H segments, apart from HD2 day 78 KLH^{spec} mBC, where J_H6 was found to be used most often (50%) followed by the J_H4 (20%) segments. Yet, employing a χ^2 goodness-of-fit test again to compare the individual used J_H distributions with the J_H segment usage distribution of naïve B cells (156) revealed that KLH^{spec} B cell subsets from all donors exhibited significant differences in this regard to the naïve B cell repertoire ($p\chi^2<0.001$ in all cases). Furthermore, comparably to the V_H segment family usage in HD1, KLH^{spec} mBC exhibited a significantly distinct distribution compared to primary PB ($p\chi^2<0.01$) as well as secondary PB ($p\chi^2<0.001$). Also in HD2, the mBC showed a significant different J_H distribution compared to primary PB ($p\chi^2<0.001$) while secondary PB did not.

However, as the number of sequences and experiment repetition is small, the statistical power of these χ^2 tests is limited and precludes firm conclusions. Thus this data can only serve as an indication that selection of the KLH^{spec} B cell repertoire occurred and was presumably re-initiated during the re-challenge.

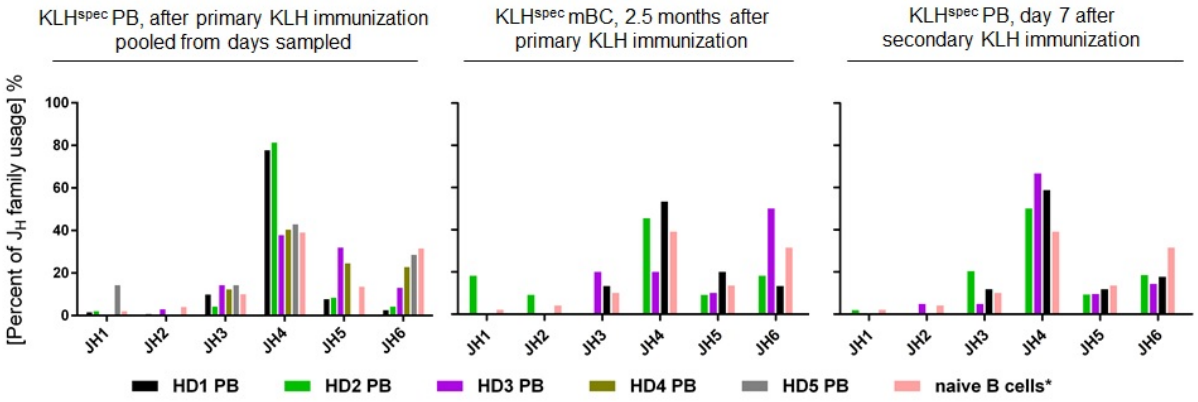

Figure 5-12 J_H family usage within the expressed variable heavy chain regions from KLH^{spec} B cell subsets.
Distribution of J_H family segment usage for KLH^{spec} PB pooled for each donor from the sampled days after primary immunization, from KLH^{spec} mBC and secondary PB. For orientation frequencies of J_H usage from naïve B cells* are additionally shown, *from Wu et al. 2010 (156).

Analyzing the recombination of V_H to J_H segments revealed that members of the V_H3 gene family were recombined with J_H1, J_H3, J_H4, J_H5 and J_H6 gene segments, re-

spectively, all to a comparable extent while members of the V_H4 family were most frequently found in combination with J_H4, J_H5 or J_H6.

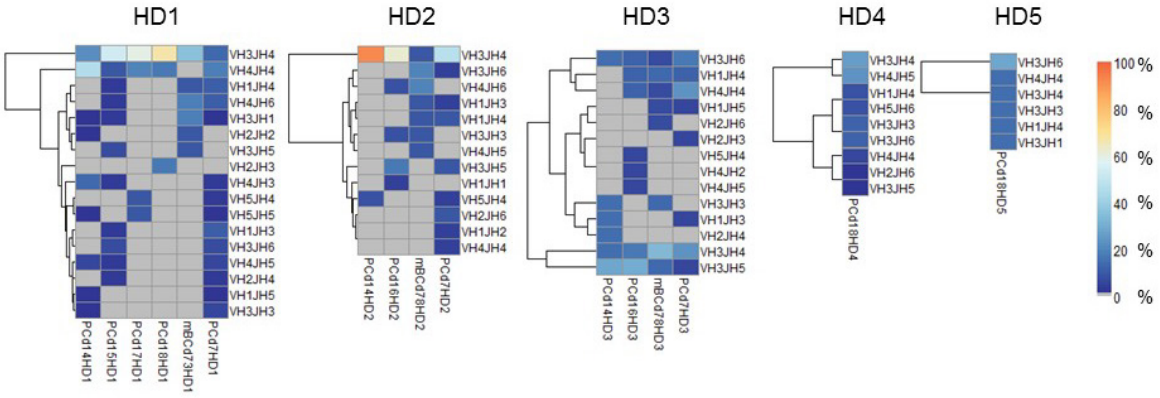

Figure 5-13 Heatmaps of V_H to J_H family segment combinations used by KLH^{spec} PB and mBC after primary and secondary immunization.
PC = KLH^{spec} PB; d= day. The heatmaps were generated using R (pheatmap-package; euclidean distance and hierarchical clustering (complete) were used (131, 157)).

5.1.11 Simultaneous presence of low and highly mutated primary KLH^{spec} PB sequences

Next, to gain insights into the maturation status of the response, the frequency and imprints of SHM in the V_H regions (FWR1 through FWR3) as compared to their predicted germline gene sequences were examined. The results are shown in Table 5-1 and Figure 5-14 A.

Table 5-1 Summary of molecular properties of expressed IGH sequences of KLH^{spec} B cells.

Donor	Day post immunization	KLH^{spec} B Cell Type	Sequences mutated %	Number of mutations per V_H region median (range)	accumulated R/S ratio CDRH1&2	accumulated R/S ratio FWR 1-3	Total number of nucleotides	Total number of mutations	Median mutation rate***	Number of sequences	Number of unique sequences (clones)
HD1	14	PB	100	7 (1-25)	5.4	1.7	8283	306	0.00074	37	18
HD1	15	PB	93	19.5 (0-32)	9	1.6	6780	480	0.00198	30	19
HD1	17	PB	100	25 (5-28)	28.5	1.8	2226	199	0.00215	10	5
HD1	18	PB	100	20 (5-25)	4	1.5	1362	104	0.00161	6	4
HD1	73	mBC	91	9 (0-19)	4	1.3	2469	100	n/a	11	11
HD1	7*	PB	100	18 (9-62)	3.6	1.5	12168	1027	n/a	54	49
HD2	14	PB	100	9 (8-24)	1.5	1.8	2616	158	0.00106	12	5
HD2	16	PB	100	15 (3-29)	3.6	1.5	5357	378	0.00139	24	12
HD2	78	mBC	100	16 (7-26)	4.8	2.1	2181	158	n/a	10	9
HD2	7*	PB	100	14 (7-30)	4.5	2	4623	321	n/a	21	17
HD3	14	PB	100	26 (3-46)	3.9	1.7	1578	180	0.00276	7	6
HD3	16	PB	100	12 (2-22)	4.8	1.5	3819	210	0.00109	17	15
HD3	78	mBC	100	6 (4-17)	5.4	2.2	3351	125	n/a	15	14
HD3	7*	PB	100	13 (6-47)	4.7	1.7	3756	273	n/a	17	14
HD4	18	PB	77	8 (0-40)	2.4	1.7	12857	453	0.0006	57	32
HD5	18	PB	29	0 (0-21)	n.a.**	n.a.**	1620	30	0	7	7

* days post secondary immunization
** no silent mutations were observed.
*** mutations/bp/generation (with 8 hours cell cycle)

This analysis revealed that 187 out of 207 IgH gene rearrangements obtained from primary KLH^{spec} PB, i.e. 90%, were mutated. Only few unmutated sequences were

found in donors HD1, HD4 and HD5. The decrease and increase of average SHM between the days did not allow deduction of a universal pattern. In detail, in HD1 and HD2 an increase of the median mutation frequency from day 14 to days 15-18 to relatively high average mutation frequencies of 8.7%-11% (HD1, days 15-18) and 6.7% (HD2, day 16), respectively was found. In contrast, in HD3, the median mutation frequency decreased from day 14 (11.6%) to day 16 (5.3%).

Nevertheless, a striking universal pattern regarding the presence of highly mutated sequences among these primary KLH^{spec} PB was identified in all donors, i.e. 36% of the primary PB sequences carried 15 mutations or more (mutation frequency ≥ 7%) in their expressed V_H region genes. Such high mutation frequencies were found to be largely independent of the underlying isotype, with the exception of the in total 5 V_H transcripts from $C\gamma3$ and $C\gamma4$ rearrangements that were completely unmutated (Figure 5-14 B).

Next, the pattern of SHM was further analyzed. Antigen-driven selection of the antigen-binding variable region of the BCR in the framework of a GC reaction influences the pattern of SHM. Of interest here is a comparison of the ratios of replacement (R) to silent (S) mutations in the FWR and the R/S ratio in the CDRH which provides insight into selection processes. The FWR R/S ratio should decrease and the CDRH R/S ratio should increase as the GC reaction proceeds and functional selection on the basis of improved antigen binding occurs (158). The pattern of SHM of primary KLH^{spec} PB IgH sequences sampled over several days fit this hypothesis of antigenic selection, i.e. in HD1-HD3 CDRH R/S mutation ratio progressively rose from day 14 to day 16 or day 17, respectively (Table 5-1) and primary KLH^{spec} PB FWR R/S ratios were generally smaller than R/S ratios from CDRH (CDRH1 and CDRH2), with the exception of day 14 PB from HD2.

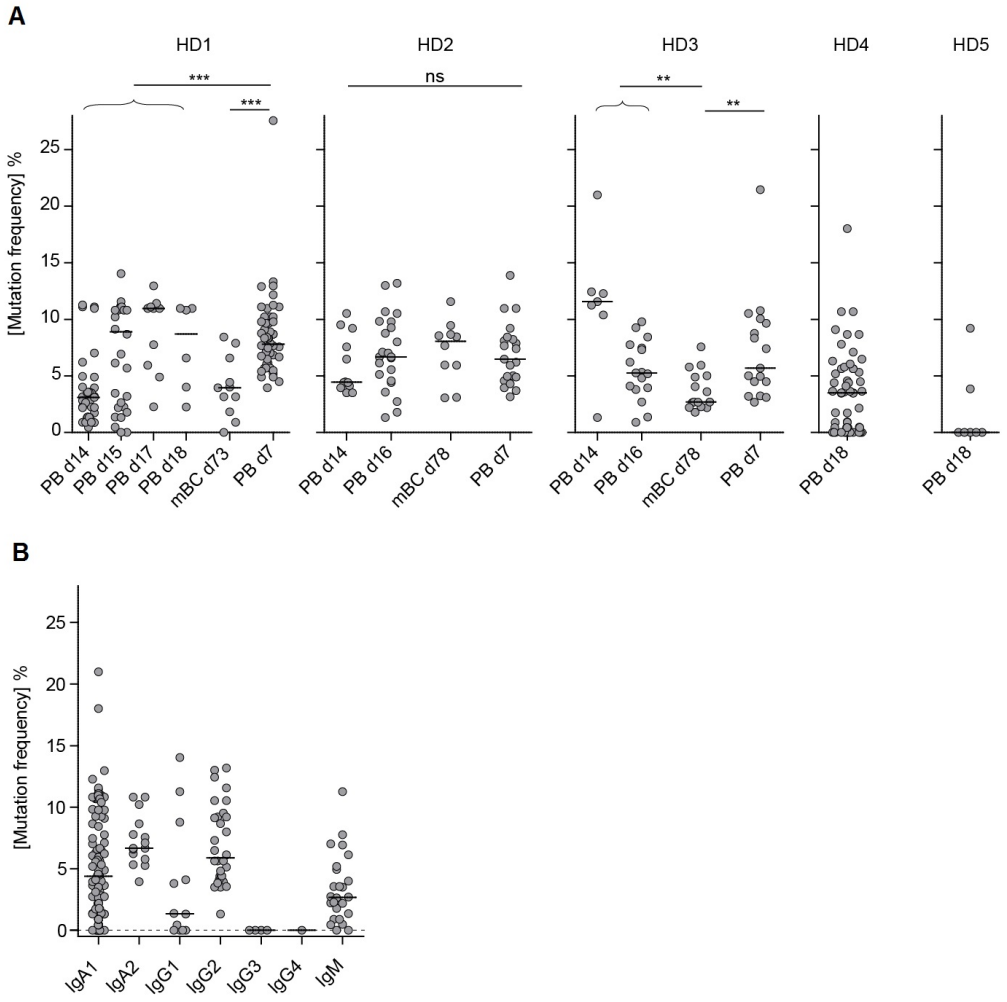

Figure 5-14 Somatic hypermutation within V_H segments of KLH^{spec} PB and mBC.
A Frequencies of SHM within V_H regions (FWR1-FWR3) from individual KLH^{spec} PB or mBC for each donor on indicated days (d). Mann-Whitney tests were performed with p≤0.001 represented by ***, p≤0.01 represented by ** and p>0.05 considered as no significant difference (ns). For reasons of visual clarity, only significant differences revealed by testing are indicated for HD1 and HD3 while for HD2 no significant differences were found at all. **B** Mutation frequencies for each V_H according to its corresponding IgH isotype subclass of primary KLH^{spec} PB were pooled from all donors for this graph.

5.1.12 Mutation rate of the highly mutated primary KLH^{spec} PB

The simultaneous occurrence of un- to low mutated primary KLH^{spec} PB sequences together with the highly mutated sequences, of which the latter comprised approximately one third of the primary KLH^{spec} PB repertoire, prompted the investigation whether the highly mutated PB could be generated from naïve B cells within 2-3 weeks under the known pre-requisites, i.e. a SHM rate ranging from $4x10^{-4}$ to $1.1x10^{-3}$ mutations per bp per division (159-163) and general cell division times between 6 hours to 18 hours (24, 129, 164). More detailed analyses of the actual murine GC B cell division time arrived at estimates between 6-8 hours (129).

Accordingly, a hypothetical maximum mutation rate for each primary PB sequence was calculated, based on the number of mutations observed per analyzed nucleotides, i.e. V_H sequence length, on the respective day (Figure 5-15 and Equation 1). Assuming 8 hours per cell cycle the calculation revealed that 22% of the primary KLH^{spec} PB IgH sequences would have been exhibited to mutation rates of $2x10^{-3}$ mutations/bp/generation or higher corresponding to at least two times higher mutation rates than the maximum rates described (Figure 5-15 A). Moreover, this calculation also showed that on 8 out of the 10 sampling time points from all donors, the average mutation rate of the primary PB was above that of $1x10^{-3}$ mutations/bp/generation, when the unmutated PB were excluded, accordingly to the calculations described in the literature (Figure 5-15 B). Even when unmutated PB were included this notion was still true for 7 out of the 10 sampling time points (not shown).

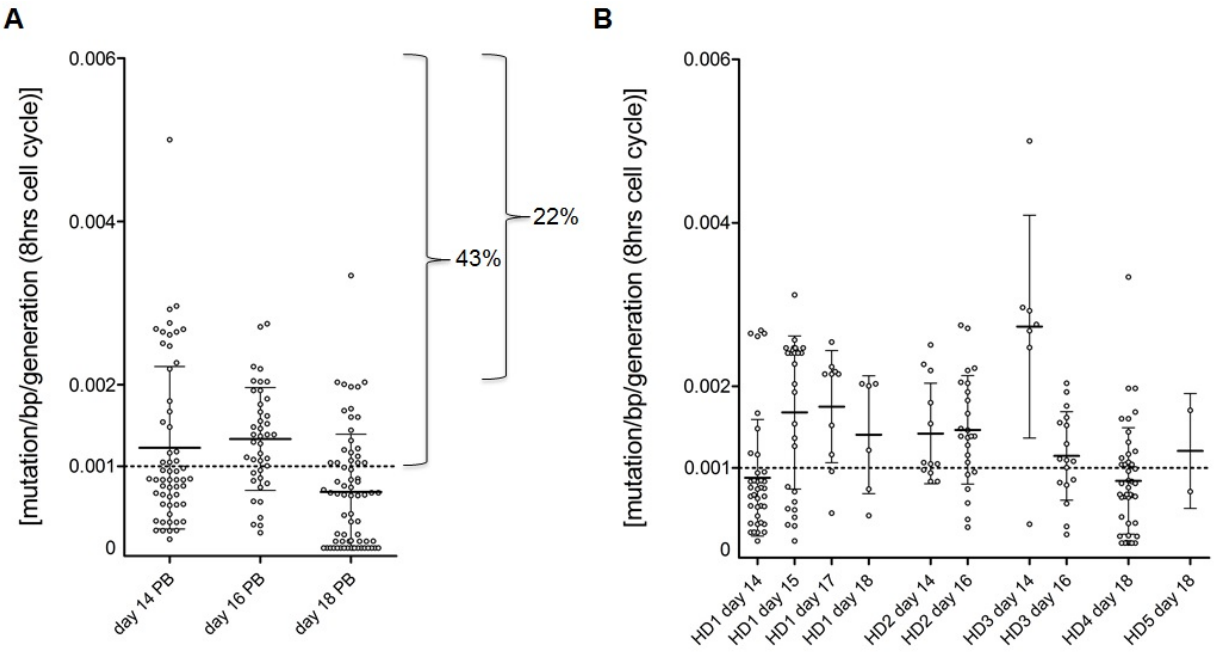

Figure 5-15 Mutation rate of primary KLH^{spec} PB.
A Calculated hypothetical mutation rates from individual KLH^{spec} primary PB sequences determined from the number of mutations per analyzed nucleotides (bp) of the respective V_H segment with an assumed cell cycle length of 8 hours (hrs). For orientation, a previously described and later confirmed mutation rate is shown by the dotted line, i.e. $1x10^{-3}$ mutations/bp/generation (159, 163). Brackets and frequencies indicate percentage of sequences that theoretically underwent mutation rates higher than $1x10^{-3}$ (43%) or $2x10^{-3}$ (22%) mutations/bp/generation. Unmutated sequences were included in calculation of the average rate. **B** Mutation rates calculated as under **A**, but day and donor individual shown for the mean calculation whereby unmutated sequences were excluded.
Bar indicates mean ± standard deviation.

Importantly, these calculations refer to peripheral blood PB and not to GC B cells, for which the previous rates were inferred. Furthermore these calculations do not con-

sider any lag phase or time for GC-, division- or SHM onset nor any kind of selection factor, time for PB differentiation or for tissue egress. Thus the calculated rates will underestimate the actual rates required to obtain the numbers of mutations observed. In consequence, mutation frequencies and rates of at least 22% of these primary PB are inconsistent with prior described observations and assumptions. Unless there are unknown or missing assumptions, e.g. mutation rates in humans could be generally higher than in murine B cells which however would in turn be inconsistent with the simultaneous presence of the low and highly mutated primary PB on the same days, I put forward the hypothesis that the highly mutated primary PB are the progeny of presumably cross-reactive mBC recruited into this response.

5.1.13 SHM from the primary- to the memory- to the secondary repertoire did not follow a gradual increase

The circulating KLH^{spec} mBC 2.5 months after primary immunization from HD1 and HD3 lacked highly mutated sequences (Figure 5-14 A and Table 5-1) either suggesting that the mBC precursors left the GC response earlier than the PB precursors or that the progenitors of the highly mutated primary PB sequences could not compete with the lower mutated sequences and were deleted from the repertoire. More detailed sequence repertoire analyses will permit more subtle insights into these aspects.

Upon secondary immunization, all V_H sequences were found somatically mutated. However, in HD2 and HD3, compared to primary KLH^{spec} PB no significant increase of the median mutation frequency and number could be detected whereas in HD1 the average increase of somatic mutations was significant (Mann-Whitney test, $p<0.001$; Figure 5-14 A). Whether this increase comprised additional SHM within V_H sequences of PB detected during primary immunization, i.e. indicative of SHM re-initiation upon re-challenge, or whether the secondary response comprised an underlying different sequence repertoire will also be revealed by a more detailed analysis of the primary PB, mBC and secondary PB clonal repertoires (see below).

5.1.14 Circulating primary KLH^{spec} PB repertoires showed within donor between day variations

We next studied the KLH^{spec} IgH sequences for their CDRH3 length distribution (Figure 5-16) as restricted antigen-specific antibody responses have been shown to select for CDRH3 loops of particular lengths (45, 165, 166). Moreover the CDRH3 region allows first conclusions on the clonality of an immune response.

For the primary KLH^{spec} PB it was thereby apparent that a broad range of CDRH3 lengths was found, with donor-specific values for minimum and maximum lengths, overall ranging from 18 to 78 bp, indicative of a relatively unrestricted response. However donor-specific accumulations of certain lengths could be identified, partly resulting from clonally related cells (described below). As the CDRH3 region is the main site of specific contact between the antibody and the antigen, it is reasonable to assume that similar antigenic recognition sequence patterns may be present in between the donors at this site. Therefore a search for sequence motifs within CDRH3 regions was conducted using the MEME suite, ClustalW and Weblogo (125-128). However, no common amino acid sequence motifs could be identified, neither between KLH^{spec} CDRH3 sequences within a donor nor across donors (data not shown).

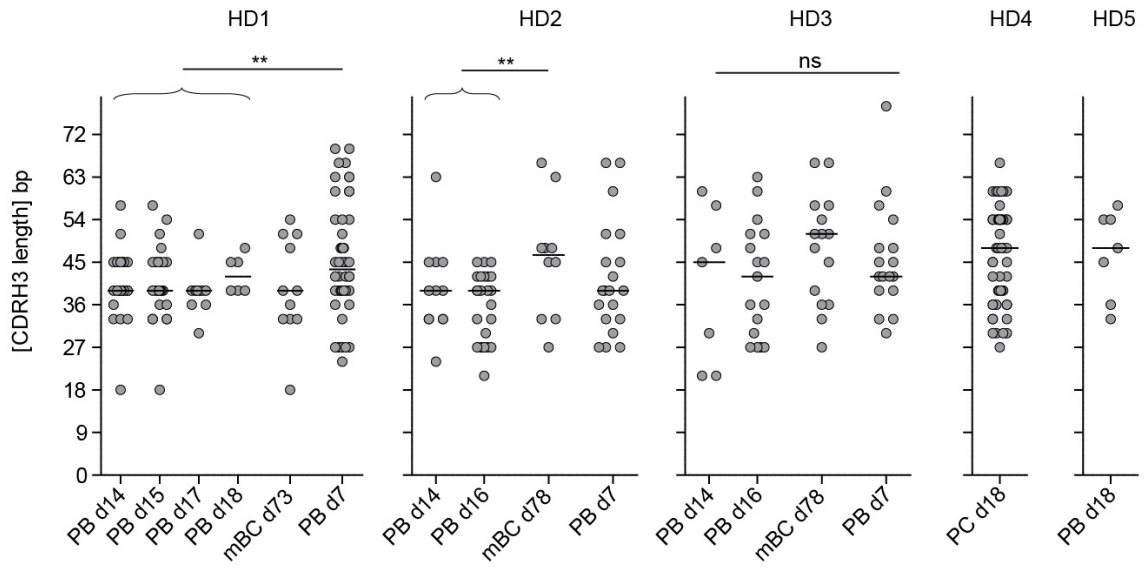

Figure 5-16 CDRH3 sequence lengths of KLH^{spec} primary PB, mBC and secondary PB.
Distribution of CDRH3 lengths in base pairs (bp) of KLH^{spec} B cell subsets for each donor and day (d) as indicated. Bar indicates median. Mann-Whitney tests were performed with $p \leq 0.01$ represented by ** and $p > 0.05$ considered as no significant difference (ns). For reason of visual clarity, only significant differences revealed by testing are indicated for HD1 and HD2 while for HD3 no significances were found at all.

As the distribution of the CDRH3 lengths of KLH^{spec} primary PB indicated oligo- to low order polyclonal repertoires with a certain underlying day-wise exchange of the circulating pools (Figure 5-16) the IgH sequences were further analyzed for clonally expanded cells. A clone was defined by its unique IgH variable region sequence including the CDRH3 length and sequence, as described by us before (38). This analysis identified trees of clonally related and expanded PB and mBC within the KLH^{spec} B cell pools of HD1-HD4 and no sequences qualifying as clonally related were found between individual donors. Pies of the circulating KLH^{spec} primary PB, mBC and secondary PB repertoires are shown in Figure 5-17.

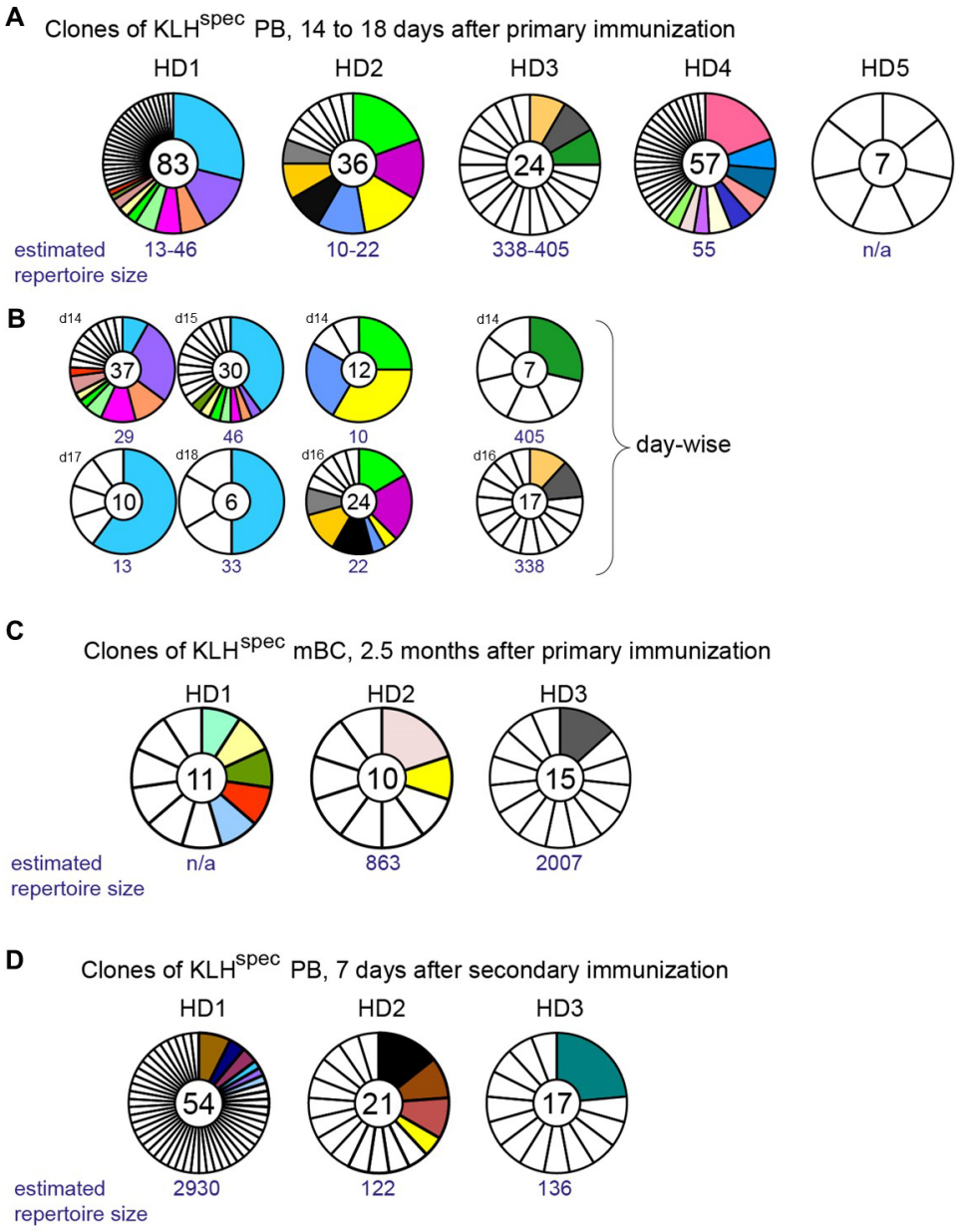

Figure 5-17 Donor individual KLH^{spec} B cell clone repertoires and relationships through the KLH response.

Pie charts representing the different clonal families of KLH^{spec} PB and mBC. White slices denote those sequences found only once during the entire response. Circled number within each pie chart denotes the total number of sequences and slices are unique clones and proportional to clone size. Numbers underneath the pies are the one-sided 95% confidence limits of the maximum likelihood estimates of the statistical repertoire sizes, calculated with the Stirling's numbers of the second kind, as described before (130). **A** Pies of donor individual pooled primary PB are shown for days 14-18. KLH^{spec} PB sequences found only once between days 14-18 of that yet clonally related cells were found in the KLH^{spec} mBC or secondary PB compartment were also marked by a color piece. **B** Day-wise primary clonal repertoires for HD1 – HD3.
Pie charts of KLH^{spec} mBC are shown under **C** and for KLH^{spec} secondary PB under **D**.

As has been already indicated by the CDRH3 length distribution for HD1 - HD3, the detailed sequence repertoire analyses revealed a within donor between day variation for the primary KLH^{spec} PB (Figure 5-17 A and B). To support this notion further a statistical prediction of the theoretical repertoire sizes based on the isolated repertoires was made using a statistical repertoire size estimation, as described (130). With this approach a maximum likelihood estimate *n* $(P(d)_{max})$ for each donor and day and a 95% one-sided confidence limit *n* $(P(d)_{<0.05}$; Table 5-2) could be calculated. To shortly explain, *d* is the number of distinct gene rearrangements, *r* is the number of all examined gene rearrangements and *n* is the theoretical statistical calculated quantity of different clones within one individual, to ensure the empirical found numbers of observed distinct sequences among all of the examined sequences (see Equation 2). This calculation yielded differing daily repertoire sizes (i.e. rearrangement events) and thus supported the suggestion that the circulating primary PB were partially exchanged between the sampled days (Figure 5-17 B and Table 5-2).

Table 5-2 Statistical calculations of repertoire sizes

Donor	Day post immunization	Cell Type	$P(d)_{<0.05}$ for n=	$P(d)_{max}$ for n=	d	r
HD1	14	PC	29	21	18	37
HD1	15	PC	46	29	19	30
HD1	17	PC	13	5	5	10
HD1	18	PC	33	6	4	6
HD1	73	mBC	n/a	n/a	11	11
HD1	7	PC	2930	270	49	54
HD2	14	PC	10	5	5	12
HD2	16	PC	22	14	12	24
HD2	78	mBC	865	42	9	10
HD2	7	PC	122	45	17	21
HD3	14	PC	405	19	6	7
HD3	16	PC	338	64	15	17
HD3	78	mBC	2007	100	14	15
HD3	7	PC	136	41	14	17
HD4	18	PC	55	43	32	57
HD5	18	PC	n/a	n/a	7	7

5.1.15 Largely unrelated circulating KLH^{spec} primary, memory and secondary B cell repertoires

Next, also KLH^{spec} mBC and secondary PB were analyzed for their clonal composition. For HD2 and HD3, one mBC was found for each donor of which a related sequence was isolated already from the respective circulating primary PB pool. For HD1, four related KLH^{spec} mBC of which primary PB clones existed were found (Figure 5-17 C). Thus, in conclusion the majority of primary KLH^{spec} PB clones were not reflected in the analyzed circulating KLH^{spec} mBC, which interestingly appeared to be more poly- than oligoclonal in comparison to the primary PB repertoire.

From the secondary PB sequences we could retrieve in total 4 clones that were related to primary PB. Thus clonal relationships between the secondary and primary repertoire were even more infrequent than from the primary to the mBC repertoire (Figure 5-17 D). Further, only in HD1 and HD2 individual secondary PB sequences were found that were related to the analyzed mBC after 2.5 months. Hence, the secondary KLH^{spec} PB repertoire exhibited a considerable deviation to the KLH^{spec} primary PB and mBC repertoire (Figure 5-17). Notably, theoretical repertoire size calculations revealed for HD1 and HD2 more diverse secondary KLH^{spec} PB (progenitor) repertoires compared to the primary KLH^{spec} PB.

In summary, these analyses disclosed largely different circulating KLH^{spec} B cell repertoires between the primary and secondary effector cells and the steady state mBC, as illustrated in Figure 5-18.

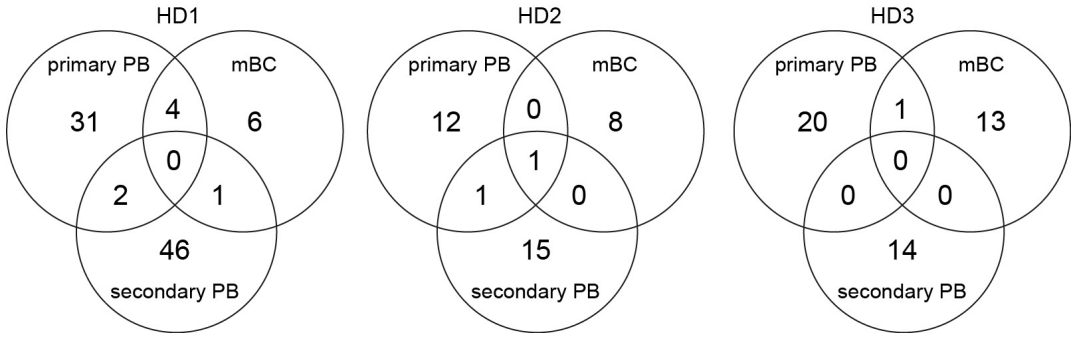

Figure 5-18 Venn diagrams of clonal overlap between KLH^{spec} B cell pools.
The Venn diagrams show clonal overlap of KLH^{spec} primary PB, mBC and secondary PB sequences for HD1-HD3. Given are the numbers of unique and overlapping clones in the respective compartment.

5.1.16 Absence of a universal affinity maturation and CSR axis within clonally expanded KLH^{spec} B cell genealogy trees

Finally, analysis of genealogic trees of clonally expanded KLH^{spec} B cells in more detail was performed to assess whether individual clones converged toward a single (higher mutated) variant on a clonal branch or diverged across multiple options along diversification in several branches independently and to uncover potential common maturation axes.

A selection of such trees from HD1 to HD4 is shown in Figure 5-19 a-m. This analysis found examples of divergent branches of subclonal variants (a-k) where further diversification (independent of the underlying mutation load) occurred and other examples where no such diversification was evident (l,m). Within some of these trees both possibilities were found (a,b,c,e,i,j,k).

Also examples of clonally related cells were identified which diverged across antibody classes (a,b,c,f,g,j,l,m) and other examples where they did not (d,e,h,i,k) leaving room for speculation on switch cues and differentiation environments for equally mutated clones with distinct isotype usage.

In donors HD1-HD3, where few clonally related KLH^{spec} primary PB and mBC could be retrieved (a,b,d,g,i), two examples of mBC that were less mutated than the corresponding PB (a, d) were found whereas in the other examples mBC exhibited a higher mutation load (b,g,i).

In the few cases of clonally-related KLH^{spec} primary and secondary PB some of these trees suggested that re-diversification of the precursors may have occurred while other examples did clearly not support that notion, including examples of both possibilities even within the same trees (i,h and c,h respectively).

These results indicate that clonal diversification and selection processes are very dynamic and complex for this response. Potentially, larger sampling sizes and more sampling time points could help to unravel existent directional maturation axes. The data here do not allow conclusions about the latter nor do they provide clarification to whether mBC re-enter GC upon reactivation, as the data here are indicative of both pathways, i.e. GC-dependent and GC-independent PB generation from mBC.

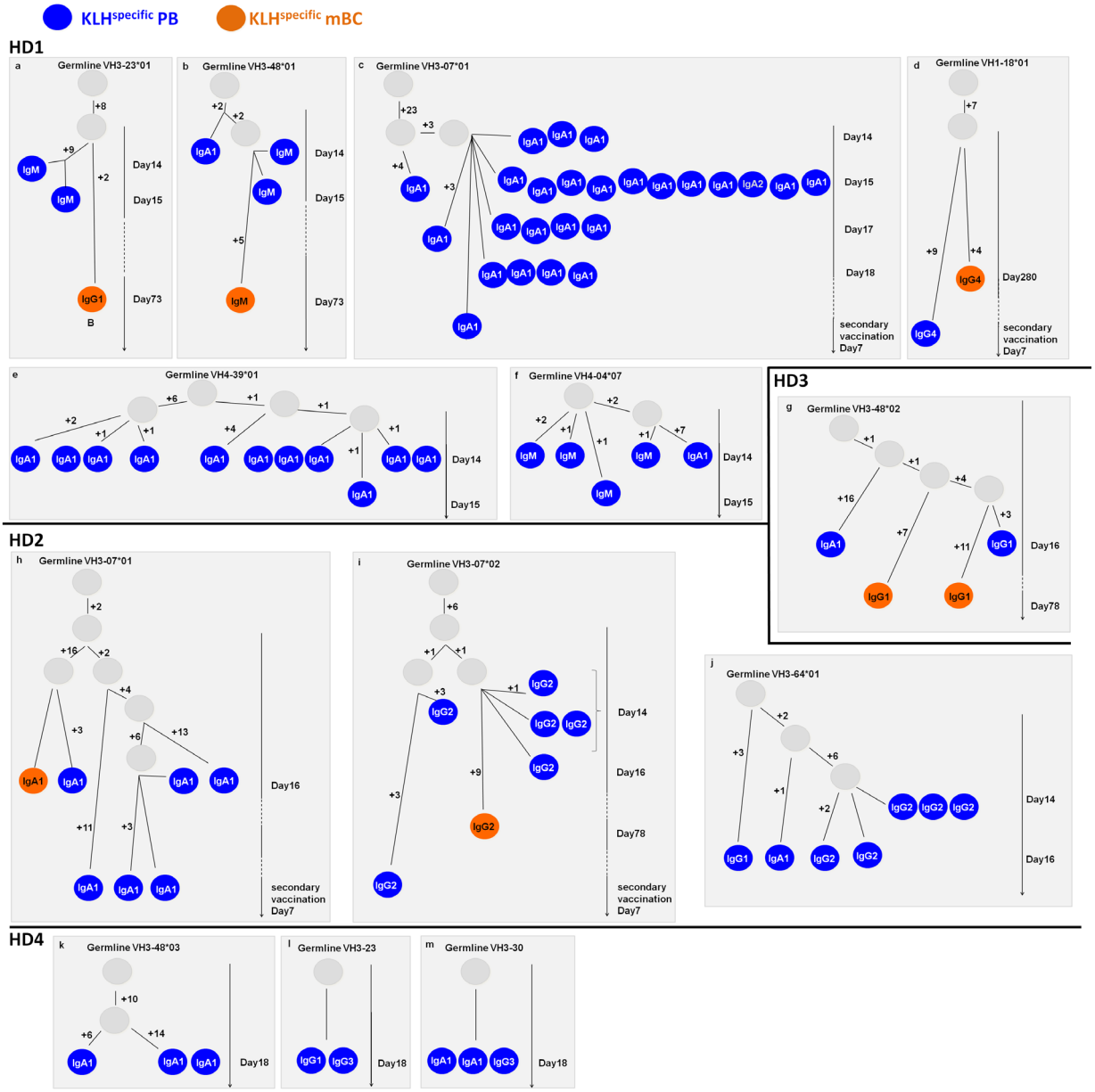

Figure 5-19 Genealogic trees of individual expanded B cell clones.
Selected genealogic trees of different primary PB, mBC and secondary PB clonally related cells from HD1 – HD4, found on indicated days. In donor HD5, no clonally related cells were found. Grey circles denote hypothetical logical precursors. The predicted germline sequence is printed above each clone. Numbers on branches indicate numbers of shared mutations of the successive cells. Isotype printed within the circles are the isotype of the respective cell. Blue circles: KLH^{spec} PB sequence. Orange circles: KLH^{spec} mBC sequence.

5.2 Tissue distribution and related phenotype of human memory B cells

One result from the previous investigation was that primary KLH immunization induced an immunological memory. For the B cell memory compartment such memory consists of long-lived PC and mBC. Whereas it is acknowledged that long-lived PC preferentially reside in niches in the BM (65, 68) as well as in spleen (67, 86) and tonsil (87, 167), little is known about potential survival niches for mBC and the role of certain organs in mBC maintenance and functionality. To address this question a comprehensive mapping, including quantification and phenotyping of mBC within different lymphoid organs, i.e. spleen, BM and tonsil compared to peripheral blood, during steady state conditions was conducted. Furthermore, effects on circulating mBC proportions potentially resulting from the absence of spleen and tonsil, respectively, were investigated.

5.2.1 Tissue-specific compartmentalization of human B cells

To gain a first overview of the general lymphocyte subset composition in humans, the tissues under study were analyzed for their relative $CD19^{pos}$ B cell to $CD3^{pos}$ T cell content (Figure 5-20).

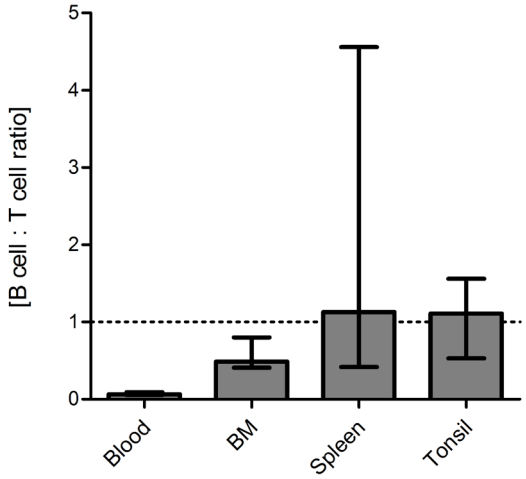

Figure 5-20 B cell and T cell proportion is intrinsic to the tissue.
Shown is the ratio of B cell:Tcell numbers determined by flow cytometry from isolated mononuclear cells from the tissues (blood n=15, BM n=14, spleen n=7, tonsil n=11), given as median ± interquartile range.

Whereas spleen and tonsil contained similar numbers of B and T cells with a tendency of higher B cell than T cell numbers in the spleen, the amount of T cells outnumbered that of B cells in blood by 6.5- to 23-fold and in BM by 0.7- to 4.3-fold, for the latter including one example where the T cell number was below that of the B cell number.

Subsequently, a detailed assessment of B cell frequencies was conducted and is shown in Figure 5-21 A. A relative enrichment of $CD19^{pos}$ B cells was found in the BM (median 19%), spleen (33%) and tonsil (43%) compared to those circulating in peripheral blood (4%). This relative distribution was transformed into absolute B cell numbers, based on lymphocyte numbers per organ as described (121). This approximation yielded highest B cell content in spleen, followed by 2.5- to 3.5-fold less B cell numbers in BM and tonsil, respectively, which all contained substantially higher (20- to 70-fold) total numbers of B cells than blood.

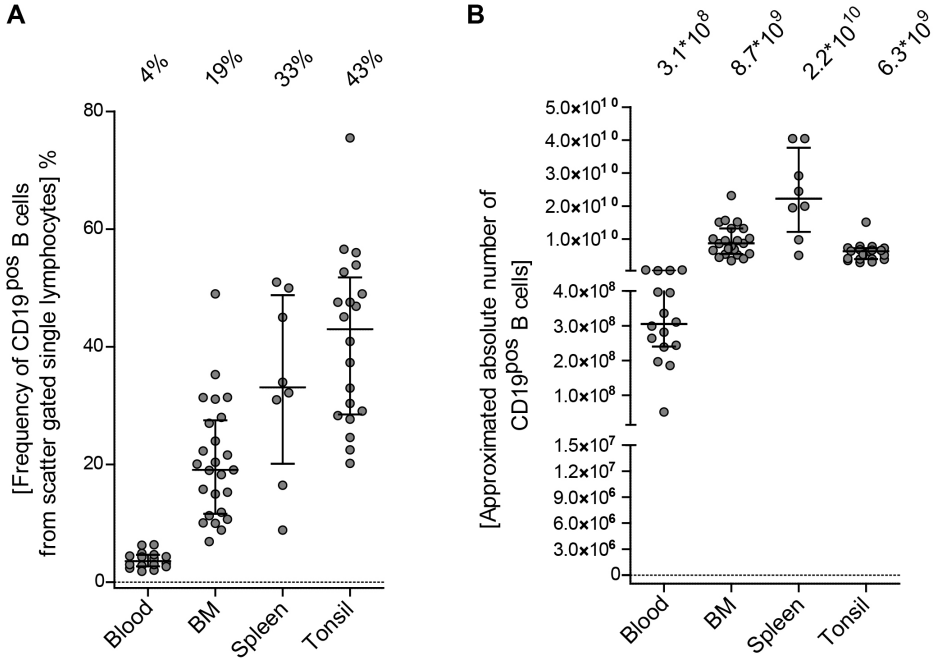

Figure 5-21 Distribution of B cells in blood and different lymphoid organs.
A Isolated mononuclear cells from human peripheral blood (n=16), BM (n=25), spleen (n=8) and tonsil (n=20) were analyzed for their frequencies of $CD3^{neg}CD14^{neg}CD19^{pos}$ B cells from living scatter gated lymphocytes. **B** Transformed absolute numbers of those $CD19^{pos}$ B cells in the different tissues based on the ratio of gated B cells to all lymphocytes, multiplied with absolute lymphocyte numbers of the respective tissue as previously described by Trepel (121). Bar indicates median ± interquartile range.

Next, the B cell population within each tissue was analyzed regarding its subpopulation constitution (Figure 5-22) with a focus on mBC subsets. Depending on the type of tissue of interest, a variety of markers can be selected to define the specific B cell subsets. For tonsil and later also for blood for example, the *B mature* classification

was used defining B cells according to their activation and differentiation stages based on the surface expression of CD38 and IgD (101, 168). However, for other tissues, e.g. BM and spleen, this system has not been validated. Another widely used B cell classification is by surface expression of CD20 and CD27. CD27 is regarded as a pan-mBC marker as it has proven its usefulness in separating reactive antigen-experienced non-cycling B cells from mature naïve B cells and antibody-secreting PB/PC (91, 143, 144, 169-172). Further, the resolution of this system can be considerably enhanced with regard to IgD expression, i.e. mBC can be divided into IgD^{pos} and IgD^{neg} subsets (173) and a small population of $CD27^{neg}IgD^{neg}$ mBC can be determined (174, 175), amongst other. As the *B mature* classification impedes analysis of these various (blood) mBC subsets, in this study the CD20/CD27 classification was used.

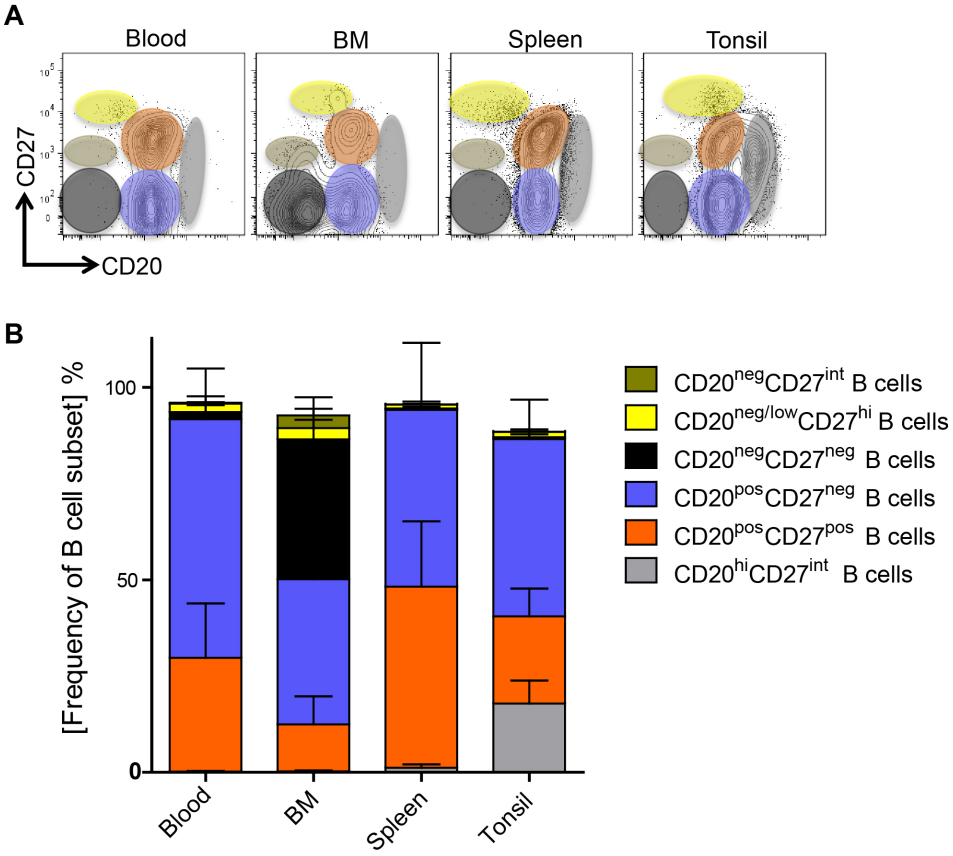

Figure 5-22 B cell subset frequency within the different tissues.
$CD19^{pos}CD3^{neg}CD14^{neg}$ B cells isolated from blood (n=15), BM (n=14), spleen (n=7) and tonsil (n=11) were separated by their CD20 and CD27 expression. **A** Representative dot plots from flow cytometry analysis with indicated gating areas, starting in the lower left corner, clockwise: $CD20^{neg}CD27^{neg}$ cells (black circle), $CD20^{neg}CD27^{pos}$ cells (khaki), $CD20^{neg/low}CD27^{high}$ cells (yellow), $CD20^{pos}CD27^{pos}$ cells (orange), $CD20^{high}CD27^{int}$ cells (grey) and $CD20^{pos}CD27^{neg}$ cells (purple). **B** Frequency of B cell subset distribution within the different tissues, given as mean ± standard deviation.

For the general B cell analysis this staining revealed at least 6 $CD19^{pos}$ B cell subsets, i.e. $CD20^{neg}CD27^{neg}$ cells, $CD20^{neg}CD27^{pos}$ cells, $CD20^{neg/low}CD27^{high}$ cells, $CD20^{pos}CD27^{pos}$ cells, $CD20^{high}CD27^{int}$ cells and $CD20^{pos}CD27^{neg}$ cells, for which tissue-specific patterns could be identified.

In detail, spleen and blood contained in their majority three main B cell populations, i.e. $CD20^{pos}CD27^{neg}$ cells, comprising naïve B cells in their majority but also transitional B cells and few mBC, $CD20^{pos}CD27^{pos}$ cells which are considered as mBC in their large majority and $CD20^{neg/low}CD27^{high}$ cells, which are acknowledged to be antibody-secreting PB and PC in their majority. In addition to those three B cell subsets, tonsils contained a $CD27^{int}CD20^{high}$ B cell population which resembled a GC B cell phenotype, confirmed by their high expression levels of CD38 and negativity for CD24 (not shown) as described elsewhere (71, 176). This subset was also traceable in spleens from young adults but largely absent in spleens from elderly. In addition to the former three populations, BM contained two largely exclusive populations. One prominent population with the phenotype $CD20^{neg}CD27^{neg}$, which presumably are B cell precursor stages and a smaller population of $CD27^{int}CD20^{neg}$ cells which are of unknown identity so far.

5.2.2 Defining a mBC gating strategy

The composition of the B cell populations within the different tissues revealed a $CD20^{neg}CD27^{int}$ B cell subset within BM of which the origin and potential relationship to the mBC compartment is currently unknown. Therefore, as mBC can classically be defined as class-switched (small and quiescent) B cells, IgG and IgA expressing B cells, respectively, were mapped for their localization in the CD20/CD27 system. This was carried out to test whether the BM $CD20^{neg}CD27^{int}$ B cells may constitute a (class-switched) mBC population (Figure 5-23).

This analysis identified IgA^{pos} and IgG^{pos} class-switched B cells in the $CD20^{high}CD27^{int}$, $CD20^{neg/low}CD27^{high}$ and in the $CD20^{pos}CD27^{pos}$ population but not in the BM $CD20^{neg}CD27^{int}$ B cell population. This does not exclude its mBC identity but prompted us to exclude them from our mBC analysis at this point as further studies will be required to determine their origin. As a result, in the following analyses mBC were identified as $CD20^{pos}CD27^{pos}$ B cells in all tissues.

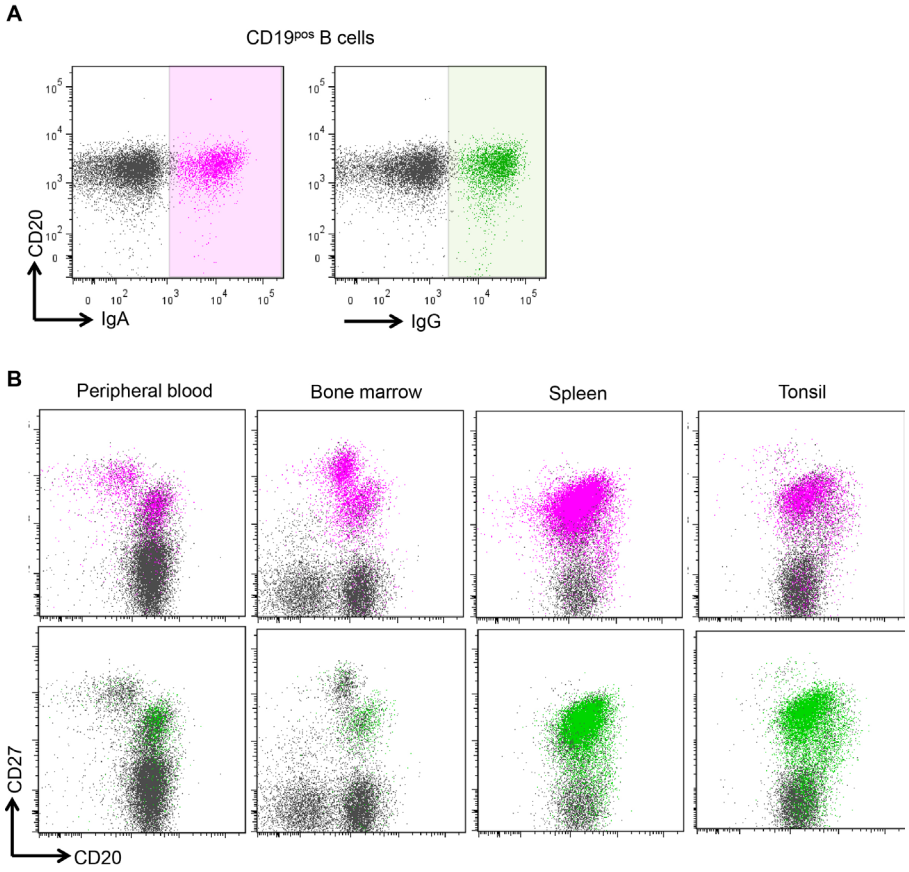

Figure 5-23 Mapping of IgA and IgG B cells in the CD20/CD27 classification.
A Dot plots of gating for IgA- (left; pink marked cells) and IgG- (right, green marked cells) surface expressing B cells. **B** Representative dot plots of mapping the as under **A** gated IgA (pink, upper row) and IgG (green, lower row) B cells, respectively, in the CD20/CD27 classification.

5.2.3 Distribution of human mBC in different lymphoid organs

Subsequently, frequencies of mBC among CD19^{pos} B cells were determined. This analysis yielded an on average higher frequency of mBC detected in the spleen (46%) as compared to peripheral blood (30%) and tonsil (21%), whereas the BM contained a substantially lower mBC frequency (8%; Figure 5-24).

With respect to approximated absolute numbers, significantly more mBC were found in the spleen and tonsil (median 9.1x10^9 and 1.1x10^9, respectively) compared to peripheral blood (8.2x10^7) and BM (6.6x10^8). This equals 111-fold enrichment of mBC in spleen compared to blood, and 14- and 8-fold more mBC in spleen compared to BM and tonsil, respectively.

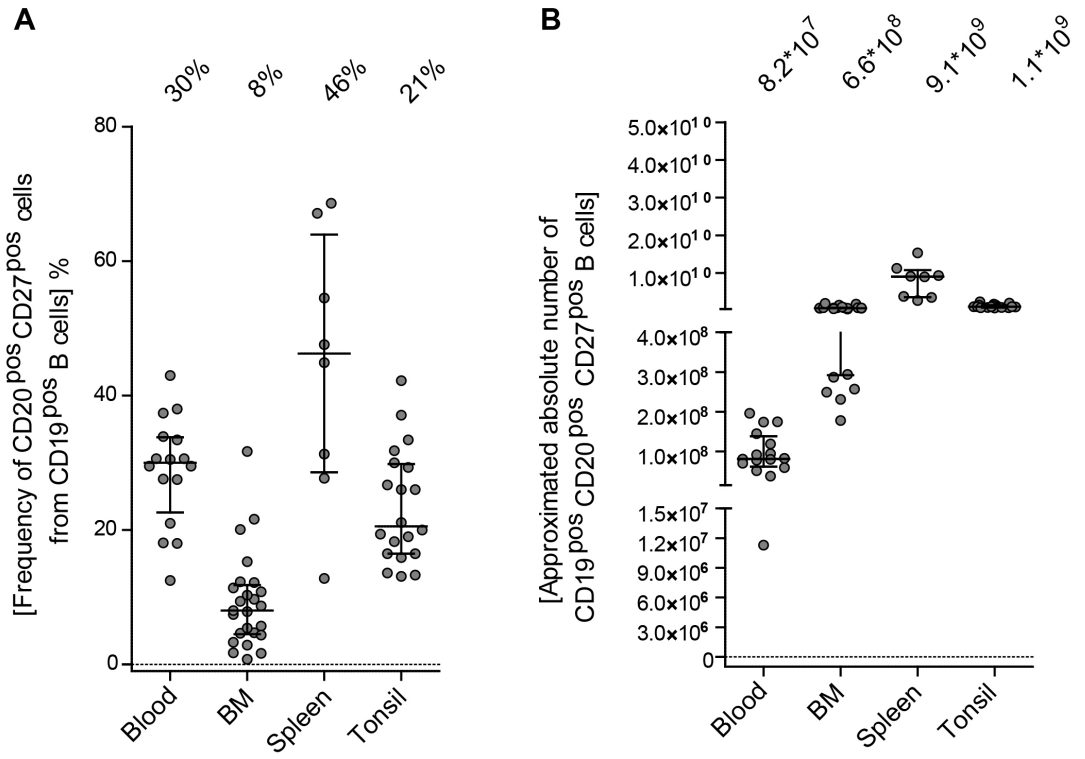

Figure 5-24 Tissue distribution of human mBC.
A Isolated mononuclear cells from human peripheral blood (n=16), BM (n=25), spleen (n=8) and tonsil (n=20) were analyzed for their frequencies of $CD20^{pos}CD27^{pos}$ mBC within $CD3^{neg}CD14^{neg}CD19^{pos}$ B cells. **B** Transformed absolute numbers of mBC in different tissues.
Bars and numbers indicate median, respectively, error bar is the interquartile range.

5.2.4 Age dependence of mBC accumulation within the tissues

We further investigated whether an age dependence of mBC frequency in the different tissues under study existed (Figure 5-25). Notably, we did not have access to samples from children under the age of 10 years for our analyses. In this regard it is important to acknowledge that blood $CD27^{pos}$ B cells increase gradually with age, most prominent during the first 10-15 years of life (170).

The results from our analysis show that during adulthood, throughout 35 to 82 years of age, mBC frequencies remained low in BM whereas the spleen constantly contained a high proportion of mBC, for ages ranging from 16 – 79 years, with one exception. For both tissues, no significant linear age-mBC frequency dependence could be found using the Spearman's rank correlation test. In blood the frequencies of mBC varied considerably between the individuals with ages ranging between 23 and 63 years, and also no linear age-mBC frequency dependence was detectable, which was also true for tonsil.

Figure 5-25 Age dependence of relative mBC accumulation within the tissues.
Relation of donor age to mBC frequency for peripheral blood (n=40), BM (n=34), spleen (n=10) and tonsil (n=20) samples. No significant correlation was observed in any of the tissues (Spearman's rank correlation coefficient).

5.2.5 Expression of markers associated with tissue residency

For tissue-resident resting CD4^{pos} memory T cells, different studies identified that 60-100% of these expressed CD69 whereas in contrast, only few (1-20%) blood memory T cells expressed that marker (177) and therefore CD69 was considered as a marker for tissue resident T cells. Further, it has been described that CD69 suppresses Sphingosine-1-phosphate receptor 1 (S1PR1) and therefore inhibits tissue egress (178, 179) consistent with a role of CD69 in lymphocyte tissue retention. Therefore, we next analyzed CD69 expression of the tissue-residing mBC in contrast to circulating mBC (Figure 5-26).

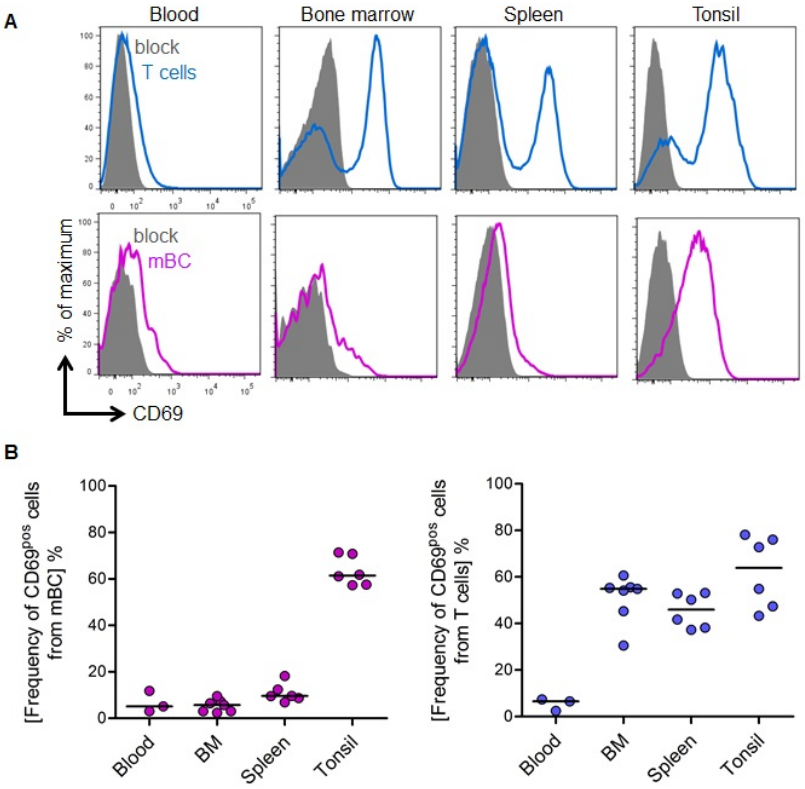

Figure 5-26 CD69 expression of lymphoid organ and blood mBC and T cells.

A Histograms of CD69 expression of $CD3^{pos}$ T cells (upper row, shown for comparison only) and of mBC (lower row). **B** Frequency of CD69 expressing mBC (right) and for comparison only, of $CD3^{pos}$ T cells. As control (grey histogram) blocking with unlabeled CD69 was performed prior to the staining. Bar indicates median.

This analysis demonstrated that with overall 2% -18% of mBC from blood, BM and spleen, the minority expressed CD69 in these tissues (Figure 5-26 B). By contrast, the majority of tonsillar mBC were $CD69^{pos}$, with expression found on 57% - 71% mBC here.

Yet, as evident already by visual inspection of the representative histograms (Figure 5-26 A) the tonsillar mBC CD69-expression level was below that of tissue-residing T cells, which was exemplarily analyzed for three tonsillar mBC and T cell pairs (Figure 5-27).

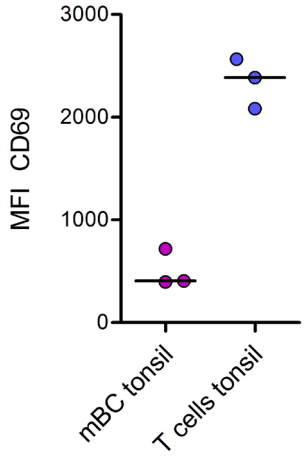

Figure 5-27 CD69 expression levels of tonsillar mBC and T cells.
Three tonsils were additionally analyzed for the CD69 median fluorescence intensities (MFI) of $CD69^{pos}$ mBC and T cells. Bar indicates median.

Next, as CD69 was originally described to be an immediate early activation marker, being rapidly and transiently induced upon T cell activation and was associated with lymphocyte proliferation (180), the expression of the proliferation-associated marker Ki-67 (181) was investigated as the environment of the tonsil is immunologically far more active than that of spleen, BM or blood. Thus the tonsillar $CD69^{pos}$ mBC could simply constitute an activated B cell population. However, this analysis showed that Ki-67 was generally only expressed in a minor fraction of tissue-residing mBC, i.e. on 0.5% - 13%, indicative that the identified overall and tonsillar mBC populations are indeed mostly quiescent in terms of proliferation (Figure 5-28), in contrast to approximately 50% of the tonsillar GC B cell population (Figure 5-28 A).

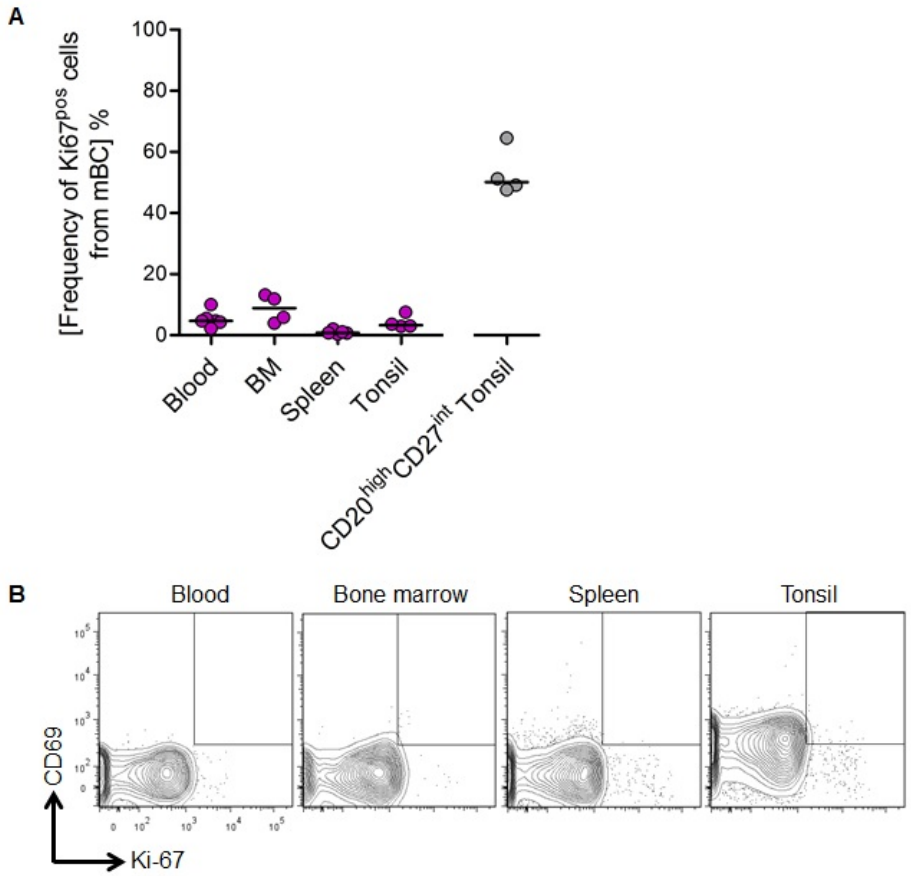

Figure 5-28 Expression of Ki-67 on tissue-residing and circulating mBC.
A Proportion of Ki-67^{pos} mBC from their parent population. For comparison only, the tonsillar CD20^{high}CD27^{int} B cell population, i.e. GC B cells, is also shown regarding its percentage of Ki-67^{pos} cells. Bar indicates median. **B** Representative dot plots showing Ki-67 and CD69 expression by mBC, the rectangle gate marks the co-expressing mBC population.

Furthermore, the Ki-67^{pos} mBC population did not co-express CD69 (Figure 5-28 B). Hence, it appears likely that the CD69 expression on tonsillar mBC is indeed associated to tissue retention and these mBC should consequently be non-migratory.

To investigate this aspect further, expression of CD62L, a molecule involved in active lymphocyte recirculation and trafficking, also known as L-selectin, was analyzed (Figure 5-29).

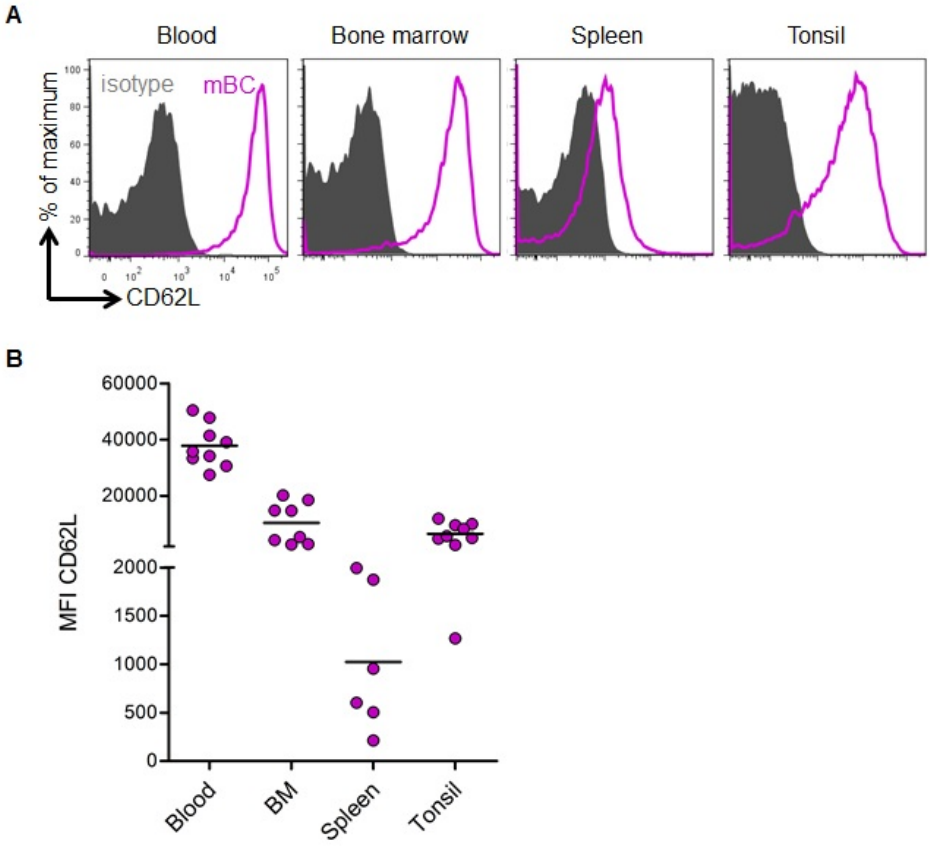

Figure 5-29 Expression of CD62L on lymphoid organ and circulating mBC.
A Representative histograms of CD62L expression on mBC. As control, the isotype staining is shown (grey histogram). **B** Median fluorescence intensities (MFI) of CD62L on tissue and circulating mBC. Bar indicates mean.

CD62L was highly expressed on blood mBC (37800 ± 7646; mean MFI ± standard deviation), at lower levels on BM (10428 ± 7349) and on tonsillar mBC (6551 ± 3581) and exhibited strongly reduced expression on splenic mBC (1024 ± 745; Figure 5-29 B). Thus tonsillar mBC exhibited reduced CD62L expression in contrast to circulating mBC but expressed it well above the level of splenic mBC that are described to be recirculating (182).

The inhibitory receptor receptor-like protein 4 (FcRL4) has been described to be expressed on human mBC which reside in epithelial tissues (183) and on an mBC subset in tonsils (184). Therefore, the expression of FcRL4 was analyzed to investigate whether it identifies a tissue-resident mBC population (Figure 5-30).

As can be seen in Figure 5-30, the majority of $CD20^{pos}CD27^{pos}$ mBC in blood as well as in the tissues under study, including tonsils, did not express FcRL4.

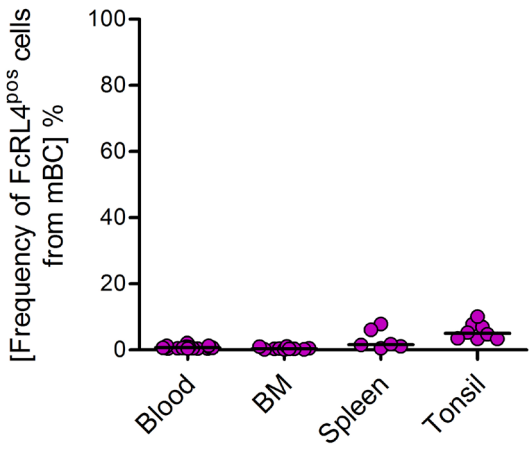

Figure 5-30 Expression of FcRL4 on tissue and circulating mBC.
Proportion of FcRL4^{pos} mBC from their parent population. Bar indicates median.

5.2.6 Differentiation and migration marker expression by human mBC obtained from different human tissues

For tissue-resident long-lived BM PC it has been described that these expressed a more mature phenotype compared to tonsillar and blood PB/PC, i.e. decreased expression of HLA-DR, CD95, CD45 and CD21 among others (167). Following this idea, tissue and blood mBC were next analyzed for their expression of markers associated to an advanced maturation stage and distinct homing and migration behavior. Representative histograms from a series of experiments are summarized in Figure 5-31 A. The differentiation and activation markers CD24, CD45, CD21 and HLA-DR were expressed on almost all mBC, comparably in all tissues analyzed (Figure 5-31 B) and deviations were detectable on a statistical level but did not lead to disclosure of considerable separate negative populations. The ICOSL was expressed at low levels on mBC from blood (525 ± 101; mean MFI ± standard deviation) and BM (604 ±135) but was largely absent on mBC from spleen (179 ± 127) and tonsil (134 ± 24; Figure 5-31 C). Analysis of lymphocyte trafficking and adhesion markers showed that CD54 (ICAM-1) was expressed on almost all mBC from all tissues which was also true for CD31 (PECAM-1), yet for the latter the frequencies of mBC from spleen (96.5% ± 1.9%) and BM (95.9% ± 1.9%) expressing this molecule was greater compared to those of blood (79.5% ± 6.3%) and tonsil mBC (81.2% ± 4.0%).

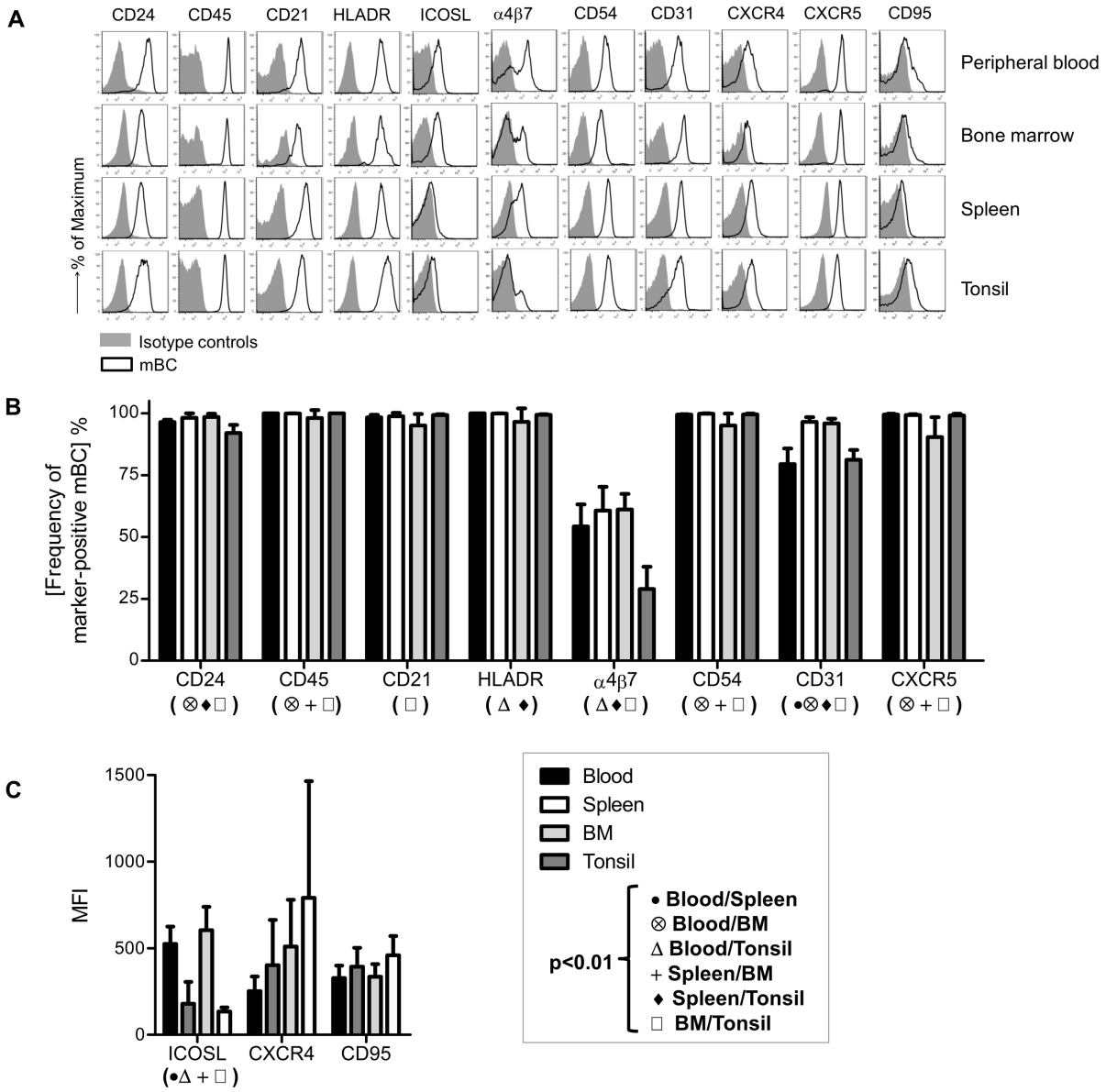

Figure 5-31 Comparative analysis of the pattern of expression of differentiation, survival and migration associated molecules by mBC from different tissues.
A Representative examples of molecule expression associated to differentiation and activation (ICOSL, CD21, CD24, HLADR, CD45), lymphocyte trafficking and adhesion (CXCR4, CXCR5, α4β7 integrin, CD54, CD31) and survival (CD95) by blood, BM, spleen and tonsil mBC (black line). As control, corresponding isotype controls are shown (grey). **B** Frequencies of mBC expressing the markers as indicated. **C** Median fluorescence intensities (MFI) of indicated markers expressed by mBC from each tissue.
Symbols underneath the diagrams indicate significant differences between tissues as indicated by the legend (Mann-Whitney tests were performed with p≤0.01 considered as significant difference). Number of samples ranged between 5-10 for each marker and tissue. Bar indicates mean. Error bars represent the standard deviation.

The chemokine receptor CXCR5, involved in B cell migration into B cell follicles from spleen and Peyer's patches (185), was homogenously expressed by nearly all mBC from all tissues analyzed, apart from a small portion of BM mBC (6.6% ± 3.3%).

CXCR4, also involved in lymphocyte follicle positioning and homing behavior to the BM (186), was found to be expressed somewhat higher on splenic (MFI 402 ± 262), BM (510 ± 270) and tonsillar (791 ± 674) mBC compared to circulating mBC (253 ± 84). The death receptor CD95 (FAS/APO-1) was expressed at similar low densities on the majority of mBC obtained from all tissues.

Interestingly, the mucosal (gut-) homing adhesion molecule β7 integrin, which can be considered as representative for α4β7 integrin expression (187), was found to be present on a proportion of mBC from all tissues, yet in tonsil, a mucosal associated tissue, a significantly smaller mBC population expressed β7 integrin (29% ± 9%) in contrast to mBC from blood, spleen and BM, respectively (54.3% ± 8.9%, 60.7% ± 9.6% and 61.2% ± 6.2%, respectively). Further analysis of pre- and post-switch mBC population revealed that IgD^{pos} mBC expressed significantly higher levels of β7 integrin than IgD^{neg} mBC consistently in all tissues (Figure 5-32).

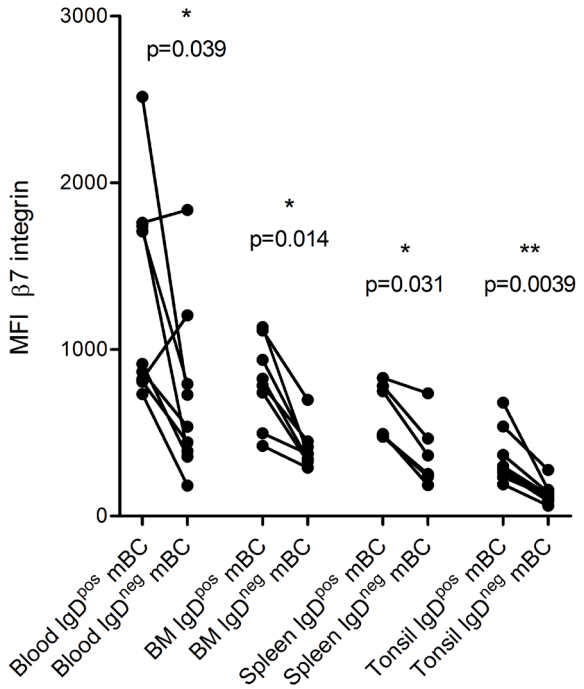

Figure 5-32 β7 integrin expression levels of IgD^{pos} and IgD^{neg} mBC from the different lymphoid organs and blood.
Median fluorescence intensities of surface expression of β7 integrin on mBC as indicated. Wilcoxon signed rank tests were performed.

In summary and albeit small detectable differences, none of these yielded identification of mBC populations consistent with differential maturation stages or survival capacities between the different tissues studied.

5.2.7 Distinct distribution of IgA, IgG or IgM/IgD-expressing mBC in different tissues

Next, compartmentalization of different isotype expressing mBC populations including $CD20^{pos}CD27^{neg}IgD^{neg}$ B cells was assessed. The gating strategy of a representative example is shown in Figure 5-33 A.

This analysis demonstrated that circulating and BM mBC contained similar frequencies of surface IgA (median 17.3% and 20.0%, respectively) and IgG expressing mBC (22.9% and 22.6%, Figure 5-33 B). In contrast to the other tissues, tonsillar mBC contained a larger frequency of surface IgA^{pos} mBC (26.1%) whereas surface IgG^{pos} mBC were present to similar frequencies in spleen (31.7%) and tonsil (36.6%) and thus enriched compared to blood and BM. The pre-switched mBC population (IgM^{pos}/IgD^{pos}) was reduced in tonsil (25.6%) compared to the populations present in blood (48.9%), spleen (45.0%) and BM (37.9%). Yet, with respect to absolute numbers, the spleen contained the largest populations of IgA^{pos}, IgG^{pos} and IgM^{pos}/IgD^{pos} mBC, respectively (Figure 5-33 D). Notably, tonsils represented a site of relative accumulation of classic (IgA^{pos} and IgG^{pos}) post-switched mBC, whereas pre-switched mBC appeared de-enriched.

As described above and in line with previous reports, within the $CD27^{neg}$ B cell population mutated and class-switched B cells, considered to be mBC, can be found in blood (174, 175). Therefore, in this analysis the $CD20^{pos}CD27^{neg}IgD^{neg}$ B cell population (double-negative mBC) was included in our BCR-isotype cross-tissue comparison (Figure 5-33 C and E). We found that double-negative mBC comprised IgG expressing cells in their majority, consistent for blood (median frequency 1.9% of $CD19^{pos}$ B cells), spleen (2.6%) and tonsil (1.6%). In contrast, the frequency of IgA and IgG double-negative mBC, respectively, appeared more balanced in BM (0.2% IgA and 0.5% IgG). In absolute numbers double-negative IgG^{pos} B cells were present in higher quantities than double-negative IgA^{pos} B cells in all tissues under study (Figure 5-33 E). With regard to the $CD20^{pos}CD27^{pos}$ mBC, overall absolute numbers of both double-negative mBC subsets were 4- to 17-fold less than that of the isotype-corresponding $CD27^{pos}$ mBC subset (Figure 5-33 D and E).

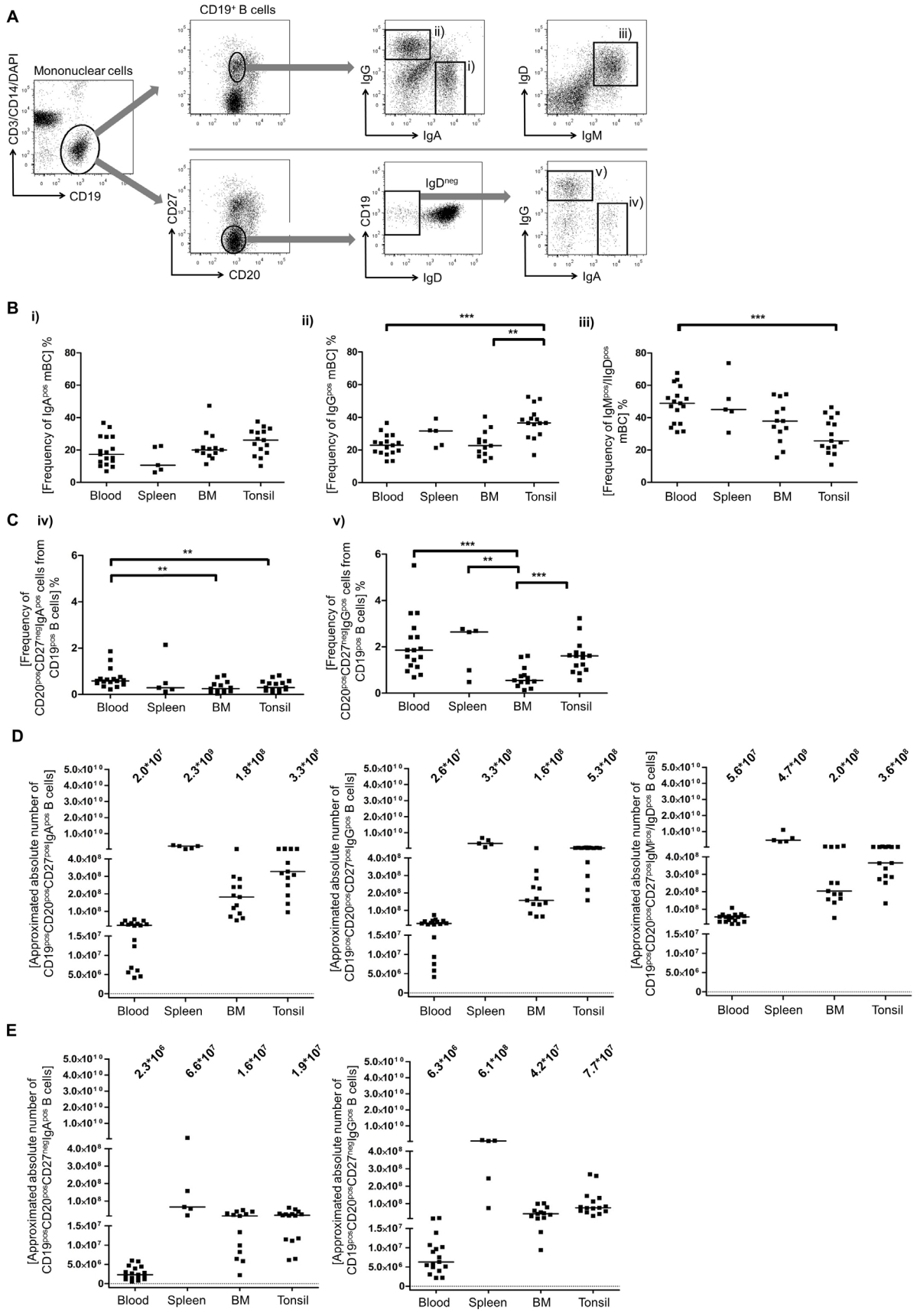

Figure 5-33 Expression of surface isotypes by lymphoid organ and CD27^{pos} circulating mBC and CD20^{pos}CD27^{neg}IgD^{neg} B cells.

A Gating strategy for isotype-specific mBC (IgA: i); IgG: ii) and IgM/IgD: iii); all upper row) and for CD19^{pos}CD20^{pos}CD27^{neg}IgD^{neg} B cells (IgA: iv) and IgG: v), lower row), exemplarily shown from tonsil. **B** Frequency of IgA^{pos}, IgG^{pos} or IgM^{pos}/IgD^{pos} mBC from a series of experiments. Mann-Whitney test, **: p<0.01; ***: p<0.001. **C** Frequency of IgA^{pos} and IgG^{pos} CD20^{pos}CD27^{neg}IgD^{neg} B cells, respectively, from CD19^{pos} B cells. **D** and **E** Transformed absolute numbers of respective indicated B cell populations, calculated as described in Figure 5-21.

5.2.8 TT^{spec} mBC are enriched in the spleen followed by tonsil

In addition to the overall picture of mBC distribution described above, subsequent analysis evaluated the presence and distribution of an antigen-specific mBC population. Here, TT^{spec} mBC were analyzed exemplarily, as most individuals have been immunized against TT. Thus, this specificity could help to reveal whether systemically induced mBC distributed in the tissues under study similarly or potentially preferred residence within the one or other organ. For this analysis again the direct TT^{spec} B cell staining, as described in section 5.1.1, was used. This analysis frequently identified TT^{spec} mBC in peripheral blood (median on average 0.04%), in the spleen (0.04%) and in the tonsil (0.06%). In BM, TT^{spec} mBC could only be infrequently detected (Figure 5-34 A).

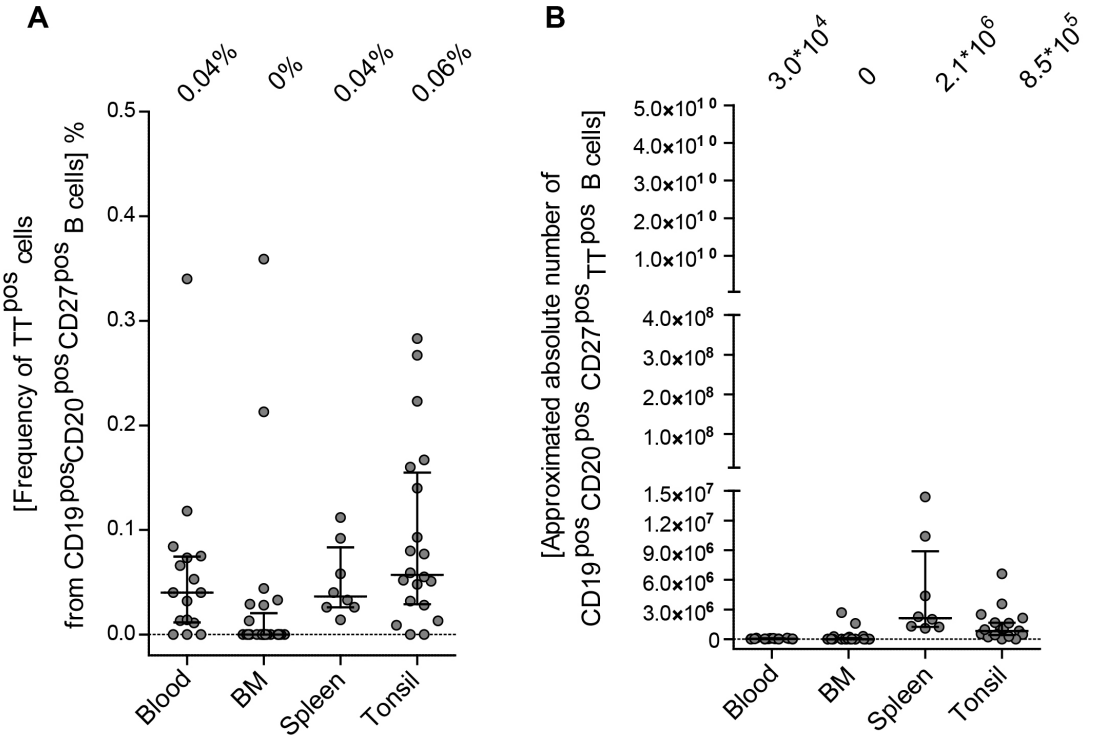

Figure 5-34 Tissue distribution of human TT^{spec} mBC.
A Isolated mononuclear cells from human peripheral blood (n=16), BM (n=22), spleen (n=8) and tonsil (n=19) were analyzed for their frequencies of TT^{spec} cells (here TT^{pos}) within CD3^{neg}CD14^{neg}CD19^{pos}CD20^{pos}CD27^{pos} B cells. **B** Transformed absolute numbers of mBC in different tissues. Bars and numbers indicate median, respectively, error bar is the interquartile range.

In absolute numbers (Figure 5-34 B), the spleen accommodated most TT^{spec} mBC (median $2.1x10^6$) followed by those prevalent within the tonsil ($8.5x10^5$) and blood ($3.0x10^4$). Their detection in the BM was too infrequent for general conclusions at this point.

5.2.9 Influence of splenectomy and tonsillectomy on circulating mBC

Since the spleen and tonsil have been found to be very intriguing mBC accommodating organs, finally, the consequences of absence of spleen or tonsil, i.e. in humans either splenectomized or tonsillectomized, on blood mBC homeostasis was investigated (Figure 5-35).

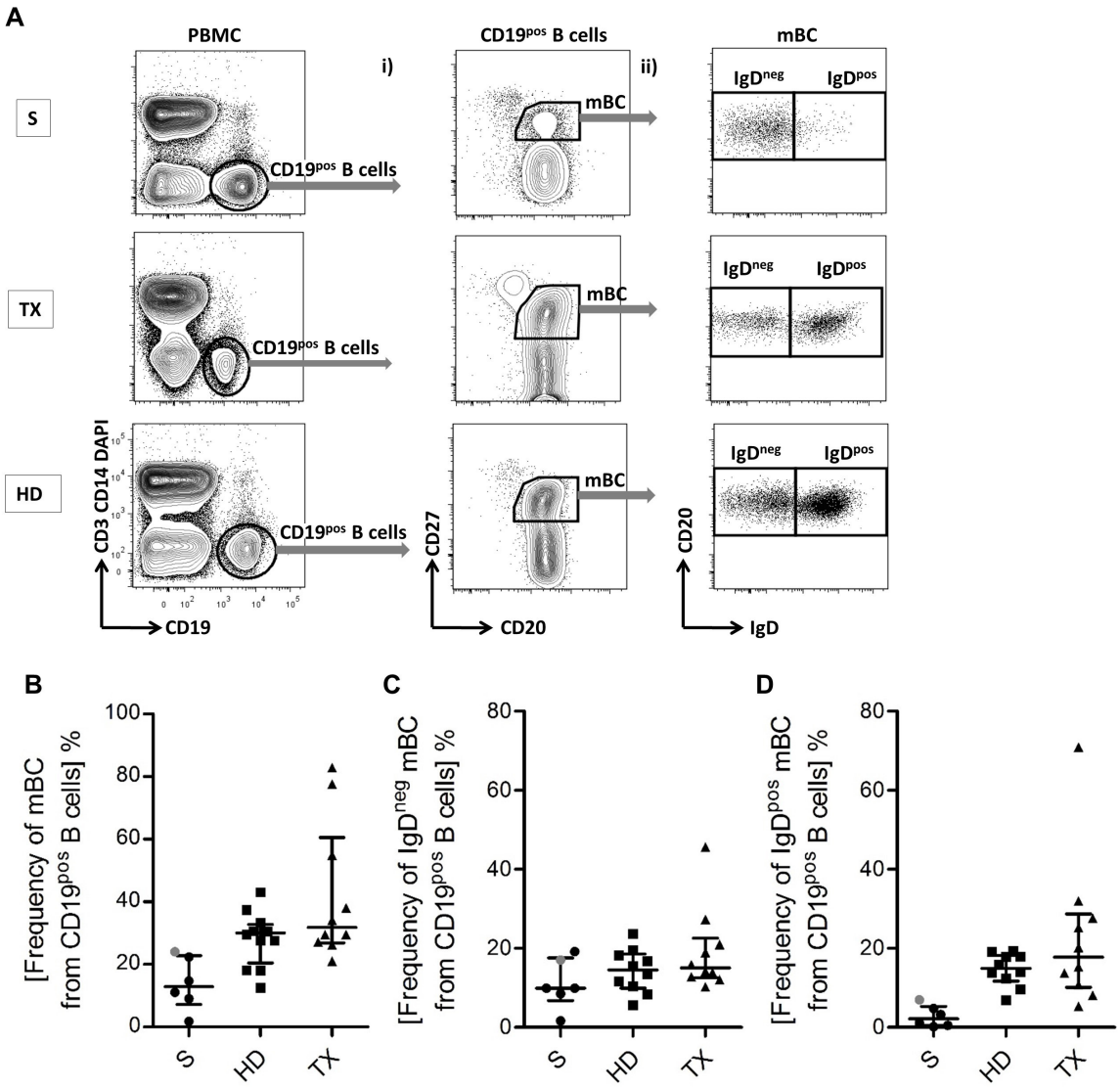

Figure 5-35 Circulating mBC are reduced in splenectomized versus healthy controls and tonsillectomized donors.
A Representative dot plots of the gating strategy. PBMC were gated with an extended forward scatter gate with subsequent exclusion of non-single cells (not shown) and subsequent gating on B cells.

Frequencies of mBC (i) and subsequently of IgD^{pos} and IgD^{neg} subsets were analyzed (ii). Upper row: Splenectomized patient (S). Middle row: tonsillectomized HD (TX). Lower row: HD. Frequencies of mBC (**B**), IgD^{neg} mBC (**C**) and IgD^{pos} mBC (**D**) are expressed as percentage from $CD19^{pos}$ B cells. Bar indicates median, error bar is the interquartile range. Grey dot: respective frequencies from splenectomized individual S2 who had the shortest time period after splenectomy (7 months) and considered short-term splenectomized in contrast to the other splenectomized individuals.

This analysis clearly showed that four long-term splenectomized individuals S1 (2 years splenectomized), S3 (35 years), S4 (13 years) and S5 (4 years) exhibited reduced frequencies of circulating mBC (11.0%, 9.0%, 1.7% and 14.7% for S1, S3, S4 and S5 respectively), whereas patients S6 (40 years, long-term splenectomized) and S2 (7 months, classified as short-term splenectomized) did not show such a drastic change (22.4% and 24.0%, respectively) compared to 10 HD (30.0%; Figure 5-35 A and B). In contrast, tonsillectomized individuals (n=10) exhibited no change of circulating mBC frequencies (median 31.8%) in comparison to the HD cohort at all.

Separate analysis of pre- and post-switch mBC (Figure 5-35 C and D) showed that all splenectomized individuals had reduced circulating IgD^{pos} mBC (median 2.2%) including S2 (6.7%) and S6 (3.2%) compared to HD (median 14.9%;) and tonsillectomized donors (17.8%), respectively. In contrast, post-switch mBC were reduced only to a minor extent in the splenectomized group (median 9.9%) compared to HD (14.5%) and tonsillectomized HD (15.0%, Figure 5-35 C).

6. Discussion

The humoral immune response is mediated by B cells and their soluble effector molecules produced upon antigenic challenge. Such challenges can be of a primary or secondary, i.e. repeated, nature and have been shown to consequently elicit distinct response kinetics which differ quantitatively and qualitatively. Most of our knowledge in this regard derives from animal models and is unfortunately not unlimited transferrable to humans, as we have an approximately 50-times higher life expectancy together with a more complex immunological history. As many immune system related diseases or abnormalities, e.g. autoimmunity and hypersensitivities, appear during adulthood a thorough knowledge base of the adults' immune system and immune response mechanisms is of importance not only for a basic understanding but also for future therapeutic interventions.

This study aimed to enhance our knowledge of underlying mechanisms of primary and secondary immune responses in human adults as well as of B cell memory induction, maintenance and its reactivation. To achieve this, in the first part a comprehensive study of anti-KLH serum antibody levels and B cellular kinetics in conjunction with the expressed variable and constant IgH sequence repertoire of KLH^{spec} primary PB, secondary PB and mBC was conducted. Overall, this approach permitted unique insights into a specific B cell repertoire's composition, diversity and dynamics. In the second part a thorough description of B cell and mBC distribution and related phenotype of the latter represents a systematic study of tissue-residing mBC and revealed some aspects worth further investigations.

6.1 The serum and cellular response to KLH immunization

This is the first study to document a detailed antibody response together with B cellular kinetics in conjunction with the molecular information of the expressed antigen-specific Ig involved in responses to a primary immunization in human adults.

Upon primary KLH immunization, specific antibody, PB and mBC responses were delayed and of lower magnitude compared with the response to KLH booster immunization of the same individuals. This concurs with the widely accepted concept of primary and secondary immune responses, concluded from studies in animal models

and children (77, 188, 189). Further, these results affirm the differences in immune responses that relate to a pre-existing antigen-specific immune memory in contrast to a naïve immune system.

Noteworthy is one specific report though, which showed that upon rabies immunization in adults, PB in the naïve volunteer group appeared later in blood (peak at day 10) than in the already immune group (peak at day 7) and were of lower frequency (63), which is in accordance with the previously described kinetics and concurs with our findings here. However, that study further found that IgM antibodies did not precede the appearance of IgG and IgA antibodies and therefore contrasts a prototypic primary immune responses, where IgM antibodies should precede the appearance of IgG antibodies. This deviating pattern was also observed in another KLH study conducted in adults (190). Thus both of these studies are consistent with our observations here (section 5.1.2) suggesting that the immune history of an individual indeed affects primary immune response kinetics to hitherto un-encountered antigens.

Another uncommented but notable finding of the previous rabies study, which we also observed, is the frequent appearance of IgA antibodies and circulating IgA^{pos} PB upon primary parenteral immunization. This consistent parenteral IgA induction, most likely independent from participation of the mucosal immune system (Figure 5-9), suggests a certain underappreciated importance of serum IgA for systemic protection as indicated by studies analyzing parenteral influenza and pneumococcal immunizations in elderly people. In these studies, the lack of protection correlated with significantly reduced IgA responses (191, 192). Admittedly, in contrast to our and the rabies study, which were pure parenteral immunizations, prior natural sensitization via mucosal surfaces is most likely in the case of pneumococcal and influenza immunizations/infections consequently potentially causing still pronounced IgA responses during re-challenges. At least, this would be consistent with results from a previous KLH study (193). In that study it was shown that primary intranasal KLH immunization primed the volunteers for strong IgA (but also IgG) serum responses to subsequent subcutaneous immunizations. In contrast, in our KLH study we detected a reduced serum IgA response upon the parenteral re-challenge.

Unfortunately, we cannot deduce or test implications for immune protection or inflammation conferred by the anti-KLH IgA as one cannot “protect” an individual from KLH and test it. It should be pointed out though that selective IgA deficiency is a relatively common primary immune deficiency in Caucasians remaining an inapparent to

only mild illness in approximately 50% of affected individuals. However, those who seek help often suffer from significant illness, including a high susceptibility to infections, autoimmune diseases and allergies (194-196) pointing towards complex regulatory mechanisms related to selective IgA absence. Taken together, these results suggest that future investigations of human protective immune responses and potential failure of those as well as “misguided” systemic immune responses (e.g. autoimmunity) should include measurements of specific serum IgA antibodies supplementary to the IgG and IgM responses, which is so far not routinely done.

6.1.1 Two blood antibody repertoires: the cellular and the serologic

The IgH sequence analysis of circulating KLH^{spec} PB detected a predominance of IgA-expressing PB which led to an interesting disparity to anti-KLH serum IgG to IgA ratios (Figure 5-8 B). Such discordances between the specific humoral immunity and the circulating PB and IgH gene repertoire, respectively, elicited by immunization have been described before (39, 197), while the underlying mechanisms remained unclear. One explanation is offered by the results from the oral immunization study from Czerkinsky and colleagues, in which it was demonstrated that the specific circulating antibody-secreting cells did not contribute to an increase of specific serum antibody levels while specific antibodies were found increased in saliva and tears. This suggests that the circulating PB were migrating to their designated survival or usage site to produce antibodies locally which did not emerge in the serum. In consequence, circulating PB induced by systemic immunization might represent to the BM migrating cells, which may become main serum antibody producers only when established in their niche.

The underlying mechanisms determining which GC-derived PB is entitled to recirculate remain undefined. Also, whether IgA PB might either be more migratory-prone than IgG or IgM PB, or alternatively are generally sparse antibody producers compared to the other two, or are less well accommodated in e.g. the BM niche compared to IgG PC remains to be shown. The latter possibility might be supported by a recent study showing that the more mature $CD19^{neg}$ BM PC compartment holds more IgG than IgA PC whereof potential reasons remain to be elucidated (198).

Alternatively, at least for the primary response, the majority of serum IgM, IgG and IgA antibodies could be derived from unmutated extra-follicular short-lived PB/PC as first line of defense which have been described to be non-migratory (35).
Anyhow, in line with the aforementioned KLH study (197), the circulating PB between days 14-18 would not be the major cellular correlates for the serum antibodies at that time point. Clarifying the raised possibilities here will require further studies addressing the circulatory and sessile tissue PB/PC compartments in conjunction with serum antibodies in more depth. In this regard, one study delineated the constituent antibodies of the human serum IgG repertoire after vaccination and examined their relationship to the antibody variable gene repertoire encoded by circulating B cells. The results revealed the molecular composition and characteristics of the vaccine-specific serum antibody repertoire and demonstrated differences between the end-point response (the serum antibodies after 9 months) and the day 7 peripheral PB (39). However, this study did not comment on chronological coinciding PB and serum antibody repertoires.

6.1.2 Mechanistic insights through analysis of KLH^{spec} IgH sequences

Analysis of the expressed variable and constant IgH repertoire of KLH^{spec} PB and mBC during the response allowed insights into the mechanism and composition of a human primary response repertoire. A detailed study of the sequences revealed that KLH^{spec} B cell repertoires were far more diverse than previous studies suggested for primary responses in rodents (199-201). The diversity in the V_H and J_H segment usage together with the relatively broad CDRH3 length distribution were indicative of an unrestricted response, i.e. availability of diverse epitopes on KLH. Yet, in contrast to the extensive genetic diversity of available naïve B cell receptors, the V_H-J_H combinations together with statistical estimations on the KLH^{spec} PB repertoire sizes suggested a relatively small pool of involved clones, indicative of strong antigenic selection. This finding concurs with a previous report that showed that the complexity of the antigenic surface of tetanus toxoid also caused an unrestricted but selected B cell response (37).
Alignment of V_H and CDRH3 regions led to retrieval of clonally related expanded clusters of KLH^{spec} B cells. We thereby found a within donor between day variation of the circulating primary KLH^{spec} PB repertoires (Figure 5-17 B) suggesting that these

cells presumably left secondary lymphoid tissues to migrate via the blood stream to their potential survival niche, e.g. the BM (64, 78, 167, 198), which would be consistent with the above mentioned PB migration hypothesis.
In contrast to a previous study conducted in mice which showed a gradual increase of the SHM load of circulating PB/PC between day 7, 10, 14 and day 28 after primary immunization (64), we could not detect a steady axis of SHM increment in the primary circulating KLH^{spec} PB although a principle repertoire turnover was detectable. Noteworthy is also our, so far in the literature not described, consistent observation that approximately one third of the primary specific PB exhibited high mutation frequencies (further discussed below).

6.1.3 A human B cell repertoire shift?

Further very interesting findings were revealed when the clonal overlap between the KLH^{spec} primary PB, mBC and secondary PB repertoires was investigated. Firstly, the presence of the yet few clonally-related primary and secondary PB sequences is a direct genetic measurement of mBC establishment and reactivation, which has been presumed from many previous studies but remained to be shown in humans until now.
Secondly, only few clonal overlaps between the KLH^{spec} primary PB, mBC and secondary PB repertoires were found. Moreover, the secondary PB pool appeared clonally even more diverse than the primary PB pool with the emergence of largely new clones. This is intriguing as one would logically assume that prominent expanded clones observed in the primary PB pool would seed into the mBC pool and reappear upon its reactivation in response to immunization with the very same antigen.
Yet, conform to our results, and although this finding is against expectations, this observation has been described in the murine system before by Berek and colleagues who referred to it as “repertoire shift” (41, 43, 202). With reference to their model antigen oxazolone, Berek and Milstein speculated that the reason for this phenomenon may be firstly the higher affinity for the antigen of a canonical variable region combination (i.e. V_H-Ox1) dominating the primary response and its high frequency in the naïve available repertoire. In contrast, the V_HM21-$V\kappa$-Ox1 variable region combination, which was an important component in their reported repertoire shift, had a much lower frequency in the pre-immunization repertoire. Speculating that during matura-

tion of the primary response, certain clones will proliferate faster as they acquire advantageous mutations while others may fail to increase their affinity adequately, an initial advantage may not be of sufficient value in the longer term to successfully compete in the arising antigen-specific B cell pool.

Our study extents this concept to humans and in a more real-life scenario of a maturing primary and secondary response. The suggested scenario would offer an explanation for the initial presence of extensively expanded KLH^{spec} clonal families, some even with high mutation frequencies, of which the potential origin will be discussed below, that disappeared largely in the mBC repertoire and the secondary response, respectively.

Additionally, the antibodies arising from the canonical activated primary clones will cover their epitopes on the antigen, which in consequence blocks the interaction of the (canonical combination) GC B cells and antigen-antibody complexes on the surface of FDC. This would additionally give a competitive advantage to potentially low affinity (KLH^{spec}) B cell clones recognizing different epitopes over time, which we may not have isolated during the time frame of our sampling but which may have seeded into the mBC pool. These possibilities remain unproven at this point but offer logical explanations as to why the mature response is distinct from the primary repertoire and more diverse in gene combinations, i.e. clones.

Yet, an important aspect to point out is that it is unknown which proportion from the entirety of available antigen-specific cells is represented in peripheral blood and how well that pool mirrors the ongoing immunization-induced processes in lymphoid tissues. That the circulating PB pool can only be a minor fraction of the entire available specific PB repertoire is apparent by the fact that the blood can only hold a small proportion of B cells at any time compared to spleen, BM and other lymphoid tissues as shown in this very study (section 5.2) and by others (203, 204). Results from a mouse study further showed that antigen-specific PB in blood exhibited delayed SHM load compared to splenic PB, but paralleling SHM load to that of BM PB/PC, supporting the notion, that the circulating compartment is established directly by blood-borne PB and secondly, suggests that analysis of circulating PB will lead to underestimation of affinity maturation processes still ongoing in GC within secondary lymphoid organs (64).

6.1.4 Origin of highly mutated KLH^{spec} primary PB and potential underlying mechanisms

As mentioned before, the analysis of IgH sequences from circulating primary KLH^{spec} PB revealed a considerable proportion of cells with an unexpected high mutation load compared to, the only available data in this regard, primary immunization responses in rodents (45, 47, 62, 64, 82, 158, 162, 205-207). Based on the here presented calculations of the theoretical underlying mutation rates required to generate such highly mutated V_H genes from germline sequences and in due consideration of acknowledged cell cycle durations and mutation rates, it appears unlikely that unmutated naïve B cells can be the precursors of these early PB (described in section 5.1.12). Thus, alternative explanations have to be considered.

Firstly, duration of cell division of human B cells could be considerably shorter than of murine B cells. Yet, this possibility appears unlikely since human embryonic stem cells, which are considered as very fast dividing cells, already require 16 hours (208) to complete one cycle while other human fast dividing cells are described to take 22-24 hours and others even considerably longer (209). Besides, even if human GC B cells could take as little as 8 hours per division, as assumed in our calculations here, they would not constantly divide over the 14 to 18 days as at least selection has to intervene in between.

Therefore, secondly, the mutation rate in humans could indeed be considerably higher than described for rodents. Yet, it needs emphasis that the SHM rate has profound consequences for the fate of mutating B cells, i.e. whereas low rates may fail to produce sufficient genetic variation for efficient affinity-based maturation, too high mutation rates would lead to poor clonal expansion due to a high frequency of deleterious mutations. Therefore we can assume that the rate cannot exceed a certain value. In this regard, computer simulations found, with consideration of clonal expansion together with sufficient diversification both consistent with observed affinity maturation values, that the SHM rates would have to range optimally between 0.5-1.0x10^{-3} mutations/bp/generation (210-212). These considerations appear also valid for humans.

Therefore, I suggest a third possibility. I propose that the highly mutated primary KLH^{spec} PB were descendants of presumably cross-reactive mBC. In contrast to children and most laboratory rodents, human adults theoretically possess a B cell repertoire available for primary immune responses that comprises not only naïve B cells

but also a considerable population of mBC. The latter constitute approximately 15-50% of the entire B cell compartment (Figure 5-24; (213)) and it would be unlikely and pose un-economical to reserve this repertoire only for the original inducing antigens. An identifiable property of such a cross-reactive mBC recruitment would be the presence of highly mutated germline genes early in the response next to un- and low mutated ones, as evidently observed in the current KLH study. As such highly mutated B cell clones were not identified in primary responses in the murine system so far is this the first description of this phenomenon.

In contrast, during secondary KLH immunization no unmutated KLH^{spec} PB were observed and even the lower mutated sequences could not be generated within 7 days, based on the same calculations as performed for the primary KLH^{spec} PB (not shown). Hence, participation of presumably cross-reactive mBC in a primary response may occur whereas, in accordance with the literature, the other way around, participation of naïve B cells in higher order responses is not indicated. Possible reasons for that are likely based on out-competition of naïve B cells by mBC due to their increased frequencies and intrinsic properties, as reviewed elsewhere (214), as well as the presence of memory T cells in a primed system (215).

Nevertheless, the proposed recruitment of cross-specific mBC in this primary response did not result in kinetics characteristic of memory responses (77, 188). It is possible that the KLH-cross-reactive mBC were of such low frequency that their resulting effector cells and antibodies were not detectable before day 10-14. Inconsistent with that suggestion is however that in 4 of the 5 donors pre-primary immunization circulating KLH-binding mBC frequencies ranged from 0.1% to 0.6% which is concurrent with described mBC frequencies of other antigen specificities, resulting in expected secondary response kinetics upon challenge (203, 216-218).

Besides, it is unknown how many mBC are required to mount bona fide secondary responses. In this regard it has been indicated that as few as 25 mBC might be sufficient (219), and these numbers were readily exceeded by the here identified blood KLH-binding mBC frequencies.

Another possible explanation is that the potential activation of cross-reactive mBC has an altered pattern compared to mBC re-activation to their anamnestic antigen. Yet, reasons for this have to remain subject to speculation as this study did not address the following possibilities in the experiments. It could be that mBC require indeed help from memory T cells to mount memory responses. A previous human KLH

study did not identify significant *in vitro* KLH^{spec} (memory) T cell responses before KLH immunization in naïve donors (136). Hence, KLH-binding mBC would receive help from naïve but not memory T cells, consequently presumably leading to the observed primary kinetics. In line with this suggestion, one study indicated that B cell reactivation/GC participation is faster in the presence of pre-existing T cell help compared to kinetics resulting from de novo development of helper T cells from naïve T cells (220). However, while it is generally acknowledged that T cell help is critical to the generation of B cell memory (221, 222), the principle requirement of T cell help for mBC (re-)activation remains unclear and is under current investigation. One recent study in mice showed that IgM mBC do not depend on T cell help to generate antibodies while class-switched mBC did largely not generate antibody-secreting cells in absence of T cell help indicating that mBC greatly, although not absolutely depend on T cell help for their reactivation (154). In line, a study conducted with human mBC upon vaccination with a polysaccharide-conjugate vaccine highlighted a critical role of T cells in the differentiation of mBC into antibody-secreting cells (223). The here proposed mBC reactivation under absence of memory T helper cells could be consistent with these observations. However, other studies indicated that the effect of T cell depletion on generation of antibodies from mBC is only minimal and therefore T cell help for mBC activation would be dispensable (219, 224).

Nevertheless, a consensus exists that mBC reactivation appears to require at least a specific microenvironment including interactions with other cells as previous experiments demonstrated that homing of mBC to intact lymphoid follicle structures including presence of FDC was a necessity for mBC reactivation (219, 225).

In the present study, we may have observed tissue homing of the KLH-binding mBC as these cells were detectable in the periphery prior to primary immunization but not shortly afterwards followed by their later re-appearance. This suggests their recruitment to lymphoid tissues and their temporary retention. Such specific immune response-related lymphocyte behavior has been observed before. In few animal studies it was shown that pre-immunization circulating antigen-specific lymphocytes were reduced in the periphery by antigen injection presumably due to their temporary retention in secondary lymphoid organs (226-228) and one study conducted in humans reported reduction of circulating B and T cell numbers 7 to 14 days after yellow fever vaccination and their recovery to baseline levels afterwards (229). The time frame of lymphocyte disappearance and re-appearance of the latter study is indeed

consistent with the disappearance and re-appearance kinetics of the KLH^{spec} mBC in the current study.

In this regard another observation deserves attention. As can be seen in Figure 5-6, the pre-primary immunization KLH-binding mBC were poorly blockable which yet did not constitute mere unspecific background as such background should remain stable over time. Instead, the observation was that subsequently the KLH-binding mBC were decreased as described above and the later re-appearing well blockable KLH^{spec} mBC did not add on top of these pre-immunization mBC frequencies. Together with their blood appearance kinetics, this suggests that the pre-immunization KLH-binding mBC were not only retained in secondary lymphoid organs but underwent maturation and selection. Supposedly, in this process low affine mBC, consistent with poor blocking efficiency, either increased their affinity or were negatively selected from the repertoire.

I will close this part of the discussion by returning to a point raised earlier. Theoretically, every large protein antigen, including self-antigens, can be recognized by a specific BCR. It follows that BCR from mBC are not excluded. As poly- and autoreactivity appear to be not specifically counter selected in the mBC generation during a GC reaction (230-233), likely due to low abundance or unexpressed self-antigen in close proximity to the GC environment (234), there must be a mechanism preventing those mBC's uncontrolled reactivation. Otherwise, if mBC acted without such licensing *in vivo,* the associated uncontrolled mBC response would facilitate the initiation, diversification and establishment of long-lived auto-antibody responses as soon as their cross-reactive auto-antigen becomes available through cell rupture or other incidences. Thus, in the framework of autoimmunity the potential mechanism(s) controlling such unrestricted recruitment and activation of cross-specific mBC requires future attention and investigation.

6.2 Tissue distribution of mBC

The second part of this study describes the distribution and compartmentalization of human mBC within different lymphoid organs and the related phenotype compared to in blood circulating mBC. General B and T lymphocyte subset compositions indicated an organ and blood specific compartmentalization of both lineages that was in accordance with a previous study (177). Tissue-dependent compartmentalization was

revealed to be further evident on the B cell subset level, with subsets exclusively present in the one or other organ. Thereby, (CD19^{pos})CD20^{neg}CD27^{neg} B cells exclusively found in the BM presumably constitute a pre-mature B cell population as CD19 represents the earliest B cell lineage determinant and the expression of other B cell-lineage antigens follows thereafter (235). The identity of the in BM found CD20^{neg}CD27^{pos} B cells has to remain elusive at this point but future studies addressing their state of Ig diversification and their stimulatory potential may assist in clarifying their origin.

On the other hand, CD20^{pos}CD27^{neg} (naïve) B cells were always abundantly present in every tissue. Yet in the spleen they were outnumbered by CD20^{pos}CD27^{pos} B cells (mBC). In this regard, analyses of mBC in the organs revealed that these cells did not simply correlate with the relative distribution of CD19^{pos} B cells but showed enrichment in the spleen followed by tonsil. Previous studies described the presence of mBC in the spleen (99, 104, 106), tonsil (101, 106, 236, 237) and BM (96) but a comparable and comprehensive analysis of these was not conducted.

Interestingly, the current study found no indication of any correlation of age to mBC-accumulation in adult lymphoid organs. This suggests that the diverse lifestyles, immune history and genetic heterogeneity within the here representative analyzed donor population did not result in large variations of mBC content in the respective organ over time. Moreover, together with the results from the absolute number approximations, each tissue/organ appears to have a certain pre-defined capacity to maintain B cells and mBC. Such notable consistencies have been identified before for human T cells (177).

Unfortunately we did not have access to tissue samples from younger children, which should however be addressed in future studies as especially the mBC compartment is established during the first 10-15 years of life, as mentioned before (section 5.2.4). It would be interesting to determine the accumulation of mBC during these years in the one or other organ and correlate that to potential effects of responsiveness to vaccination and to the potential to establish long lasting antibody titers. It has been shown that the splenic marginal zone which accommodates IgD^{pos} mBC in its majority but also IgD^{neg} mBC requires development over the first 2 years of life which is correlated with a lack of response to polysaccharide vaccines and a high incidence of encapsulated bacterial infections (108, 182).

Notably, also for the BM PC niche a certain requirement of development is indicated since early life TD antibody responses are characterized by a rapid decline of serum titers, such that antigen-specific IgG antibodies revert to baseline levels within months following infant immunization (238). It has been speculated that early-life BM stromal cells fail to provide the molecular signals that support PB survival and differentiation into surviving PC (239). Nevertheless, as conjugate vaccines and other TD immunization are functional in children and induce at least a reactive B cell memory, i.e. mBC, even when antibody titers constantly decline, we can assume that the classical mBC's survival and/or maintenance differs from the other two either in location, micro-environmental factors or in the principle requirement of a certain survival niche (240).

6.2.1 Phenotype of tissue-residing mBC

The overall mBC phenotype analysis conducted here (Figure 5-31) found that blood and splenic, BM and tonsillar mBC were largely similar in most of the markers analyzed. Yet, some differences identified in the isotype distribution, CD69, CD62L and β7 integrin expression leave room for speculation on mBC subset homing behavior and tissue residency.

Firstly, a certain tissue-intrinsic compartmentalization of the different isotype-specific mBC pools was detectable. Tonsillar mBC showed a relative enrichment of IgA^{pos} and IgG^{pos} cells as compared to spleen, BM and blood and a reduced presence or even de-enrichment of double-positive mBC. This may reflect the different functions of the tonsils as part of the mucosa-associated immune system and/or may be the result of the recurrent bacterial infections, as cause of the tonsillectomy. Yet, tonsillistis is usually caused by streptococcus or pneumococcus infections for which $IgD^{pos}CD27^{pos}$ mBC were shown to specifically impart the protective immune response (241) and from that one would expect an accumulation of these cells in the tonsils. However, as it is in principle possible that such initial TI responses convert to TD responses including switching to IgA or IgG then this would be consistent with the here found results again. To address this further, subsequent experiments should include detailed BCR sequence analyses to elucidate consequent resulting interrelationships between the pre- and post-switch tonsillar mBC compartments, besides determination of their specificities.

Another very interesting observation was that tonsillar mBC expressed the lymphocyte mucosal homing associated molecule β7 integrin less frequently compared to splenic mBC for example. It has been shown that recirculation of murine lymphocytes to the mucosae involves binding of α4β7 integrin to the mucosal vascular addressin cell adhesion molecule 1 (MAdCAM-1), which is predominantly expressed on venules in the gut-associated lymphoid tissue (GALT) and intestinal lamina propria (242). In humans there is only indirect evidence suggesting that α4β7 expressing (T) lymphocytes migrate selectively to the intestine and that it is a ligand for MAdCAM-1 (243-245) while it is generally accepted that α4β7 integrin is involved in lymphocyte mucosal homing behavior and mucosa-associated responses (152). The infrequent expression of β7 integrin by mBC in a mucosa-associated organ, i.e. tonsil, and the role of β7 integrin on splenic mBC in such abundance pose an interesting finding and suggests for the latter either their gut mucosal origin or their potential of re-circulation to the gut mucosal tissues.

In mice, it was shown that a splenic side population seeded into the gut and was responsible to replenish the intestinal B1 B cells pool (246) illustrating that splenic B cells (precursors) can seed into the gut B cell pool. For the human system, based on the following indications, I put forward the hypothesis that splenic marginal zone (IgD^{pos}) mBC, which are thought to confer protection from bacterial infections, may even traffic between the gut mucosae and the spleen presumably via the blood. In humans MAdCAM-1-expressing fibroblasts draw a ring like structure within the human splenic marginal zone (107) which I propose may specifically retard the $CD27^{pos}$ mBC in this area. This suggestion would be consistent with the observation that the human splenic marginal zone exhibits an accumulation of IgD^{pos} mBC which I could show here possess a higher density of β7 integrin than IgD^{neg} mBC (Figure 5-32). The proposed gut-spleen interrelation could consequently induce a systemic protection to gut-originating pathogens. This may prove vital in the case of mucosal barrier damage and pathogen leakage into the blood stream.

That an exchange of marginal zone and gut B cells can principally occur is evident by the fact that MALT lymphomas frequently populate the splenic marginal zone (shortly summarized by Jo Spencer (247)).

Strikingly, MAdCAM-1 expression is completely absent in human tonsils (245).

Another noticeable finding was revealed when analyzing expression of CD69 and CD62L. MBC from tonsils expressed low levels of CD69 contrasting circulating, splenic and BM mBC in which CD69 expression was absent. CD69 is an acknowledged marker of early (T) cell activation which consequently should coincide with proliferation (248). As the here conducted analysis of the cell-proliferation marker Ki-67 showed that mBC from all tissues were quiescent cells in their large majority, we can assume that CD69 does not mark an activated mBC population within the tonsil. Therefore a second function of CD69 expression may be of interest here. CD69 has been indicated to have a potential role in thymocyte egress and lymphocyte migration (249). In this regard, Shiow and colleagues further showed that CD69 negatively regulates S1PR1 surface expression and consequently hinders lymphocyte tissue egress (250). Specifically, tissue resident memory T cells populations (T_{RM}) have been found to lack expression of the transcription factor Krüppel-like Factor 2 (KLF2) and its target S1PR1 whereof in consequence surface expression of CD69 is elevated and this expression has been linked to their retention (251-256). With regard to B cells, direct cell surface staining of S1PR1 on B cells has proven difficult (257) but elevated CD69 expression can serve as a surrogate marker for its reduced expression (258, 259). Therefore, the here found $CD69^{pos}$ tonsillar mBC could constitute a true tissue-resident mBC subset in contrast to BM and splenic mBC. Noteworthy though, CD62L has also been shown to be under positive control of KLF2, i.e. upregulation of CD69 should coincide with a loss or at least a strong reduction of CD62L surface expression (260) and consistently T_{RM} do not express it anymore. In this study we found an interesting variability of CD62L expression on human tissue-residing mBC not consistent with this just described CD69-CD62L counter-expression described for T_{RM}. As expected CD62L was highly expressed on circulating mBC and a marginal but significant reduction was detectable on BM and tonsillar mBC. For the latter, the still high abundance of CD62L is not consistent with properties described for tissue-resident cells. Yet, at least for mouse B cells, regulation of trafficking-associated molecules under KLF2 appears distinct compared to T cells (259-261) whereas these aspects require clarification in the human system.

However, CD62L was strongly reduced on splenic mBC which poses an interesting discrepancy. Upon CD62L engagement, e.g. entry into a lymph node, the molecule is normally shedded. However, migration or rather recirculation through the spleen has been shown to be independent of CD62L (262, 263) which is why it should not have

been shedded on the recirculating splenic mBC populations which essentially should resemble blood mBC in this regard. Although the level of expression might not essentially be related with the functional capacity, as e.g. known for CXCR4 expression levels and the resultant migratory capacity towards CXCL12 (78, 186), the strong reduction to absence of CD62L on the supposedly recirculatory mBC populations in the spleen was not expected (182) and the underlying mechanisms require future investigations.

Albeit absence/low concentration of CD62L, in further support of a recirculatory nature of splenic mBC is the here reported finding that splenectomy reduced peripheral blood mBC frequencies (Figure 5-35). This is also in accordance with results from other investigations (108-110). And notably, this contrasts the ineffectual absence of tonsils on circulating mBC proportions, which is its notable first description to the best of our knowledge. Thus, the here described $CD69^{pos}$ tonsillar mBC do not appear to contribute to the circulatory pool and therefore may indeed constitute a tissue resident mBC pool.

To address tissue-residency versus circulatory behavior of (memory) B cells in the human system from a more functional angle, current biopharmaceutical therapies may be of assistance. It is acknowledged that B cell depletion during therapy with the anti-CD20 antibody rituximab requires recirculation of affected B cells since the liver has been identified as the major site for the cell depletion (264). Therefore, studies addressing the B cell depletion status in different tissues can serve as an indicator for the resident versus circulatory nature of the organ's (memory) B cell populations. Unfortunately, such studies are only scarcely available for humans. Few studies could show that rituximab largely depletes splenic $CD20^{pos}$ B cells (70, 265, 266) consistent with their suggested recirculatory nature, mature B cells in BM (265, 267, 268) and largely also in lymph nodes (269). In contrast, B cells resident in the GALT tissues appear resistant to rituximab treatment (270). However, no such data is available for human tonsils and therefore final conclusions on tissue-resident mBC in tonsils cannot be drawn at this point.

We reported on a splenectomized patient that provided instructive data exhibiting a normal B cell memory recall response to TT immunization despite having undergone splenectomy 13 years previously, was not booster immunized in between and subsequently required 3 treatment cycles with rituximab because of refractory ITP (203), but was B cell-repleted when we immunized her. Although this is only a one case

report, it indicates that even when the entire circulating mBC compartment was eliminated and the spleen absent, which holds the largest (TT^{pos}) mBC population (section 5.2.8) there must be a compartment of mBC surviving elsewhere. This conclusion would be consistent with publications by Gowans and colleagues where it was described that cannulation and drainage of the rat thoraic duct for several days was associated with progressive decrease of lymphocytes in the lymph, lymph nodes and spleen (271). In extension of these experiments they showed that depletion of these circulating lymphocytes prior to booster immunization did not affect a secondary response (272) suggesting that the sessile lymphocyte compartments were the response eliciting ones.

Potential sites offering mBC survival niches are the mucosal/intestinal tissues, the skin or other non-lymphoid tissues, as shown for $T_{RM.}$ Or even the tonsil, as discussed above. Notably, the tonsil was found to contain TT^{pos} mBC. Since an experiment demonstrated that parenteral TT immunization did not induce local responses in tonsils at all (273), these mBC must have migrated there from their site of induction but may not seed back into recirculation which however remains to be determined.

The presence of mBC, and even of TT^{pos} mBC, continuously circulating in peripheral blood indicates that a certain mBC pool constantly patrols the body. Yet, the relationship to tissue-residing mBC and whether there is a constant turnover has to remain unclear at this point.

The discussed aspects raise important questions and contradictions which are worthwhile addressing in future studies to clarify the existence, whereabouts and requirements of potential tissue-resident human mBC and their regulation in support of development of long-lasting immunity induced by vaccines but also for immunotherapies targeting pathogenic mBC.

6.3 Outlook and concluding remarks

This study contributes to our understanding of human B cell memory induction, maintenance and reactivation. Nevertheless open questions remain and even new questions arose. To start with, the results presented in the KLH immunization study should be confirmed by experiments using a different primary immunization, whereby e.g. yellow fever, tick-borne encephalitis or hepatitis B immunizations would be candidates. In such experiments the data collection should be expanded though.

Firstly, to address the question whether mBC, specific to originally unrelated antigens, are cross-recruited into such a (primary) immune response based on binding of their BCR to the new (immunizing) antigen, isolation and BCR sequencing of pre-immunization antigen-binding mBC should be performed.

Secondly, in addition, also pre-immunization bulk naïve B cell and pre- and post-switch mBC populations should be FACS sorted and their BCR repertoire sequenced using a next-generation sequencing approach, as described and performed for other problems before (39, 156, 274). These sequences could be subsequently investigated for their relationships with the later in blood appearing immunizing-antigen-specific PB and mBC. In addition, the antigen-specific B cell populations should be monitored longer, including sorting and sequencing, which could assist in clarifying whether the proposed repertoire shift already occurs late in the primary response or upon recall, provided that this is visible in the circulating B cell populations.

The suggested experiments could also contribute to an understanding of whether different mBC layers existed in humans which however would include also sorting and sequencing experiments prior to the secondary immunization. Another aspect of major importance is the monitoring of T cells in such a response and to define, if present or absent, how (cross-specific) memory T cell help can influence primary immune responses in humans. Detection of antigen-specific T cells can be performed by *in vitro* stimulation of PBMC with the antigen and detection, characterization and enumeration of $CD154^{pos}$ T cells, i.e. antigen-specific cells, several hours afterwards (275, 276). In a broader sense such knowledge may help optimizing vaccination strategies and could also contribute to an enhanced understanding of underlying mechanisms involved in autoimmunity.

The data of this thesis further provide an assessment of human mBC distribution and characteristics, including defined antigen-specific (TT^{pos}) mBC. Beyond their identification and characterization, it is unclear if these mBC share the same molecular and functional characteristics. To address this, investigations of tissue-residing mBC populations (IgG^{pos} versus IgA^{pos} versus IgM^{pos}/IgD^{pos}) should be extended to more tissues, e.g. skin, intestine and lymph nodes. Also such a new study should include sorting of the different mBC populations and subsequent BCR sequencing as only such an approach could grant insights into mBC repertoire relationships between the different tissues and also to blood mBC. However, a concern here is that since BCR repertoires vary considerably between individuals, to generate interpretable results,

such a comparative analysis would have to be performed on mBC isolated from tissues from one donor, e.g. from organ donors, which may pose ethically difficult. Alternatively, matched blood-tissue samples could be used however, that approach would have obvious limitations. Yet, an experiment which could be performed is the sorting and sequencing of mBC populations within an organ which also has not been performed so far but could contribute clarification to the debate of the relationships of IgD^{neg} and IgD^{pos} mBC (277).

Finally, the BM has been known to provide niche conditions supporting the survival of antibody-secreting PC and also for memory T cells. As quiescence in terms of proliferation and activation appears a favorable condition to sustain also reactive memory lymphocytes, since a frequent reactivation could cause their exhaustion or exterminate them from the repertoire, the non-inflammatory environment together with the niche conditions provided would make the BM an ideal tissue for memory lymphocyte maintenance. Yet, the here described features of tissue mBC do not suggest that these are preferentially maintained in the BM, in contrast to memory T cells and long-lived PC. Hence, future exploration of this aspect is of importance as knowledge about human mBC maintenance and survival requirements could be used for development of new vaccination but also therapeutic intervention strategies.

7. References

1. Silverstein AM. *A History of Immunology.* 1989.
2. Finn OJ. Immuno-oncology: understanding the function and dysfunction of the immune system in cancer. *Annals of oncology : official journal of the European Society for Medical Oncology / ESMO.* 2012;23 Suppl 8(viii6-9.
3. Sallusto F, Lanzavecchia A, Araki K, and Ahmed R. From vaccines to memory and back. *Immunity.* 2010;33(4):451-63.
4. Reth M. Antigen receptors on B lymphocytes. *Annual review of immunology.* 1992;10(97-121.
5. Hozumi N, and Tonegawa S. Evidence for somatic rearrangement of immunoglobulin genes coding for variable and constant regions. *Proceedings of the National Academy of Sciences of the United States of America.* 1976;73(10):3628-32.
6. Croce CM, Shander M, Martinis J, Cicurel L, D'Ancona GG, Dolby TW, and Koprowski H. Chromosomal location of the genes for human immunoglobulin heavy chains. *Proceedings of the National Academy of Sciences of the United States of America.* 1979;76(7):3416-9.
7. Kirsch IR, Morton CC, Nakahara K, and Leder P. Human immunoglobulin heavy chain genes map to a region of translocations in malignant B lymphocytes. *Science.* 1982;216(4543):301-3.
8. Matsuda F, Ishii K, Bourvagnet P, Kuma K, Hayashida H, Miyata T, and Honjo T. The complete nucleotide sequence of the human immunoglobulin heavy chain variable region locus. *The Journal of experimental medicine.* 1998;188(11):2151-62.
9. Ravetch JV, Siebenlist U, Korsmeyer S, Waldmann T, and Leder P. Structure of the human immunoglobulin mu locus: characterization of embryonic and rearranged J and D genes. *Cell.* 1981;27(3 Pt 2):583-91.
10. Corbett SJ, Tomlinson IM, Sonnhammer EL, Buck D, and Winter G. Sequence of the human immunoglobulin diversity (D) segment locus: a systematic analysis provides no evidence for the use of DIR segments, inverted D segments, "minor" D segments or D-D recombination. *Journal of molecular biology.* 1997;270(4):587-97.
11. Lefranc MP. Nomenclature of the human immunoglobulin lambda (IGL) genes. *Experimental and clinical immunogenetics.* 2001;18(4):242-54.
12. Lefranc MP. Nomenclature of the human immunoglobulin kappa (IGK) genes. *Experimental and clinical immunogenetics.* 2001;18(3):161-74.
13. Fugmann SD, Lee AI, Shockett PE, Villey IJ, and Schatz DG. The RAG proteins and V(D)J recombination: complexes, ends, and transposition. *Annual review of immunology.* 2000;18(495-527.
14. Gellert M. V(D)J recombination: RAG proteins, repair factors, and regulation. *Annual review of biochemistry.* 2002;71(101-32.
15. Lewis SM. P nucleotides, hairpin DNA and V(D)J joining: making the connection. *Seminars in immunology.* 1994;6(3):131-41.
16. Lewis SM. The mechanism of V(D)J joining: lessons from molecular, immunological, and comparative analyses. *Advances in immunology.* 1994;56(27-150.
17. Corcoran AE. Immunoglobulin locus silencing and allelic exclusion. *Seminars in immunology.* 2005;17(2):141-54.
18. Hartley SB, Cooke MP, Fulcher DA, Harris AW, Cory S, Basten A, and Goodnow CC. Elimination of self-reactive B lymphocytes proceeds in two stages: arrested development and cell death. *Cell.* 1993;72(3):325-35.
19. Goodnow CC, Crosbie J, Adelstein S, Lavoie TB, Smith-Gill SJ, Brink RA, Pritchard-Briscoe H, Wotherspoon JS, Loblay RH, Raphael K, et al. Altered immunoglobulin expression and functional silencing of self-reactive B lymphocytes in transgenic mice. *Nature.* 1988;334(6184):676-82.
20. Tiegs SL, Russell DM, and Nemazee D. Receptor editing in self-reactive bone marrow B cells. *The Journal of experimental medicine.* 1993;177(4):1009-20.
21. Forster I, and Rajewsky K. The bulk of the peripheral B-cell pool in mice is stable and not rapidly renewed from the bone marrow. *Proceedings of the National Academy of Sciences of the United States of America.* 1990;87(12):4781-4.
22. Carsetti R, Kohler G, and Lamers MC. Transitional B cells are the target of negative selection in the B cell compartment. *The Journal of experimental medicine.* 1995;181(6):2129-40.

23. Itano AA, McSorley SJ, Reinhardt RL, Ehst BD, Ingulli E, Rudensky AY, and Jenkins MK. Distinct dendritic cell populations sequentially present antigen to CD4 T cells and stimulate different aspects of cell-mediated immunity. *Immunity.* 2003;19(1):47-57.
24. Liu YJ, Zhang J, Lane PJ, Chan EY, and MacLennan IC. Sites of specific B cell activation in primary and secondary responses to T cell-dependent and T cell-independent antigens. *European journal of immunology.* 1991;21(12):2951-62.
25. Lanzavecchia A. Antigen-specific interaction between T and B cells. *Nature.* 1985;314(6011):537-9.
26. Cyster JG. Chemokines, sphingosine-1-phosphate, and cell migration in secondary lymphoid organs. *Annual review of immunology.* 2005;23(127-59.
27. Bar-Or A, Oliveira EM, Anderson DE, Krieger JI, Duddy M, O'Connor KC, and Hafler DA. Immunological memory: contribution of memory B cells expressing costimulatory molecules in the resting state. *Journal of immunology.* 2001;167(10):5669-77.
28. Banchereau J, Bazan F, Blanchard D, Briere F, Galizzi JP, van Kooten C, Liu YJ, Rousset F, and Saeland S. The CD40 antigen and its ligand. *Annual review of immunology.* 1994;12(881-922.
29. Blanchard D, Gaillard C, Hermann P, and Banchereau J. Role of CD40 antigen and interleukin-2 in T cell-dependent human B lymphocyte growth. *European journal of immunology.* 1994;24(2):330-5.
30. Galibert L, Durand I, Banchereau J, and Rousset F. CD40-activated surface IgD-positive lymphocytes constitute the long term IL-4-dependent proliferating B cell pool. *Journal of immunology.* 1994;152(1):22-9.
31. Renard N, Duvert V, Blanchard D, Banchereau J, and Saeland S. Activated CD4+ T cells induce CD40-dependent proliferation of human B cell precursors. *Journal of immunology.* 1994;152(4):1693-701.
32. Sharpe AH, and Freeman GJ. The B7-CD28 superfamily. *Nature reviews Immunology.* 2002;2(2):116-26.
33. MacLennan IC, Toellner KM, Cunningham AF, Serre K, Sze DM, Zuniga E, Cook MC, and Vinuesa CG. Extrafollicular antibody responses. *Immunological reviews.* 2003;194(8-18.
34. Ho F, Lortan JE, MacLennan IC, and Khan M. Distinct short-lived and long-lived antibody-producing cell populations. *European journal of immunology.* 1986;16(10):1297-301.
35. Smith KG, Hewitson TD, Nossal GJ, and Tarlinton DM. The phenotype and fate of the antibody-forming cells of the splenic foci. *European journal of immunology.* 1996;26(2):444-8.
36. Glanville J, Zhai W, Berka J, Telman D, Huerta G, Mehta GR, Ni I, Mei L, Sundar PD, Day GM, et al. Precise determination of the diversity of a combinatorial antibody library gives insight into the human immunoglobulin repertoire. *Proceedings of the National Academy of Sciences of the United States of America.* 2009;106(48):20216-21.
37. Poulsen TR, Meijer PJ, Jensen A, Nielsen LS, and Andersen PS. Kinetic, affinity, and diversity limits of human polyclonal antibody responses against tetanus toxoid. *Journal of immunology.* 2007;179(6):3841-50.
38. Frolich D, Giesecke C, Mei HE, Reiter K, Daridon C, Lipsky PE, and Dorner T. Secondary immunization generates clonally related antigen-specific plasma cells and memory B cells. *Journal of immunology.* 2010;185(5):3103-10.
39. Lavinder JJ, Wine Y, Giesecke C, Ippolito GC, Horton AP, Lungu OI, Hoi KH, DeKosky BJ, Murrin EM, Wirth MM, et al. Identification and characterization of the constituent human serum antibodies elicited by vaccination. *Proceedings of the National Academy of Sciences of the United States of America.* 2014;111(6):2259-64.
40. Eisen HN. Affinity enhancement of antibodies: how low-affinity antibodies produced early in immune responses are followed by high-affinity antibodies later and in memory B-cell responses. *Cancer immunology research.* 2014;2(5):381-92.
41. Cumano A, and Rajewsky K. Clonal recruitment and somatic mutation in the generation of immunological memory to the hapten NP. *The EMBO journal.* 1986;5(10):2459-68.
42. Gearhart PJ, Johnson ND, Douglas R, and Hood L. IgG antibodies to phosphorylcholine exhibit more diversity than their IgM counterparts. *Nature.* 1981;291(5810):29-34.
43. Berek C, Griffiths GM, and Milstein C. Molecular events during maturation of the immune response to oxazolone. *Nature.* 1985;316(6027):412-8.
44. Griffiths GM, Berek C, Kaartinen M, and Milstein C. Somatic mutation and the maturation of immune response to 2-phenyl oxazolone. *Nature.* 1984;312(5991):271-5.

45. Kaartinen M, Griffiths GM, Markham AF, and Milstein C. mRNA sequences define an unusually restricted IgG response to 2-phenyloxazolone and its early diversification. *Nature.* 1983;304(5924):320-4.
46. Rudikoff S, Pawlita M, Pumphrey J, and Heller M. Somatic diversification of immunoglobulins. *Proceedings of the National Academy of Sciences of the United States of America.* 1984;81(7):2162-6.
47. Wysocki L, Manser T, and Gefter ML. Somatic evolution of variable region structures during an immune response. *Proceedings of the National Academy of Sciences of the United States of America.* 1986;83(6):1847-51.
48. MacLennan IC. Germinal centers. *Annual review of immunology.* 1994;12(117-39.
49. Kroese FG, Timens W, and Nieuwenhuis P. Germinal center reaction and B lymphocytes: morphology and function. *Current topics in pathology Ergebnisse der Pathologie.* 1990;84 (Pt 1)(103-48.
50. MacLennan IC. Somatic mutation. From the dark zone to the light. *Current biology : CB.* 1994;4(1):70-2.
51. Goossens T, Klein U, and Kuppers R. Frequent occurrence of deletions and duplications during somatic hypermutation: implications for oncogene translocations and heavy chain disease. *Proceedings of the National Academy of Sciences of the United States of America.* 1998;95(5):2463-8.
52. Laffleur B, Denis-Lagache N, Peron S, Sirac C, Moreau J, and Cogne M. AID-induced remodeling of immunoglobulin genes and B cell fate. *Oncotarget.* 2014;5(5):1118-31.
53. Di Noia JM, and Neuberger MS. Molecular mechanisms of antibody somatic hypermutation. *Annual review of biochemistry.* 2007;76(1-22.
54. Neuberger MS, and Rada C. Somatic hypermutation: activation-induced deaminase for C/G followed by polymerase eta for A/T. *The Journal of experimental medicine.* 2007;204(1):7-10.
55. Maul RW, and Gearhart PJ. AID and somatic hypermutation. *Advances in immunology.* 2010;105(159-91.
56. Maul RW, and Gearhart PJ. Controlling somatic hypermutation in immunoglobulin variable and switch regions. *Immunologic research.* 2010;47(1-3):113-22.
57. Maizels N. Immunoglobulin gene diversification. *Annual review of genetics.* 2005;39(23-46.
58. de Vinuesa CG, Cook MC, Ball J, Drew M, Sunners Y, Cascalho M, Wabl M, Klaus GG, and MacLennan IC. Germinal centers without T cells. *The Journal of experimental medicine.* 2000;191(3):485-94.
59. Tew JG, Wu J, Qin D, Helm S, Burton GF, and Szakal AK. Follicular dendritic cells and presentation of antigen and costimulatory signals to B cells. *Immunological reviews.* 1997;156(39-52.
60. Allen CD, Okada T, Tang HL, and Cyster JG. Imaging of germinal center selection events during affinity maturation. *Science.* 2007;315(5811):528-31.
61. Stavnezer J, Guikema JE, and Schrader CE. Mechanism and regulation of class switch recombination. *Annual review of immunology.* 2008;26(261-92.
62. Berek C. The development of B cells and the B-cell repertoire in the microenvironment of the germinal center. *Immunological reviews.* 1992;126(5-19.
63. Blanchard-Rohner G, Pulickal AS, Jol-van der Zijde CM, Snape MD, and Pollard AJ. Appearance of peripheral blood plasma cells and memory B cells in a primary and secondary immune response in humans. *Blood.* 2009;114(24):4998-5002.
64. Blink EJ, Light A, Kallies A, Nutt SL, Hodgkin PD, and Tarlinton DM. Early appearance of germinal center-derived memory B cells and plasma cells in blood after primary immunization. *The Journal of experimental medicine.* 2005;201(4):545-54.
65. Manz RA, Thiel A, and Radbruch A. Lifetime of plasma cells in the bone marrow. *Nature.* 1997;388(6638):133-4.
66. Amanna IJ, Carlson NE, and Slifka MK. Duration of humoral immunity to common viral and vaccine antigens. *The New England journal of medicine.* 2007;357(19):1903-15.
67. Slifka MK, Antia R, Whitmire JK, and Ahmed R. Humoral immunity due to long-lived plasma cells. *Immunity.* 1998;8(3):363-72.
68. Slifka MK, Matloubian M, and Ahmed R. Bone marrow is a major site of long-term antibody production after acute viral infection. *Journal of virology.* 1995;69(3):1895-902.
69. Schittek B, and Rajewsky K. Maintenance of B-cell memory by long-lived cells generated from proliferating precursors. *Nature.* 1990;346(6286):749-51.

70. Mamani-Matsuda M, Cosma A, Weller S, Faili A, Staib C, Garcon L, Hermine O, Beyne-Rauzy O, Fieschi C, Pers JO, et al. The human spleen is a major reservoir for long-lived vaccinia virus-specific memory B cells. *Blood.* 2008;111(9):4653-9.
71. Liu YJ, Barthelemy C, de Bouteiller O, Arpin C, Durand I, and Banchereau J. Memory B cells from human tonsils colonize mucosal epithelium and directly present antigen to T cells by rapid up-regulation of B7-1 and B7-2. *Immunity.* 1995;2(3):239-48.
72. Hayakawa K, Ishii R, Yamasaki K, Kishimoto T, and Hardy RR. Isolation of high-affinity memory B cells: phycoerythrin as a probe for antigen-binding cells. *Proceedings of the National Academy of Sciences of the United States of America.* 1987;84(5):1379-83.
73. Gray D, and Skarvall H. B-cell memory is short-lived in the absence of antigen. *Nature.* 1988;336(6194):70-3.
74. Dunn-Walters AAAaD. Immune Responses: Primary and Secondary. *Ecyclopedia of Life Sciences (ELS) John Wiley & Sons, Ltd: Chichester.* 2010.
75. Kenneth Murphy PT, Mark Walport. Janeway's immunobiology. 2008;7th ed(ISBN 0-8153-4123-7).
76. MacLennan IC, Liu YJ, Oldfield S, Zhang J, and Lane PJ. The evolution of B-cell clones. *Current topics in microbiology and immunology.* 1990;159(37-63.
77. Fink K. Origin and Function of Circulating Plasmablasts during Acute Viral Infections. *Frontiers in immunology.* 2012;3(78.
78. Odendahl M, Mei H, Hoyer BF, Jacobi AM, Hansen A, Muehlinghaus G, Berek C, Hiepe F, Manz R, Radbruch A, et al. Generation of migratory antigen-specific plasma blasts and mobilization of resident plasma cells in a secondary immune response. *Blood.* 2005;105(4):1614-21.
79. Lane P, Burdet C, McConnell F, Lanzavecchia A, and Padovan E. CD40 ligand-independent B cell activation revealed by CD40 ligand-deficient T cell clones: evidence for distinct activation requirements for antibody formation and B cell proliferation. *European journal of immunology.* 1995;25(6):1788-93.
80. Arpin C, Dechanet J, Van Kooten C, Merville P, Grouard G, Briere F, Banchereau J, and Liu YJ. Generation of memory B cells and plasma cells in vitro. *Science.* 1995;268(5211):720-2.
81. Callard RE, Herbert J, Smith SH, Armitage RJ, and Costelloe KE. CD40 cross-linking inhibits specific antibody production by human B cells. *International immunology.* 1995;7(11):1809-15.
82. Rada C, Gupta SK, Gherardi E, and Milstein C. Mutation and selection during the secondary response to 2-phenyloxazolone. *Proceedings of the National Academy of Sciences of the United States of America.* 1991;88(13):5508-12.
83. McHeyzer-Williams LJ, Milpied PJ, Okitsu SL, and McHeyzer-Williams MG. Class-switched memory B cells remodel BCRs within secondary germinal centers. *Nature immunology.* 2015;16(3):296-305.
84. McHeyzer-Williams MG, Nossal GJ, and Lalor PA. Molecular characterization of single memory B cells. *Nature.* 1991;350(6318):502-5.
85. Wrammert J, Smith K, Miller J, Langley WA, Kokko K, Larsen C, Zheng NY, Mays I, Garman L, Helms C, et al. Rapid cloning of high-affinity human monoclonal antibodies against influenza virus. *Nature.* 2008;453(7195):667-71.
86. Ellyard JI, Avery DT, Phan TG, Hare NJ, Hodgkin PD, and Tangye SG. Antigen-selected, immunoglobulin-secreting cells persist in human spleen and bone marrow. *Blood.* 2004;103(10):3805-12.
87. Medina F, Segundo C, Jimenez-Gomez G, Gonzalez-Garcia I, Campos-Caro A, and Brieva JA. Higher maturity and connective tissue association distinguish resident from recently generated human tonsil plasma cells. *Journal of leukocyte biology.* 2007;82(6):1430-6.
88. Radbruch A, Muehlinghaus G, Luger EO, Inamine A, Smith KG, Dorner T, and Hiepe F. Competence and competition: the challenge of becoming a long-lived plasma cell. *Nature reviews Immunology.* 2006;6(10):741-50.
89. Chu VT, Frohlich A, Steinhauser G, Scheel T, Roch T, Fillatreau S, Lee JJ, Lohning M, and Berek C. Eosinophils are required for the maintenance of plasma cells in the bone marrow. *Nature immunology.* 2011;12(2):151-9.
90. Klein U, Goossens T, Fischer M, Kanzler H, Braeuninger A, Rajewsky K, and Kuppers R. Somatic hypermutation in normal and transformed human B cells. *Immunological reviews.* 1998;162(261-80.
91. Klein U, Rajewsky K, and Kuppers R. Human immunoglobulin (Ig)M+IgD+ peripheral blood B cells expressing the CD27 cell surface antigen carry somatically mutated variable region

genes: CD27 as a general marker for somatically mutated (memory) B cells. *The Journal of experimental medicine.* 1998;188(9):1679-89.
92. Tokoyoda K, Hauser AE, Nakayama T, and Radbruch A. Organization of immunological memory by bone marrow stroma. *Nature reviews Immunology.* 2010;10(3):193-200.
93. Tokoyoda K, Zehentmeier S, Chang HD, and Radbruch A. Organization and maintenance of immunological memory by stroma niches. *European journal of immunology.* 2009;39(8):2095-9.
94. Tokoyoda K, Zehentmeier S, Hegazy AN, Albrecht I, Grun JR, Lohning M, and Radbruch A. Professional memory CD4+ T lymphocytes preferentially reside and rest in the bone marrow. *Immunity.* 2009;30(5):721-30.
95. Mayo MS, Paramithiotis E, and Cooper MD. B lymphocyte migration to the bone marrow of humans is not random. *Statistics in medicine.* 1999;18(2):223-31.
96. Paramithiotis E, and Cooper MD. Memory B lymphocytes migrate to bone marrow in humans. *Proceedings of the National Academy of Sciences of the United States of America.* 1997;94(1):208-12.
97. Spencer J, Finn T, Pulford KA, Mason DY, and Isaacson PG. The human gut contains a novel population of B lymphocytes which resemble marginal zone cells. *Clinical and experimental immunology.* 1985;62(3):607-12.
98. Stein H, Bonk A, Tolksdorf G, Lennert K, Rodt H, and Gerdes J. Immunohistologic analysis of the organization of normal lymphoid tissue and non-Hodgkin's lymphomas. *The journal of histochemistry and cytochemistry : official journal of the Histochemistry Society.* 1980;28(8):746-60.
99. Tangye SG, Liu YJ, Aversa G, Phillips JH, and de Vries JE. Identification of functional human splenic memory B cells by expression of CD148 and CD27. *The Journal of experimental medicine.* 1998;188(9):1691-703.
100. Vitetta ES, Berton MT, Burger C, Kepron M, Lee WT, and Yin XM. Memory B and T cells. *Annual review of immunology.* 1991;9(193-217.
101. Pascual V, Liu YJ, Magalski A, de Bouteiller O, Banchereau J, and Capra JD. Analysis of somatic mutation in five B cell subsets of human tonsil. *The Journal of experimental medicine.* 1994;180(1):329-39.
102. Arpin C, Banchereau J, and Liu YJ. Memory B cells are biased towards terminal differentiation: a strategy that may prevent repertoire freezing. *The Journal of experimental medicine.* 1997;186(6):931-40.
103. Dono M, Burgio VL, Tacchetti C, Favre A, Augliera A, Zupo S, Taborelli G, Chiorazzi N, Grossi CE, and Ferrarini M. Subepithelial B cells in the human palatine tonsil. I. Morphologic, cytochemical and phenotypic characterization. *European journal of immunology.* 1996;26(9):2035-42.
104. Ettinger R, Sims GP, Robbins R, Withers D, Fischer RT, Grammer AC, Kuchen S, and Lipsky PE. IL-21 and BAFF/BLyS synergize in stimulating plasma cell differentiation from a unique population of human splenic memory B cells. *Journal of immunology.* 2007;178(5):2872-82.
105. Steiniger B, Timphus EM, and Barth PJ. The splenic marginal zone in humans and rodents: an enigmatic compartment and its inhabitants. *Histochemistry and cell biology.* 2006;126(6):641-8.
106. Steiniger B, Timphus EM, Jacob R, and Barth PJ. CD27+ B cells in human lymphatic organs: re-evaluating the splenic marginal zone. *Immunology.* 2005;116(4):429-42.
107. Steiniger BS, Wilhelmi V, Seiler A, Lampp K, and Stachniss V. Heterogeneity of stromal cells in the human splenic white pulp. Fibroblastic reticulum cells, follicular dendritic cells and a third superficial stromal cell type. *Immunology.* 2014;143(3):462-77.
108. Kruetzmann S, Rosado MM, Weber H, Germing U, Tournilhac O, Peter HH, Berner R, Peters A, Boehm T, Plebani A, et al. Human immunoglobulin M memory B cells controlling Streptococcus pneumoniae infections are generated in the spleen. *The Journal of experimental medicine.* 2003;197(7):939-45.
109. Martinez-Gamboa L, Mei H, Loddenkemper C, Ballmer B, Hansen A, Lipsky PE, Emmerich F, Radbruch A, Salama A, and Dorner T. Role of the spleen in peripheral memory B-cell homeostasis in patients with autoimmune thrombocytopenia purpura. *Clinical immunology.* 2009;130(2):199-212.
110. Cameron PU, Jones P, Gorniak M, Dunster K, Paul E, Lewin S, Woolley I, and Spelman D. Splenectomy associated changes in IgM memory B cells in an adult spleen registry cohort. *PloS one.* 2011;6(8):e23164.

111. Gowans JL, and Uhr JW. The carriage of immunological memory by small lymphocytes in the rat. *The Journal of experimental medicine.* 1966;124(5):1017-30.
112. Campbell MJ, Zelenetz AD, Levy S, and Levy R. Use of family specific leader region primers for PCR amplification of the human heavy chain variable region gene repertoire. *Molecular immunology.* 1992;29(2):193-203.
113. Thoree VC, Golby SJ, Boursier L, Hackett M, Dunn-Walters DK, Sanderson JD, and Spencer J. Related IgA1 and IgG producing cells in blood and diseased mucosa in ulcerative colitis. *Gut.* 2002;51(1):44-50.
114. Marks JD, Tristem M, Karpas A, and Winter G. Oligonucleotide primers for polymerase chain reaction amplification of human immunoglobulin variable genes and design of family-specific oligonucleotide probes. *European journal of immunology.* 1991;21(4):985-91.
115. Yavuz S, Grammer AC, Yavuz AS, Nanki T, and Lipsky PE. Comparative characteristics of mu chain and alpha chain transcripts expressed by individual tonsil plasma cells. *Molecular immunology.* 2001;38(1):19-34.
116. Corazza GR, Ginaldi L, Zoli G, Frisoni M, Lalli G, Gasbarrini G, and Quaglino D. Howell-Jolly body counting as a measure of splenic function. A reassessment. *Clinical and laboratory haematology.* 1990;12(3):269-75.
117. Boyum A. Isolation of mononuclear cells and granulocytes from human blood. Isolation of monuclear cells by one centrifugation, and of granulocytes by combining centrifugation and sedimentation at 1 g. *Scandinavian journal of clinical and laboratory investigation Supplementum.* 1968;97(77-89.
118. Shapiro HM. *Practical flow cytometry.* New York: Wiley-Liss; 2003.
119. Czerkinsky CC, Nilsson LA, Nygren H, Ouchterlony O, and Tarkowski A. A solid-phase enzyme-linked immunospot (ELISPOT) assay for enumeration of specific antibody-secreting cells. *Journal of immunological methods.* 1983;65(1-2):109-21.
120. Aarntzen EH, de Vries IJ, Goertz JH, Beldhuis-Valkis M, Brouwers HM, van de Rakt MW, van der Molen RG, Punt CJ, Adema GJ, Tacken PJ, et al. Humoral anti-KLH responses in cancer patients treated with dendritic cell-based immunotherapy are dictated by different vaccination parameters. *Cancer immunology, immunotherapy : CII.* 2012;61(11):2003-11.
121. Trepel F. Number and distribution of lymphocytes in man. A critical analysis. *Klinische Wochenschrift.* 1974;52(11):511-5.
122. Souto-Carneiro MM, Longo NS, Russ DE, Sun HW, and Lipsky PE. Characterization of the human Ig heavy chain antigen binding complementarity determining region 3 using a newly developed software algorithm, JOINSOLVER. *Journal of immunology.* 2004;172(11):6790-802.
123. Morgenstern B, Dress A, and Werner T. Multiple DNA and protein sequence alignment based on segment-to-segment comparison. *Proceedings of the National Academy of Sciences of the United States of America.* 1996;93(22):12098-103.
124. Dereeper A, Guignon V, Blanc G, Audic S, Buffet S, Chevenet F, Dufayard JF, Guindon S, Lefort V, Lescot M, et al. Phylogeny.fr: robust phylogenetic analysis for the non-specialist. *Nucleic acids research.* 2008;36(Web Server issue):W465-9.
125. Bailey TL, Boden M, Buske FA, Frith M, Grant CE, Clementi L, Ren J, Li WW, and Noble WS. MEME SUITE: tools for motif discovery and searching. *Nucleic acids research.* 2009;37(Web Server issue):W202-8.
126. Larkin MA, Blackshields G, Brown NP, Chenna R, McGettigan PA, McWilliam H, Valentin F, Wallace IM, Wilm A, Lopez R, et al. Clustal W and Clustal X version 2.0. *Bioinformatics.* 2007;23(21):2947-8.
127. Goujon M, McWilliam H, Li W, Valentin F, Squizzato S, Paern J, and Lopez R. A new bioinformatics analysis tools framework at EMBL-EBI. *Nucleic acids research.* 2010;38(Web Server issue):W695-9.
128. Crooks GE, Hon G, Chandonia JM, and Brenner SE. WebLogo: a sequence logo generator. *Genome research.* 2004;14(6):1188-90.
129. Zhang J, MacLennan IC, Liu YJ, and Lane PJ. Is rapid proliferation in B centroblasts linked to somatic mutation in memory B cell clones? *Immunology letters.* 1988;18(4):297-9.
130. Behlke MA, Spinella DG, Chou HS, Sha W, Hartl DL, and Loh DY. T-cell receptor beta-chain expression: dependence on relatively few variable region genes. *Science.* 1985;229(4713):566-70.
131. R Core Team. R: A language and environment for statistical computing. R Foundation for Statistical Computing V, Austria. URL http://www.R-project.org/. 2014.

132. Gatsogiannis C, and Markl J. Keyhole limpet hemocyanin: 9-A CryoEM structure and molecular model of the KLH1 didecamer reveal the interfaces and intricate topology of the 160 functional units. *Journal of molecular biology.* 2009;385(3):963-83.
133. Harris JR, and Markl J. Keyhole limpet hemocyanin (KLH): a biomedical review. *Micron.* 1999;30(6):597-623.
134. Husby S, Mestecky J, Moldoveanu Z, Holland S, and Elson CO. Oral tolerance in humans. T cell but not B cell tolerance after antigen feeding. *Journal of immunology.* 1994;152(9):4663-70.
135. Mestecky J, Husby S, Moldoveanu Z, Waldo FB, van den Wall Bake AW, and Elson CO. Induction of tolerance in humans: effectiveness of oral and nasal immunization routes. *Annals of the New York Academy of Sciences.* 1996;778(194-201.
136. Kapp K, Maul J, Hostmann A, Mundt P, Preiss JC, Wenzel A, Thiel A, Zeitz M, Ullrich R, and Duchmann R. Modulation of systemic antigen-specific immune responses by oral antigen in humans. *European journal of immunology.* 2010;40(11):3128-37.
137. Slovin SF, Keding SJ, and Ragupathi G. Carbohydrate vaccines as immunotherapy for cancer. *Immunology and cell biology.* 2005;83(4):418-28.
138. Lee ST, Jiang YF, Park KU, Woo AF, and Neelapu SS. BiovaxID: a personalized therapeutic cancer vaccine for non-Hodgkin's lymphoma. *Expert opinion on biological therapy.* 2007;7(1):113-22.
139. Flowers CR. BiovaxID idiotype vaccination: active immunotherapy for follicular lymphoma. *Expert review of vaccines.* 2007;6(3):307-17.
140. Shah HB, and Koelsch KA. B-Cell ELISPOT: For the Identification of Antigen-Specific Antibody-Secreting Cells. *Methods in molecular biology.* 2015;1312(419-26.
141. Frisan T, Levitsky V, and Masucci M. Limiting dilution assay. *Methods in molecular biology.* 2001;174(213-6.
142. Rawstron AC. Immunophenotyping of plasma cells. *Current protocols in cytometry / editorial board, J Paul Robinson, managing editor [et al].* 2006;Chapter 6(Unit6 23.
143. Agematsu K. Memory B cells and CD27. *Histology and histopathology.* 2000;15(2):573-6.
144. Agematsu K, Hokibara S, Nagumo H, and Komiyama A. CD27: a memory B-cell marker. *Immunology today.* 2000;21(5):204-6.
145. Cerutti A. The regulation of IgA class switching. *Nature reviews Immunology.* 2008;8(6):421-34.
146. Stavnezer J, and Kang J. The surprising discovery that TGF beta specifically induces the IgA class switch. *Journal of immunology.* 2009;182(1):5-7.
147. van Vlasselaer P, Punnonen J, and de Vries JE. Transforming growth factor-beta directs IgA switching in human B cells. *Journal of immunology.* 1992;148(7):2062-7.
148. Berlin C, Berg EL, Briskin MJ, Andrew DP, Kilshaw PJ, Holzmann B, Weissman IL, Hamann A, and Butcher EC. Alpha 4 beta 7 integrin mediates lymphocyte binding to the mucosal vascular addressin MAdCAM-1. *Cell.* 1993;74(1):185-95.
149. Camerini D, James SP, Stamenkovic I, and Seed B. Leu-8/TQ1 is the human equivalent of the Mel-14 lymph node homing receptor. *Nature.* 1989;342(6245):78-82.
150. Kishimoto TK, Jutila MA, and Butcher EC. Identification of a human peripheral lymph node homing receptor: a rapidly down-regulated adhesion molecule. *Proceedings of the National Academy of Sciences of the United States of America.* 1990;87(6):2244-8.
151. Gallatin WM, Weissman IL, and Butcher EC. A cell-surface molecule involved in organ-specific homing of lymphocytes. *Nature.* 1983;304(5921):30-4.
152. Kantele A, Kantele JM, Savilahti E, Westerholm M, Arvilommi H, Lazarovits A, Butcher EC, and Makela PH. Homing potentials of circulating lymphocytes in humans depend on the site of activation: oral, but not parenteral, typhoid vaccination induces circulating antibody-secreting cells that all bear homing receptors directing them to the gut. *Journal of immunology.* 1997;158(2):574-9.
153. Quiding-Jarbrink M, Nordstrom I, Granstrom G, Kilander A, Jertborn M, Butcher EC, Lazarovits AI, Holmgren J, and Czerkinsky C. Differential expression of tissue-specific adhesion molecules on human circulating antibody-forming cells after systemic, enteric, and nasal immunizations. A molecular basis for the compartmentalization of effector B cell responses. *The Journal of clinical investigation.* 1997;99(6):1281-6.
154. Zuccarino-Catania GV, Sadanand S, Weisel FJ, Tomayko MM, Meng H, Kleinstein SH, Good-Jacobson KL, and Shlomchik MJ. CD80 and PD-L2 define functionally distinct memory B cell subsets that are independent of antibody isotype. *Nature immunology.* 2014;15(7):631-7.

155. Dogan I, Bertocci B, Vilmont V, Delbos F, Megret J, Storck S, Reynaud CA, and Weill JC. Multiple layers of B cell memory with different effector functions. *Nature immunology.* 2009;10(12):1292-9.
156. Wu YC, Kipling D, Leong HS, Martin V, Ademokun AA, and Dunn-Walters DK. High-throughput immunoglobulin repertoire analysis distinguishes between human IgM memory and switched memory B-cell populations. *Blood.* 2010;116(7):1070-8.
157. http://CRAN.R-project.org/package=pheatmap RKpPHRpv. 2013.
158. Smith KG, Light A, Nossal GJ, and Tarlinton DM. The extent of affinity maturation differs between the memory and antibody-forming cell compartments in the primary immune response. *The EMBO journal.* 1997;16(11):2996-3006.
159. McKean D, Huppi K, Bell M, Staudt L, Gerhard W, and Weigert M. Generation of antibody diversity in the immune response of BALB/c mice to influenza virus hemagglutinin. *Proceedings of the National Academy of Sciences of the United States of America.* 1984;81(10):3180-4.
160. Berek C, and Milstein C. Mutation drift and repertoire shift in the maturation of the immune response. *Immunological reviews.* 1987;96(23-41.
161. Sablitzky F, Wildner G, and Rajewsky K. Somatic mutation and clonal expansion of B cells in an antigen-driven immune response. *The EMBO journal.* 1985;4(2):345-50.
162. Levy NS, Malipiero UV, Lebecque SG, and Gearhart PJ. Early onset of somatic mutation in immunoglobulin VH genes during the primary immune response. *The Journal of experimental medicine.* 1989;169(6):2007-19.
163. Kleinstein SH, Louzoun Y, and Shlomchik MJ. Estimating hypermutation rates from clonal tree data. *Journal of immunology.* 2003;171(9):4639-49.
164. Zaitoun AM. Cell population kinetics of the germinal centres of lymph nodes of BALB/c mice. *Journal of anatomy.* 1980;130(Pt 1):131-7.
165. Andersen PS, Haahr-Hansen M, Coljee VW, Hinnerfeldt FR, Varming K, Bregenholt S, and Haurum JS. Extensive restrictions in the VH sequence usage of the human antibody response against the Rhesus D antigen. *Molecular immunology.* 2007;44(4):412-22.
166. Adderson EE, Shackelford PG, Quinn A, Wilson PM, Cunningham MW, Insel RA, and Carroll WL. Restricted immunoglobulin VH usage and VDJ combinations in the human response to Haemophilus influenzae type b capsular polysaccharide. Nucleotide sequences of monospecific anti-Haemophilus antibodies and polyspecific antibodies cross-reacting with self antigens. *The Journal of clinical investigation.* 1993;91(6):2734-43.
167. Medina F, Segundo C, Campos-Caro A, Gonzalez-Garcia I, and Brieva JA. The heterogeneity shown by human plasma cells from tonsil, blood, and bone marrow reveals graded stages of increasing maturity, but local profiles of adhesion molecule expression. *Blood.* 2002;99(6):2154-61.
168. Bohnhorst JO, Bjorgan MB, Thoen JE, Natvig JB, and Thompson KM. Bm1-Bm5 classification of peripheral blood B cells reveals circulating germinal center founder cells in healthy individuals and disturbance in the B cell subpopulations in patients with primary Sjogren's syndrome. *Journal of immunology.* 2001;167(7):3610-8.
169. Agematsu K, Nagumo H, Shinozaki K, Hokibara S, Yasui K, Terada K, Kawamura N, Toba T, Nonoyama S, Ochs HD, et al. Absence of IgD-CD27(+) memory B cell population in X-linked hyper-IgM syndrome. *The Journal of clinical investigation.* 1998;102(4):853-60.
170. Agematsu K, Nagumo H, Yang FC, Nakazawa T, Fukushima K, Ito S, Sugita K, Mori T, Kobata T, Morimoto C, et al. B cell subpopulations separated by CD27 and crucial collaboration of CD27+ B cells and helper T cells in immunoglobulin production. *European journal of immunology.* 1997;27(8):2073-9.
171. Nagumo H, and Agematsu K. Synergistic augmentative effect of interleukin-10 and CD27/CD70 interactions on B-cell immunoglobulin synthesis. *Immunology.* 1998;94(3):388-94.
172. Klein U, Kuppers R, and Rajewsky K. Evidence for a large compartment of IgM-expressing memory B cells in humans. *Blood.* 1997;89(4):1288-98.
173. Wu YC, Kipling D, and Dunn-Walters DK. The relationship between CD27 negative and positive B cell populations in human peripheral blood. *Frontiers in immunology.* 2011;2(81.
174. Fecteau JF, Cote G, and Neron S. A new memory CD27-IgG+ B cell population in peripheral blood expressing VH genes with low frequency of somatic mutation. *Journal of immunology.* 2006;177(6):3728-36.
175. Wei C, Anolik J, Cappione A, Zheng B, Pugh-Bernard A, Brooks J, Lee EH, Milner EC, and Sanz I. A new population of cells lacking expression of CD27 represents a notable component

of the B cell memory compartment in systemic lupus erythematosus. *Journal of immunology.* 2007;178(10):6624-33.
176. Jung J, Choe J, Li L, and Choi YS. Regulation of CD27 expression in the course of germinal center B cell differentiation: the pivotal role of IL-10. *European journal of immunology.* 2000;30(8):2437-43.
177. Sathaliyawala T, Kubota M, Yudanin N, Turner D, Camp P, Thome JJ, Bickham KL, Lerner H, Goldstein M, Sykes M, et al. Distribution and compartmentalization of human circulating and tissue-resident memory T cell subsets. *Immunity.* 2013;38(1):187-97.
178. Bankovich AJ, Shiow LR, and Cyster JG. CD69 suppresses sphingosine 1-phosophate receptor-1 (S1P1) function through interaction with membrane helix 4. *The Journal of biological chemistry.* 2010;285(29):22328-37.
179. Grigorova IL, Schwab SR, Phan TG, Pham TH, Okada T, and Cyster JG. Cortical sinus probing, S1P1-dependent entry and flow-based capture of egressing T cells. *Nature immunology.* 2009;10(1):58-65.
180. Nakamura S, Sung SS, Bjorndahl JM, and Fu SM. Human T cell activation. IV. T cell activation and proliferation via the early activation antigen EA 1. *The Journal of experimental medicine.* 1989;169(3):677-89.
181. Scholzen T, and Gerdes J. The Ki-67 protein: from the known and the unknown. *Journal of cellular physiology.* 2000;182(3):311-22.
182. Weller S, Braun MC, Tan BK, Rosenwald A, Cordier C, Conley ME, Plebani A, Kumararatne DS, Bonnet D, Tournilhac O, et al. Human blood IgM "memory" B cells are circulating splenic marginal zone B cells harboring a prediversified immunoglobulin repertoire. *Blood.* 2004;104(12):3647-54.
183. Hatzivassiliou G, Miller I, Takizawa J, Palanisamy N, Rao PH, Iida S, Tagawa S, Taniwaki M, Russo J, Neri A, et al. IRTA1 and IRTA2, novel immunoglobulin superfamily receptors expressed in B cells and involved in chromosome 1q21 abnormalities in B cell malignancy. *Immunity.* 2001;14(3):277-89.
184. Ehrhardt GR, Hsu JT, Gartland L, Leu CM, Zhang S, Davis RS, and Cooper MD. Expression of the immunoregulatory molecule FcRH4 defines a distinctive tissue-based population of memory B cells. *The Journal of experimental medicine.* 2005;202(6):783-91.
185. Ansel KM, Ngo VN, Hyman PL, Luther SA, Forster R, Sedgwick JD, Browning JL, Lipp M, and Cyster JG. A chemokine-driven positive feedback loop organizes lymphoid follicles. *Nature.* 2000;406(6793):309-14.
186. Hauser AE, Debes GF, Arce S, Cassese G, Hamann A, Radbruch A, and Manz RA. Chemotactic responsiveness toward ligands for CXCR3 and CXCR4 is regulated on plasma blasts during the time course of a memory immune response. *Journal of immunology.* 2002;169(3):1277-82.
187. Rott LS, Briskin MJ, Andrew DP, Berg EL, and Butcher EC. A fundamental subdivision of circulating lymphocytes defined by adhesion to mucosal addressin cell adhesion molecule-1. Comparison with vascular cell adhesion molecule-1 and correlation with beta 7 integrins and memory differentiation. *Journal of immunology.* 1996;156(10):3727-36.
188. Heffner RR, Jr., and Schluederberg A. Specificity of the primary and secondary antibody responses to myxoviruses. *Journal of immunology.* 1967;98(4):668-72.
189. Clutterbuck EA, Oh S, Hamaluba M, Westcar S, Beverley PC, and Pollard AJ. Serotype-specific and age-dependent generation of pneumococcal polysaccharide-specific memory B-cell and antibody responses to immunization with a pneumococcal conjugate vaccine. *Clinical and vaccine immunology : CVI.* 2008;15(2):182-93.
190. Lane HC, Volkman DJ, Whalen G, and Fauci AS. In vitro antigen-induced, antigen-specific antibody production in man. Specific and polyclonal components, kinetics, and cellular requirements. *The Journal of experimental medicine.* 1981;154(4):1043-57.
191. Ademokun A, Wu YC, Martin V, Mitra R, Sack U, Baxendale H, Kipling D, and Dunn-Walters DK. Vaccination-induced changes in human B-cell repertoire and pneumococcal IgM and IgA antibody at different ages. *Aging cell.* 2011;10(6):922-30.
192. Wu YC, Kipling D, and Dunn-Walters DK. Age-Related Changes in Human Peripheral Blood IGH Repertoire Following Vaccination. *Frontiers in immunology.* 2012;3(193.
193. Waldo FB, van den Wall Bake AW, Mestecky J, and Husby S. Suppression of the immune response by nasal immunization. *Clinical immunology and immunopathology.* 1994;72(1):30-4.
194. Ballow M. Primary immunodeficiency disorders: antibody deficiency. *The Journal of allergy and clinical immunology.* 2002;109(4):581-91.

195. Hammarstrom L, Vorechovsky I, and Webster D. Selective IgA deficiency (SIgAD) and common variable immunodeficiency (CVID). *Clinical and experimental immunology.* 2000;120(2):225-31.
196. Singh K, Chang C, and Gershwin ME. IgA deficiency and autoimmunity. *Autoimmunity reviews.* 2014;13(2):163-77.
197. Czerkinsky C, Prince SJ, Michalek SM, Jackson S, Russell MW, Moldoveanu Z, McGhee JR, and Mestecky J. IgA antibody-producing cells in peripheral blood after antigen ingestion: evidence for a common mucosal immune system in humans. *Proceedings of the National Academy of Sciences of the United States of America.* 1987;84(8):2449-53.
198. Mei HE, Wirries I, Frolich D, Brisslert M, Giesecke C, Grun JR, Alexander T, Schmidt S, Luda K, Kuhl AA, et al. A unique population of IgG-expressing plasma cells lacking CD19 is enriched in human bone marrow. *Blood.* 2015;125(11):1739-48.
199. Jacob J, and Kelsoe G. In situ studies of the primary immune response to (4-hydroxy-3-nitrophenyl)acetyl. II. A common clonal origin for periarteriolar lymphoid sheath-associated foci and germinal centers. *The Journal of experimental medicine.* 1992;176(3):679-87.
200. Jacob J, Przylepa J, Miller C, and Kelsoe G. In situ studies of the primary immune response to (4-hydroxy-3-nitrophenyl)acetyl. III. The kinetics of V region mutation and selection in germinal center B cells. *The Journal of experimental medicine.* 1993;178(4):1293-307.
201. Cozine CL, Wolniak KL, and Waldschmidt TJ. The primary germinal center response in mice. *Current opinion in immunology.* 2005;17(3):298-302.
202. Reth M, Hammerling GJ, and Rajewsky K. Analysis of the repertoire of anti-NP antibodies in C57BL/6 mice by cell fusion. I. Characterization of antibody families in the primary and hyperimmune response. *European journal of immunology.* 1978;8(6):393-400.
203. Giesecke C, Frolich D, Reiter K, Mei HE, Wirries I, Kuhly R, Killig M, Glatzer T, Stolzel K, Perka C, et al. Tissue distribution and dependence of responsiveness of human antigen-specific memory B cells. *Journal of immunology.* 2014;192(7):3091-100.
204. Blum KS, and Pabst R. Lymphocyte numbers and subsets in the human blood. Do they mirror the situation in all organs? *Immunology letters.* 2007;108(1):45-51.
205. Cumano A, and Rajewsky K. Structure of primary anti-(4-hydroxy-3-nitrophenyl)acetyl (NP) antibodies in normal and idiotypically suppressed C57BL/6 mice. *European journal of immunology.* 1985;15(5):512-20.
206. Malipiero UV, Levy NS, and Gearhart PJ. Somatic mutation in anti-phosphorylcholine antibodies. *Immunological reviews.* 1987;96(59-74.
207. Berek C, and Milstein C. The dynamic nature of the antibody repertoire. *Immunological reviews.* 1988;105(5-26.
208. Becker KA, Ghule PN, Therrien JA, Lian JB, Stein JL, van Wijnen AJ, and Stein GS. Self-renewal of human embryonic stem cells is supported by a shortened G1 cell cycle phase. *Journal of cellular physiology.* 2006;209(3):883-93.
209. Baserga R. The Relationship of the Cell Cycle to Tumor Growth and Control of Cell Division: A Review. *Cancer research.* 1965;25(581-95.
210. Celada F, and Seiden PE. Affinity maturation and hypermutation in a simulation of the humoral immune response. *European journal of immunology.* 1996;26(6):1350-8.
211. Shlomchik MJ, Watts P, Weigert MG, and Litwin S. Clone: a Monte-Carlo computer simulation of B cell clonal expansion, somatic mutation, and antigen-driven selection. *Current topics in microbiology and immunology.* 1998;229(173-97.
212. Kleinstein SH, and Singh JP. Toward quantitative simulation of germinal center dynamics: biological and modeling insights from experimental validation. *Journal of theoretical biology.* 2001;211(3):253-75.
213. Sanz I, Wei C, Lee FE, and Anolik J. Phenotypic and functional heterogeneity of human memory B cells. *Seminars in immunology.* 2008;20(1):67-82.
214. Tangye SG, and Tarlinton DM. Memory B cells: effectors of long-lived immune responses. *European journal of immunology.* 2009;39(8):2065-75.
215. Rogers PR, Dubey C, and Swain SL. Qualitative changes accompany memory T cell generation: faster, more effective responses at lower doses of antigen. *Journal of immunology.* 2000;164(5):2338-46.
216. Crotty S, Felgner P, Davies H, Glidewell J, Villarreal L, and Ahmed R. Cutting edge: long-term B cell memory in humans after smallpox vaccination. *Journal of immunology.* 2003;171(10):4969-73.
217. Leyendeckers H, Odendahl M, Lohndorf A, Irsch J, Spangfort M, Miltenyi S, Hunzelmann N, Assenmacher M, Radbruch A, and Schmitz J. Correlation analysis between frequencies of

circulating antigen-specific IgG-bearing memory B cells and serum titers of antigen-specific IgG. *European journal of immunology.* 1999;29(4):1406-17.
218. Nanan R, Heinrich D, Frosch M, and Kreth HW. Acute and long-term effects of booster immunisation on frequencies of antigen-specific memory B-lymphocytes. *Vaccine.* 2001;20(3-4):498-504.
219. Weisel FJ, Appelt UK, Schneider AM, Horlitz JU, van Rooijen N, Korner H, Mach M, and Winkler TH. Unique requirements for reactivation of virus-specific memory B lymphocytes. *Journal of immunology.* 2010;185(7):4011-21.
220. Schwickert TA, Alabyev B, Manser T, and Nussenzweig MC. Germinal center reutilization by newly activated B cells. *The Journal of experimental medicine.* 2009;206(13):2907-14.
221. Pape KA, Taylor JJ, Maul RW, Gearhart PJ, and Jenkins MK. Different B cell populations mediate early and late memory during an endogenous immune response. *Science.* 2011;331(6021):1203-7.
222. McHeyzer-Williams M, Okitsu S, Wang N, and McHeyzer-Williams L. Molecular programming of B cell memory. *Nature reviews Immunology.* 2012;12(1):24-34.
223. Clarke ET, Williams NA, Findlow J, Borrow R, Heyderman RS, and Finn A. Polysaccharide-specific memory B cells generated by conjugate vaccines in humans conform to the CD27+IgG+ isotype-switched memory B Cell phenotype and require contact-dependent signals from bystander T cells activated by bacterial proteins to differentiate into plasma cells. *Journal of immunology.* 2013;191(12):6071-83.
224. Hebeis BJ, Klenovsek K, Rohwer P, Ritter U, Schneider A, Mach M, and Winkler TH. Activation of virus-specific memory B cells in the absence of T cell help. *The Journal of experimental medicine.* 2004;199(4):593-602.
225. Forster R, Mattis AE, Kremmer E, Wolf E, Brem G, and Lipp M. A putative chemokine receptor, BLR1, directs B cell migration to defined lymphoid organs and specific anatomic compartments of the spleen. *Cell.* 1996;87(6):1037-47.
226. Ciabattini A, Pettini E, Fiorino F, Prota G, Pozzi G, and Medaglini D. Distribution of primed T cells and antigen-loaded antigen presenting cells following intranasal immunization in mice. *PloS one.* 2011;6(4):e19346.
227. Rowley DA, Gowans JL, Atkins RC, Ford WL, and Smith ME. The specific selection of recirculating lymphocytes by antigen in normal and preimmunized rats. *The Journal of experimental medicine.* 1972;136(3):499-513.
228. Sprent J, Miller JF, and Mitchell GF. Antigen-induced selective recruitment of circulating lymphocytes. *Cellular immunology.* 1971;2(2):171-81.
229. Kohler S, Bethke N, Bothe M, Sommerick S, Frentsch M, Romagnani C, Niedrig M, and Thiel A. The early cellular signatures of protective immunity induced by live viral vaccination. *European journal of immunology.* 2012;42(9):2363-73.
230. Haynes BF, Fleming J, St Clair EW, Katinger H, Stiegler G, Kunert R, Robinson J, Scearce RM, Plonk K, Staats HF, et al. Cardiolipin polyspecific autoreactivity in two broadly neutralizing HIV-1 antibodies. *Science.* 2005;308(5730):1906-8.
231. Verkoczy L, Kelsoe G, Moody MA, and Haynes BF. Role of immune mechanisms in induction of HIV-1 broadly neutralizing antibodies. *Current opinion in immunology.* 2011;23(3):383-90.
232. Zhou T, Georgiev I, Wu X, Yang ZY, Dai K, Finzi A, Kwon YD, Scheid JF, Shi W, Xu L, et al. Structural basis for broad and potent neutralization of HIV-1 by antibody VRC01. *Science.* 2010;329(5993):811-7.
233. Scheid JF, Mouquet H, Ueberheide B, Diskin R, Klein F, Oliveira TY, Pietzsch J, Fenyo D, Abadir A, Velinzon K, et al. Sequence and structural convergence of broad and potent HIV antibodies that mimic CD4 binding. *Science.* 2011;333(6049):1633-7.
234. Chan TD, Wood K, Hermes JR, Butt D, Jolly CJ, Basten A, and Brink R. Elimination of germinal-center-derived self-reactive B cells is governed by the location and concentration of self-antigen. *Immunity.* 2012;37(5):893-904.
235. Uckun FM. Regulation of human B-cell ontogeny. *Blood.* 1990;76(10):1908-23.
236. Liu YJ, de Bouteiller O, Arpin C, Durand I, and Banchereau J. Five human mature B cell subsets. *Advances in experimental medicine and biology.* 1994;355(289-96.
237. Cao Y, Gordic M, Kobold S, Lajmi N, Meyer S, Bartels K, Hildebrandt Y, Luetkens T, Ihloff AS, Kroger N, et al. An optimized assay for the enumeration of antigen-specific memory B cells in different compartments of the human body. *Journal of immunological methods.* 2010;358(1-2):56-65.
238. Giuliano M, Mastrantonio P, Giammanco A, Piscitelli A, Salmaso S, and Wassilak SG. Antibody responses and persistence in the two years after immunization with two acellular

vaccines and one whole-cell vaccine against pertussis. *The Journal of pediatrics.* 1998;132(6):983-8.
239. Pihlgren M, Friedli M, Tougne C, Rochat AF, Lambert PH, and Siegrist CA. Reduced ability of neonatal and early-life bone marrow stromal cells to support plasmablast survival. *Journal of immunology.* 2006;176(1):165-72.
240. Rosado MM, Scarsella M, Pandolfi E, Cascioli S, Giorda E, Chionne P, Madonne E, Gesualdo F, Romano M, Ausiello CM, et al. Switched memory B cells maintain specific memory independently of serum antibodies: the hepatitis B example. *European journal of immunology.* 2011;41(6):1800-8.
241. Takizawa M, Sugane K, and Agematsu K. Role of tonsillar IgD+CD27+ memory B cells in humoral immunity against pneumococcal infection. *Human immunology.* 2006;67(12):966-75.
242. Brandtzaeg P, Farstad IN, and Haraldsen G. Regional specialization in the mucosal immune system: primed cells do not always home along the same track. *Immunology today.* 1999;20(6):267-77.
243. Erle DJ, Briskin MJ, Butcher EC, Garcia-Pardo A, Lazarovits AI, and Tidswell M. Expression and function of the MAdCAM-1 receptor, integrin alpha 4 beta 7, on human leukocytes. *Journal of immunology.* 1994;153(2):517-28.
244. Wang X, Xu H, Gill AF, Pahar B, Kempf D, Rasmussen T, Lackner AA, and Veazey RS. Monitoring alpha4beta7 integrin expression on circulating CD4+ T cells as a surrogate marker for tracking intestinal CD4+ T-cell loss in SIV infection. *Mucosal immunology.* 2009;2(6):518-26.
245. Bourges D, Wang CH, Chevaleyre C, and Salmon H. T and IgA B lymphocytes of the pharyngeal and palatine tonsils: differential expression of adhesion molecules and chemokines. *Scandinavian journal of immunology.* 2004;60(4):338-50.
246. Rosado MM, Aranburu A, Capolunghi F, Giorda E, Cascioli S, Cenci F, Petrini S, Miller E, Leanderson T, Bottazzo GF, et al. From the fetal liver to spleen and gut: the highway to natural antibody. *Mucosal immunology.* 2009;2(4):351-61.
247. Spencer J, and Dogan A. A common migratory highway between human spleen and mucosa-associated lymphoid tissues; data from nature's own experiments. *Mucosal immunology.* 2009;2(5):380-2.
248. Ziegler SF, Ramsdell F, and Alderson MR. The activation antigen CD69. *Stem cells.* 1994;12(5):456-65.
249. Feng C, Woodside KJ, Vance BA, El-Khoury D, Canelles M, Lee J, Gress R, Fowlkes BJ, Shores EW, and Love PE. A potential role for CD69 in thymocyte emigration. *International immunology.* 2002;14(6):535-44.
250. Shiow LR, Rosen DB, Brdickova N, Xu Y, An J, Lanier LL, Cyster JG, and Matloubian M. CD69 acts downstream of interferon-alpha/beta to inhibit S1P1 and lymphocyte egress from lymphoid organs. *Nature.* 2006;440(7083):540-4.
251. Gebhardt T, Wakim LM, Eidsmo L, Reading PC, Heath WR, and Carbone FR. Memory T cells in nonlymphoid tissue that provide enhanced local immunity during infection with herpes simplex virus. *Nature immunology.* 2009;10(5):524-30.
252. Gebhardt T, Whitney PG, Zaid A, Mackay LK, Brooks AG, Heath WR, Carbone FR, and Mueller SN. Different patterns of peripheral migration by memory CD4+ and CD8+ T cells. *Nature.* 2011;477(7363):216-9.
253. Mackay LK, Stock AT, Ma JZ, Jones CM, Kent SJ, Mueller SN, Heath WR, Carbone FR, and Gebhardt T. Long-lived epithelial immunity by tissue-resident memory T (TRM) cells in the absence of persisting local antigen presentation. *Proceedings of the National Academy of Sciences of the United States of America.* 2012;109(18):7037-42.
254. Casey KA, Fraser KA, Schenkel JM, Moran A, Abt MC, Beura LK, Lucas PJ, Artis D, Wherry EJ, Hogquist K, et al. Antigen-independent differentiation and maintenance of effector-like resident memory T cells in tissues. *Journal of immunology.* 2012;188(10):4866-75.
255. Masopust D, Choo D, Vezys V, Wherry EJ, Duraiswamy J, Akondy R, Wang J, Casey KA, Barber DL, Kawamura KS, et al. Dynamic T cell migration program provides resident memory within intestinal epithelium. *The Journal of experimental medicine.* 2010;207(3):553-64.
256. Skon CN, Lee JY, Anderson KG, Masopust D, Hogquist KA, and Jameson SC. Transcriptional downregulation of S1pr1 is required for the establishment of resident memory CD8+ T cells. *Nature immunology.* 2013;14(12):1285-93.
257. Lo CG, Xu Y, Proia RL, and Cyster JG. Cyclical modulation of sphingosine-1-phosphate receptor 1 surface expression during lymphocyte recirculation and relationship to lymphoid organ transit. *The Journal of experimental medicine.* 2005;201(2):291-301.

258. Cinamon G, Matloubian M, Lesneski MJ, Xu Y, Low C, Lu T, Proia RL, and Cyster JG. Sphingosine 1-phosphate receptor 1 promotes B cell localization in the splenic marginal zone. *Nature immunology.* 2004;5(7):713-20.
259. Matloubian M, Lo CG, Cinamon G, Lesneski MJ, Xu Y, Brinkmann V, Allende ML, Proia RL, and Cyster JG. Lymphocyte egress from thymus and peripheral lymphoid organs is dependent on S1P receptor 1. *Nature.* 2004;427(6972):355-60.
260. Hart GT, Wang X, Hogquist KA, and Jameson SC. Kruppel-like factor 2 (KLF2) regulates B-cell reactivity, subset differentiation, and trafficking molecule expression. *Proceedings of the National Academy of Sciences of the United States of America.* 2011;108(2):716-21.
261. Carlson CM, Endrizzi BT, Wu J, Ding X, Weinreich MA, Walsh ER, Wani MA, Lingrel JB, Hogquist KA, and Jameson SC. Kruppel-like factor 2 regulates thymocyte and T-cell migration. *Nature.* 2006;442(7100):299-302.
262. Steeber DA, Green NE, Sato S, and Tedder TF. Lyphocyte migration in L-selectin-deficient mice. Altered subset migration and aging of the immune system. *Journal of immunology.* 1996;157(3):1096-106.
263. Morrison VL, Barr TA, Brown S, and Gray D. TLR-mediated loss of CD62L focuses B cell traffic to the spleen during Salmonella typhimurium infection. *Journal of immunology.* 2010;185(5):2737-46.
264. Montalvao F, Garcia Z, Celli S, Breart B, Deguine J, Van Rooijen N, and Bousso P. The mechanism of anti-CD20-mediated B cell depletion revealed by intravital imaging. *The Journal of clinical investigation.* 2013;123(12):5098-103.
265. Kneitz C, Wilhelm M, and Tony HP. Effective B cell depletion with rituximab in the treatment of autoimmune diseases. *Immunobiology.* 2002;206(5):519-27.
266. Audia S, Samson M, Guy J, Janikashvili N, Fraszczak J, Trad M, Ciudad M, Leguy V, Berthier S, Petrella T, et al. Immunologic effects of rituximab on the human spleen in immune thrombocytopenia. *Blood.* 2011;118(16):4394-400.
267. Laurent C, de Paiva GR, Ysebaert L, Laurent G, March M, Delsol G, and Brousset P. Characterization of bone marrow lymphoid infiltrates after immunochemotherapy for follicular lymphoma. *American journal of clinical pathology.* 2007;128(6):974-80.
268. Douglas VK, Gordon LI, Goolsby CL, White CA, and Peterson LC. Lymphoid aggregates in bone marrow mimic residual lymphoma after rituximab therapy for non-Hodgkin lymphoma. *American journal of clinical pathology.* 1999;112(6):844-53.
269. Cioc AM, Vanderwerf SM, Peterson BA, Robu VG, Forster CL, and Pambuccian SE. Rituximab-induced changes in hematolymphoid tissues found at autopsy. *American journal of clinical pathology.* 2008;130(4):604-12.
270. Mei HE, Frolich D, Giesecke C, Loddenkemper C, Reiter K, Schmidt S, Feist E, Daridon C, Tony HP, Radbruch A, et al. Steady-state generation of mucosal IgA+ plasmablasts is not abrogated by B-cell depletion therapy with rituximab. *Blood.* 2010;116(24):5181-90.
271. Gowans JL. The effect of the continuous re-infusion of lymph and lymphocytes on the output of lymphocytes from the thoracic duct of unanaesthetized rats. *British journal of experimental pathology.* 1957;38(1):67-78.
272. Gowans JL, Mc GD, and Cowen DM. Initiation of immune responses by small lymphocytes. *Nature.* 1962;196(651-5.
273. Quiding-Jarbrink M, Granstrom G, Nordstrom I, Holmgren J, and Czerkinsky C. Induction of compartmentalized B-cell responses in human tonsils. *Infection and immunity.* 1995;63(3):853-7.
274. DeKosky BJ, Ippolito GC, Deschner RP, Lavinder JJ, Wine Y, Rawlings BM, Varadarajan N, Giesecke C, Dorner T, Andrews SF, et al. High-throughput sequencing of the paired human immunoglobulin heavy and light chain repertoire. *Nature biotechnology.* 2013;31(2):166-9.
275. Frentsch M, Arbach O, Kirchhoff D, Moewes B, Worm M, Rothe M, Scheffold A, and Thiel A. Direct access to CD4+ T cells specific for defined antigens according to CD154 expression. *Nature medicine.* 2005;11(10):1118-24.
276. Schoenbrunn A, Frentsch M, Kohler S, Keye J, Dooms H, Moewes B, Dong J, Loddenkemper C, Sieper J, Wu P, et al. A converse 4-1BB and CD40 ligand expression pattern delineates activated regulatory T cells (Treg) and conventional T cells enabling direct isolation of alloantigen-reactive natural Foxp3+ Treg. *Journal of immunology.* 2012;189(12):5985-94.
277. Seifert M, Przekopowitz M, Taudien S, Lollies A, Ronge V, Drees B, Lindemann M, Hillen U, Engler H, Singer BB, et al. Functional capacities of human IgM memory B cells in early inflammatory responses and secondary germinal center reactions. *Proceedings of the National Academy of Sciences of the United States of America.* 2015;112(6):E546-55.

8. Abbreviations

Abbreviation	Meaning
%	Percent
°C	Degree centigrade
µ	Micro
aDigFITC	Digoxigenin-specific FITC-labeled $F(ab)_2$
AID	Activation induced deaminase
APC	Allophycocyanin
APC-H7	Allophycocyanin-HiLyteFluor^{TM}750Bis-NHS-ester
BCR	B cell receptor
BD	Becton Dickinson
BM	Bone marrow
bp	Base pair
BSA	Albumin, Bovine Fraction V
Cµ	Ig mu constant heavy chain region
Ca1	Ig alpha-1 constant heavy chain region
CB	Centroblast(s)
CD	Cluster of differentiation
cDNA	Complementary deoxyribonucleic acid
CDR	Complementary determining region
CDRH	CDR from IgH chain
Cg	Ig gamma constant heavy chain region
C_H	Constant heavy
CSR	Class switch recombination
Cy	Cyanine
d	Day
D	Diversity heavy chain segment
DAPI	4,6 diamidino-2-phenylindole
DC	Dendritic cell
Dig	Digoxigenin
DNA	Deoxyribonucleic acid
dNTP	Deoxy-nucleotide-triphosphate
DTT	Dithiothreitol
DZ	Dark zone
EDTA	Ethylenediaminetetraacetic acid
ELISA	Enzyme Linked Immunosorbent assay
ELISpot	Enzyme-linked immunospot assay
FACS	Fluorescence activated cell sorting
FCS	Fetal calf serum
FDC	Follicular dendritic cell
FITC	Fluorescein isothiocyanate
FWR	Framework region
g	Gram

GALT	Gut-associated lymphatic tissue
GC	Germinal centre
HD	Healthy volunteer
HIV	Human immunodeficiency virus
HLA-DR	Human leucocyte antigen DR
hrs	Hours
i.d.	Intradermally
ICOS	Inducible costimulator
ICOSL	Inducible costimulator ligand
Ig	Immunoglobulin
IgA, IgD, IgE, IgG, IgM	Ig isotype A, D, E, G or M
IgH	Ig heavy chain
IgL	Ig light chain
int	Intermediate
ITP	Immune thrombocytopenia
J_H	Joining heavy
$J\kappa$	Joining kappa
$J\lambda$	Joining lambda
KLF2	Krüppel-like Factor 2
KLH	Keyhole Limpet Hemocyanin
KLH-Cy5	KLH labeled with Cy5
KLH-Dig	KLH labeled with Dig
KLH^{spec}	KLH-specific
L	Liter
LN	Lymph node(s)
LZ	Light zone
m	Milli
M	Molarity
MAdCAM-1	Mucosal vascular addressin cell adhesion molecule 1
mBC	Memory B cell(s)
MFI	Median fluorescence intensity
$MgCl_2$	Magnesium dichloride
MHC	Major histocompatibility complex
min	Minute(s)
MNC	Mononuclear cells
mRNA	Messenger ribonucleic acid
n	Nano
n/a	Not applicable
NaCl	Sodium chloride
Neg	Negative
p	Pico
PacB	Pacific Blue
PacO	Pacific Orange
PAMP	Pathogen-associated molecular pattern
PB	Plasmablast(s)
PBMC	Peripheral blood mononuclear cells

PBS	Phosphate buffered saline
PC	Plasma cell(s)
PCR	Polymerase chain reaction
PE	Phycoerythrin
PE-Cy7	Phycoerythrin-Cyanine7
PerCp	Peridinin-chlorophyll-protein complex
Pos	Positive
PRR	pattern recognition receptors
R	Replacement mutation
RNA	Ribonucleic acid
RSS	Recombiantion signal sequence
RT	Room temperature
RT-PCR	Reverse transcription polymerase chain reaction
S	Silent mutation
s.c.	Subcutaneously
S1/S2/S3/S4/S5/S6	Splenectomized patient 1, 2, 3, 4, 5 or 6
S1PR1	Sphingosine-1-phosphate receptor 1
sec	Second
SHM	Somatic hypermutation
T	Thymus
Taq	Thermus aquaticus
TBE	Tris-borate-EDTA
TCR	T cell receptor
TD	T cell-dependent
TFH	T follicular helper cells
TI	T cell-independent
T_{RM}	Tissue resident memory T cells
TT	Tetanus toxoid
TT-Cy5	TT labeled with Cy5
TX	Tonsillectomized HD
UV	Ultra violet
V	Volume
V_H	Variable heavy
$V\kappa$	Variable kappa
$V\lambda$	Variable lambda
V_L	Variable light

9. List of Figures

10. List of Tables

11. Statement of independent work

Hiermit erkläre ich, dass ich die vorliegende Arbeit selbständig verfasst und keine anderen als die angegebenen Quellen, Hilfen und Hilfsmittel verwendet habe. Ich versichere, dass diese Arbeit in dieser oder anderer Form noch keiner Prüfungsbehörde vorgelegt wurde. Ich habe mich anderwärts nicht um einen Doktorgrad beworben und besitze keinen anderen Doktorgrad. Der Inhalt der Promotionsordnung der Mathematisch-Naturwissenschaftlichen Fakultät I der Humboldt Universität zu Berlin vom 06.07.2009 ist mir bekannt.

Berlin,

Claudia Giesecke

12. Acknowledgement

First and foremost, I would like to express my sincere gratitude to Professor Thomas Dörner for giving me the opportunity to do my PhD studies in his group and his constant support and scientific freedom he granted me. Also, I would like to thank both, Professor Thomas Dörner and Dr. Reiner Ullrich for allowing me to work on the intriguing KLH project.
I also thank my committee members, for their time and consideration to review and evaluate my thesis.

Special thanks to the team of the DRFZ FCCF, Toralf Kaiser and Jenny Kirsch, for their excellent assistance in cell sorting and their constant readiness to answer questions about flow cytometry. In line, also special thanks to the team from the central laboratory of the DRFZ, Tuula Geske, Heidi Hecker-Kia, Heidi Schliemann and Anette Peddinghaus for antibody labelling and technical support.
For patient selection and tissue material organization I furthermore thank Rainer Kuhly, Monica Killig, Timor Glatzer, Carsten Perka, Katharina Stölzel, Antje Blankenstein, Simon Reinke and all the surgeons and nurses from the Department for General, Visceral and Transplantation Surgery, Charité.

Very special thanks to the entire “Dörner group”! Special thanks here are in order to Karin Reiter for supporting me throughout the entire time and also the good laughs we had.

Furthermore, I would like to thank Andreas Thiel, Andreas Hutloff, Markus Morkel, Tim Meyer, Christian Busse, Daniela Frölich, Andreas Radbruch, Kristen Feher, Henrik Mei, Peter Lipsky, George Georgiou, David Haselbach, Rudi Lurz, Claudia Berek and Ulf Klein for their scientific input and fruitful discussions and resulting collaborations and everything I was able to learn from them. And I thank all those I did not mention explicitly.

Finally, I want to express my deep gratitude to my family. My mum and my sister, Brigitte and Lissy Giesecke, and of course my spouse Andreas Thiel. Thank you for your love, your patience and your support in everything I did. Without your understanding and help none of this would have been possible. Thank you so much.